Research on the Estimation and Visualization of the shape of colonoscope in the colon

February 2013

Jaewoo Lee

Research on the Estimation and Visualization of the shape of colonoscope in the colon

February 2013

Waseda University
Graduate School of
Advanced Science and Engineering

Major in Bioscience
Research on Biorobotics

Jaewoo Lee

To my wife Kyungeun and

My lovely kids Juhyun, Seunghyun and Junho

Acknowledgement

I cannot forget the day when Takanishi Sensei had finally agreed on my study at the Waseda University. Without his invitation, I couldn’t get this great chance to study in Japan. So first of all, I would like to express my first and deep thanks to Takanishi Atsuo Sensei, who is a major advisor of my PhD thesis and professor in the Graduate School of Advanced science and engineering.

My young advisor, Dr. Ishii was a man who helped me to study on this laboratory. I was arranged in the ‘Jisou han’ – autonomous colonoscope robot team in 2009. He was the leader of several teams which are working on the medical robotics related research. He was cute and spoke English fluently. I would like to appreciate on his warm mind and clear manner.

In Jisou Han, there were students who had made research at the building called ‘Ramducks’ nearby the Nishi Waseda Campus. Shikanai, Ukawa and Murai were there with Gabriele from fall of 2009 to spring of 2010. I like remembering those days of Ramducks although I had a little bit suffered from difference of culture.

Nowadays I am working at the TWIns room, where I received help from Doho, Takamoto who are now a member of Jisou Han. Especially, concerning on the help of presentation of pre-public hearing, I would like to say thanks to Doho Kun on his preparation.

As my theme of research is closely related to the subject of the WB team, which is led by Dr. Massimiliano Zecca who is Italian Professor in our Laboratory, I borrowed for the purpose of use for my research their device which had been developed through several years. With these devices, WB sensors, I could make almost all experiments that are related to the essence of research. Moreover, I learned a lot of knowledge which are necessary to my research from Dr. Salvatore Sessa, Dr. Lin, my colleague Luca Bartolommeo and Master Course student, Saito Kun lots of knowledge which are needed when I use well these devices. Especially, I would like to express my gratitude and thankful mind to Dr. Massimiliano Zecca. He was the man who I had received much of knowledge and made affect on my research life. As the device which was borrowed from his team and it would be possible for the sake of other students, I especially would like to emphasize on this point and express appreciation to him.

Dr. Salvatore was very kind when I wanted to know on how I can calculate the estimated value of the sensor signals. I would like to say thank you to Dr. Salvatore on his warm mind. Dr. Lin is the man who made Matlab code for me to do continuing research. I could not finalize my research without this valuable code. Putting my heart on this gratitude, I would like to express my thankful mind to him. Saito Kun and Tokomoto Kun were students who are kind to help me on everything what I wanted to know related to the laboratory works.

Dr. Yohan, Dr. Klaus and Dr. Seki and Mr. Wang are also colleagues who were helpful to my life in the laboratory. I would like to say thank you for them. Dr. Aiman, Dr. Hashimoto and Dr. Nakadate were good and helpful advices by comments and email.

Mrs. Ohta san and Mrs. Itou were the ladies who had made me to control research life to be smart in Japan. I would like to express my special appreciation to them.

In Kyushu University experiments, I know that I had learned from the animal experiments with Professor. Hashizume Team. First of all, I hope to appreciate on the help on the experiments to him.

Professor Umezu has teached me on how to prepare the presentation material and checked the material in detail. I would like to express my thankful mind to him. Professor Fujie was the leader of GCOE, from which I could received my enough stipend. I could maintain my research life in Japan without any financial trouble. I hope to express my gratitude on this financial support to him.

Professor Fujimoto is the man who gave me the clue to how to approach pre-presentation easily. I know these advices made me find way to approach in the pre-public hearing. Professor Iseki made me think one more time on what is medically meaningful in my research. I would like to express my appreciation on these advices with heart.

Finally, I have to say to my wife Kyungeun my special gratitude; my graduation is due to her lo ng time service, endurance and love. Two daughters Juhyun and Seunghyun and my boy, Junho were always kind and understanding. They have always encouraged me with warm hear t and cheer when I feel hard time. Finally, I would like to express my special gratitude to my mother and brothers. I imagine that my father in the heaven, who I didn't s ee in 25 years ago, also would be glad to hear my news.

Contents

Table of Figures

List of Tables

Symbols and abbreviation

Symbols	Meaning
$A(z), B(z), H(z)$	z transfer function for digital filter
$\theta, \emptyset, \psi$	Roll, pitch and Yaw angle (degrees, radians)
a_x, a_y	x and y components of gravitational acceleration
x_{t+1}, x_t	State vector at time step t+1,t
A,Q	State transition matrix, process noise model
$\mathcal{N}(\mu, \sigma^2)$	Normal distribution with mean μ and variance σ^2
$\hat{x}_0$	Initial state
P_0	Initial covariance
$\hat{x}_k^-$	Estimated value of state based on prior
P_k^-	Estimated value of covariance based on prior
K_k	Kalman Gain at time step k
$\hat{x}_k$	Posterior state after updating using measurement
P_k	Posterior covariance
$\mathbb{R}^3$	Euclidian 3 dimensional space
O, O'	Origin of body coordinate frame
$\theta \in]-\pi, \pi]$	Angle of rotation in chapter 3
$q = (s, x, y, z)$	Quaternion: *s* scalar part ; *x*, *y*, *z* = vector part
$\lVert q \rVert$	Norm of quaternion
$slerp(q_1, q_2, u)$	Spherical linear interpolation between q_1, q_2
u	Parameter in parametric form of curve
Φ	Generalized angle representation in chapter 4
$< \phi_r(s), \phi_p(s), \phi_y(s) >$	Roll, pitch and yaw component of generalized angle in ch apter 4
$s = s_1, s_2, \ldots, s_n$	Sensor position in chapter 4
$Q(u) = (Q_x(u), Q_y(u))$	Parametric form of planar curve, u is parameter Q_x, Q_y are *x*, *y* components of curve
$L = \int_{u_1}^{u_2} \left\lvert \frac{dP}{du} \right\rvert du$	Arc length of curve between $u_1\ and\ u_2$
$\int_{-1}^{1} f(x)dx \cong \sum_{i=1}^{n} w_i f(x_i)$	Approximation of integration by summation of weight mul tiplied by Gaussian quadrature

$L = \sum_{i=1}^{n} w_i \, f(u_i)$	Arclength approximated by the summation of weight multi plied by Gaussian quadrature
$M(t)$	Difference between theoretical and real length
t_{n+1}, t_n	
$T_i(u)$	Chevyshev polynomial

抄　録

大腸がんをはじめとする消化器系がんの早期発見，早期治療には内視鏡検査が有用である．消化管内視鏡検査は，イメージセンサー（CCD）や光ファイバーと柔軟な構造をもったチューブ状の軟性内視鏡を口腔または肛門から消化管内に挿入することで内部の様子を鮮明な画像で、リアルタイムにモニター表示することができる．軟性内視鏡は，20世紀前半に開発されて以来，さまざまな改良がおこなわれ，今日ではもっとも重要な医療検査器機の一つになっている．消化器内視鏡検査の中で，大腸内視鏡検査はもっとも困難な手技とされている．大腸に限らず消化器の形状は，体外から直視することができない．大腸内視鏡検査において術者は，大腸の正確な形状に関する情報が得られない状況下で，大腸軟性内視鏡を肛門から挿入し，肛門から大腸（結腸と直腸）全体を観察することが求められる．その際の合併症のリスク，患者のうける苦痛の程度，検査に要する時間は，術者の技量に大きく依存する．

医療の現場では，技量の依存性が低い誰でも簡便にあつかえる軟性内視鏡のニーズがあり，ロボット工学や医用工学の分野では，自律的に腸内を移動するロボット型内視鏡に関する多数の研究がおこなわれている．大腸内視鏡検査において高い技術が求められる理由は，腸管の特性や配置に起因する．腸管は弾性と粘性のある組織で構成されており，軟性内視鏡から力が作用することで伸展や屈曲が生じる．また腹腔内において腸管は，折りたたまれたように配置されている．一方術者は，内視鏡の先端部の動作と体外に残された軟性内視鏡の出入操作によって，腸管内で内視鏡を任意の位置に移動することが求められる．例えば先端を曲げた状態で，軟性内視鏡を押し込むことで湾曲部を前進したり，内視鏡を回転したりすることで3次元的な湾曲部を無理なく通過させる．これらの手技を状況に応じて適切に切り替えることで，内視鏡を肛門から結腸へ進める．この際，術者が気付かないうちに体内で軟性内視鏡および腸管がループの形成してしまう場合がある．このようなループが発生すると，肛門から内視鏡を押し込んでも内視鏡先端は前進せず，ループの径が増大する状態に陥ってしまう．これは腸壁穿孔につながる非常に危険な事態である．一方，ループが発生してもそれを解除する内視鏡の操作を行うことで，容易にループを直線化することが可能である．そこでループが発生した際，術者がそれを可視化できれば，前述の腸壁穿孔のリスクを大きく低減することができる．このような考えから，大腸内での内視鏡の形状を計測し，それを術者に提示することで医療事故を防ぐシステムが求められ

ている．

本博士論文研究は，大腸内での内視鏡の形状を可視化し，術者に提示する手法の開発を目的としている．本研究では可視化の手法として，超小型の姿勢センサノードを内視鏡に多数装着し，それらによって得られる情報から内視鏡の形状を推定する方法を提案している．各姿勢センサノードは，MEMS（Micro Electro Mechanical System）技術によって作製された3軸加速度センサ，3軸ジャイロ，3軸地磁気センサからなる．本博士論文では，これらのセンサノードのハードウェアおよびセンサのデータから内視鏡の姿勢を推定する手法について述べている．

本研究は大きく分けて4つの要素から構成される．第1の要素は，センサノードの構成およびデータ処理である．各センサノードは，3軸加速度センサ，ジャイロ，地磁気センサからなり，これらの3種類のセンサの情報を融合させることで，センサノードのpitch，roll，yawの3軸の姿勢角を推定し，出力する．大腸内視鏡検査における術者の内視鏡に対する操作は，比較的ゆっくりとしたものが多く，内視鏡に生じる速度変化も低いと仮定して扱うことが可能である．温度などによるドリフトなどのノイズについては，フィルタリング処理によって除去している．複数のセンサから得られる時系列データに対して，カルマンフィルタを適用することで，高精度な姿勢角推定を実現している．

第2および第3の要素は，内視鏡のモデリングとモデルにもとづく内視鏡の形状推定である．本研究では内視鏡の構造を直列接続された剛体リンクとしている．内視鏡の形状を推定する際は，各リンクの姿勢角，およびその変化が非常に重要であり，深く検討している．工学では剛体の回転をオイラー角の変化として表現し，数学的に扱う手法がとられる．オイラー角による回転表現の短所の1つは特異点問題にある．本研究では，特異点を回避するために，四元数が用いられている．四元数は剛体の回転やその補間に有用なため，アニメーションやCGの分野でよく用いられている．Shoemakeらの研究を参考に，本研究ではベジェ曲線のためのde Casteljauアルゴリズムを用いて，3次元スプライン補間を単位四元数に適用している．

これに加えて，ユークリッド空間におけるセンサノード間の距離についても検討している．センサノード間の距離は既知であり，ユークリッド空間内で表現可能である．これにもとづいて，軟性内視鏡の幾何学モデルを構築している．その後，2つの視点からその幾何学モデルの順運動学的解法について検討している．初めには古典的なD-H表記法につい

て述べている．次に、アニメーションやCGに関する研究で用いられているスクリュー理論を用いた解法について述べている．スクリュー理論では，一般に二重四元数を用いて表現される．二重四元数はクリフォード代数に基づいているため，クリフォード代数についても記している．本研究ではクリフォード代数を用いることで，統一解的枠組みの中での姿勢の補間および剛体リンクに関する諸問題の解を得ている．

第4の要素は，構築した手法の妥当性の実験的検証である．本研究では2つの実験が行われている．第1の実験では，センサノードの数と推定される内視鏡の形状の精度に関する検討がなされている．実験の結果にもとづき，姿勢補間が必要な理由についても検討がなされている．第2の実験では，推定された内視鏡の形状と実際の内視鏡の形状の比較が行われている．さらに，推定された形状の描画方法についてもここで述べられている．ここでは，これらの実験にもとづき，提案する手法の有用性と問題点に関する検討がなされている．

提案する手法を臨床で使用可能な機材に実装するためには，センサノードの小型化が必要不可欠である．これについては，MEMS技術の進歩により，数年のうちに実現可能と見込まれる．センサノートーの小型化が実見されれば，本研究で提案されている手法の実用化が大いに見込まれる．さらに本研究で提案している手法は，3次元マウスなどの新たなマンマシンインターフェースにも応用可能である．デザインやアニメーションなどの分野において，3次元マウスの登場が切望されており，本研究で提案する手法は3次元的な曲線を作成する新しいインターフェースに応用可能である．また本研究で提案する手法は，機械の大規模変形の計測にも応用可能である．大型の工業機械や航空機，大型望遠鏡などの光学機器のたわみやひずみの計測への応用の可能性がある．

以上のように，本論文は，直視が不可能な大腸内の軟性内視鏡の形状を推定し，可視化する手法について詳術されている．内視鏡の可視化技術は臨床医学においてその実見が強く求められており，本研究の成果の社会的意義は大きい．また，柔軟体の変形に関する検討は機械工学における重要な問題領域の1つと認識されている．さらに本研究は柔軟体の計測技術に深く関連している機械工学のみならず計測工学の発展にも貢献するものである．よって，本論文は博士（工学）の学位論文として価値あるものと認める．

Abstract

Colonoscopy is pre-requisite device to inspect colorectal decease. The history of colonoscopy and endoscopy goes to the early of last century. As these two devices are same practically in functionality, colonoscopy only is dealt with hereafter. Colonoscope is the medical device with which physicians investigates suspicious lesions of patient's lower intestinal bowel and makes operation for removing polyps or deceased lesion. After it was developed, it had been used and improved with many people since that time. At present days in the clinic, it became prerequisite medical device in detecting decease of the digestive system of human being.

Modern commercialized colonoscope has various functions as a medical device. Commercial colonoscope has two major functions; one is function for detecting deceased lesions in the digestive system. Another major one is function for making operation such as removing polyps, suturing. For the purpose of the detection of decease, it has camera at the distal tip, light source to brighten the object. For the purpose of making operation, it has various type of forceps, snare. Besides, it has water and air ways for cleansing and ballooning.

Although its function is reliable and convenient to handle, the main demerit of endoscope is that it requires elaborate skill to handle smoothly and it takes long time and abundant experiences to get skilled with endoscope. The time to take endoscopy is inversely proportional to the inconvenience of patients and physician himself/herself together.

Modern science and technology is integrated to this medical device. Although modern colonoscopy has state-of-the-art technology in its own, desire to make better convenient and more functional device demands additional research. With the advance of technology in robotics area, the automation and robotization of colonoscopy has also been studied during past decades.

Even though commercial colonoscope system has long time history of development and improvement on its performance until now, endeavourers to the more convenient and easy to operate system is still going on. In recent days, one of main trends on the direction of development of the colonoscope system is automation and application of robotics technology. Commercial colonoscope system has a lot of function which can detect inflated lesion and make suitable operation in case of necessity. All the things such as manipulation are carried out by the physician. In other to reduce physical work and concentrate on the mental

and medical work. The complexity of skill comes from the characteristic of the intestine.

Upper intestine has the form of long thin flexible and multiply bended tube. Specially, lo wer intestine is severely folded. In order to make endoscope forward in the lower intestine, the stretching behavior of folded section is needed to go smoothly.

With this reason, flexibility of endoscope is prerequisite characteristics. But this flexibility of material of endoscope also becomes a cause of increases of complexity in skill in hand ling the endoscope. Physician carries out behaviors such as pushes, pulls or twists with gr asping body of endoscope at the entrance such as mouse or anus. In some case, even pus hing endoscope, it doesn't move forward. This phenomenon is called "looping". Once loop is formed, the endoscope is not moved forward inward the lower intestine, even though physician pushes it at the entrance. This complexity can be reduced when the shape of th e endoscope in the colon is provided. One of the important functionality that in near fut ure has to be accomplished in this area is the development of visualization of shape of co lonoscopy while operating on the colon. Physicians usually sees monitor displaying the vie w of colon which comes from the camera attaching on the distal tip of endoscopy/colonos copy.

The purpose of this research is to develop the methodology which can visualize the vivid shape of the colonoscope that is moving in the colon by the manipulation of physician an d to provide the physician the suitable information which is processed optimally to the ph ysician. In this paper, visualization method on the shape of the colonoscope when it is i n the colon of the patient is presented with the detailed hardware and methodology. As se nsing nodes for visualization, a number of orientation sensors, which consists of 3 axis of accelerometer, 3 axis of rate gyroscope and 3 axis of magnetometer, are used. Due to th e MEMS (micro electro mechanical system) technology, orientation sensors are produced m assively, resulting in low cost and smaller. With these sensors by the form of network, I t ry to approach this problem.

The proposed methodology consists of 4 major parts. Among them, first one is for t he hardware which receives raw signals to evaluate Euler angles or roll, pitch and yaw an gle. Quasi static situation is assumed in the accelerometer signals. In reality, physicians d eals with colonoscope gently and smoothly with low movement speed, this assumption ma kes sense. Noise filtering is carried out in advance to reduce the level of noise, which co mes from the source such as drift and temperature. As time changing data are dealt with here, sensor fusion technique such as Kalman filtering is also checked as a method to improve the accuracy of the sensor node.

The other 2 parts concerns on methodology: orientation interpolation, Arclength Reparametrization and modeling and analysis by using serial kinematic chain. As orientation of rigid body in the space is represented by rotation angles such as Euler angles, study on the rotation is deeply discussed. Rotation constitutes the special orthonormal group (abbreviated as SO (3)). Unlike points in the Euclidian space, rotation does not commute on the multiplication in the SO (3). Euler angles are widely used for representing rotation. It is also easy to access. Main drawback of Euler angle representation is singularity which is also called Gimbal lock. In order to avoid singularities, quaternion representation is checked. Quaternion works well in dealing with rotation operation.

Firstly, orientation interpolation in the quaternion unit sphere is described. As quaternion was a good descriptor to express rotation of body, orientation interpolation using quaternion had been used in the game and animation community. From the cornerstone paper of Ken Shoemake (1985), a lot of research had been carried out. Here with de Casteljau algorithm for Bezier curve, 3 dimensional spline interpolations are implemented on the quaternion unit sphere.

Additionally, secondly, the obtaining the length of the distance between sensors using Euclidean coordinates is studied. As the distance between sensors was known along the Arclength, this value should be known within the framework of Euclidian coordinates. Table lookup and Newton Raphson method is explained.

Finally, Kinematic chain model is described. Shape is approximated by the serial kinematic chain model. Well known forward kinematics model is described in detail in two points of view. First of all, classical method such as D-H method is expounded. In addition, as shape can be described by a particle moving in the 3 dimensional space, screw theory - rigid body motion theory – which was widely been studied in the area of computer animation and robotics discipline is implemented. As long as screw theory concerns, dual quaternion representation is essentially used. As dual quaternion lives in the Clifford algebra, Clifford algebra is inevitably introduced. With introducing Clifford algebra or recently named as Geometry Algebra we can solve this problem which constitutes orientation interpolation and kinematic chain in the consistent and unified solution framework.

Final part includes abundant experimental evidence: two kinds of experiments are carried out. Accuracy problem is firstly handled with the number of sensors in the network. This also explains why orientation interpolation is needed in this method.

Secondly, comparison between true curve and generated curve by this method is performed. Finally, the visualization is implemented with real data. These shows up that problem are remained yet. With some simulation experiments, this method shows its suitability for esti mating shape of the colonoscopy. Even though sensor which is suitable to the small sized space of modern colonoscopy was not yet developed, it will be finally developed in the near future as MEMS technology and related semiconductor industry are growing prospero usly. At that time, this method will receive spot light on commercialization at the industri al and medical fields.

Moreover, this technique does not confine its usage in the range of medical application: it can extend its utility to the area of special gesture recognition such as spatial mouse. Sp atial mouse is one of very useful device which can draw pictures on the computer monito r only by moving PC-like cellular phone. Also as a major application, measuring system for detecting large deformation in the huge structure is another potential application field. In the huge equipment field such as turbine, airplane or astronomical electromagnetic tele scope, this technique can play a major role for measuring dynamic deformation.

.

Chapter 1

Introduction

In this paper, as an important functionality of colonoscopy, I deal with the visualization method of its shape during operation. Colonoscopy is a medical device which can detect the infected lesion: tumour or polyps which can be a cause of colorectal cancer in the fut ure [1]. Before I step into main dish, I will introduce in this chapter how the colon is lik e, why colonoscopy is important and how was the history of development, which dates to the previous century. Moreover, I will talk about the prospect of the future of colonosco py after reminding ourselves of what kind of things we has contributed on this interesting subject.

Medical diagnosis has its role as a vital step to find its cause of decease before procee ding to the step of curing decease in entire medical work. In the decease on the digestive system of human, the medical device called endoscope had been used since 1900.

Colon is an organ of human body. It is a part of the digestive system of human as sho wn in figure 1.1. Unlike other organ, digestive system is open to the outside through mou se and anus. Digestive system is divided into upper digestive system and lower digestive s ystem. Colon is a part of lower digestive system. As in figure 1.1, colon consists of sigm oid colon, descending part, transverse part and ascending part and cecum. Finally it is con nected through rectum to anus.

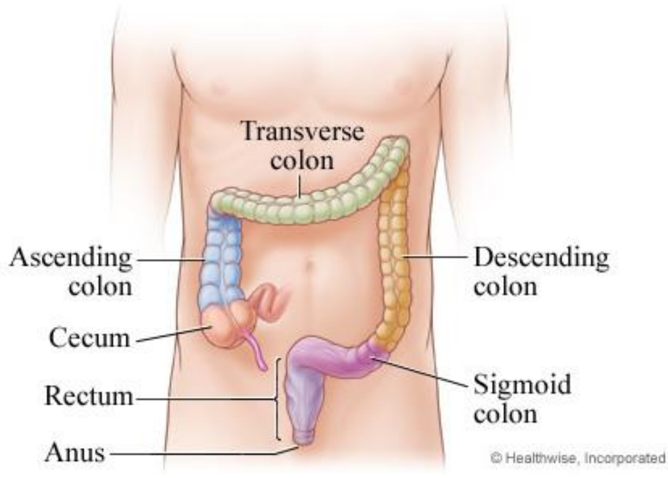

Figure 1.1 Lower intestine of Human

1.1 Colonoscope system

Colonoscope can be a system, not simple device; at least I would like to call it as a ‘s ystem’. In engineering site, system means assembly which compose of functional element. Colonoscopy can also be called by system in this aspect. Modern colonoscopy usually con sists of colonoscope tube, video processing unit, specially made lighting unit, suction pump, monitor and cart. In addition, it has lots of accessories such as various kinds of forceps. Forceps are important tools which are used to remove or grasp inflected lesion.

Figure 1.2 Modern Colonoscope (Olympus Co., ltd, Japan)

History of the colonoscope [1]

Although the first telescopes were developed in Europe in the early seventeenth century, it was Philipp Bozzini who first tried to observe inside the human body, through a rigid tube without optics. He developed an apparatus called the light conductor in 1805, which he used in his attempt to observe rectum, larynx, urethra and upper oesophagus.

In 1826, Segales in France reported on a new method for examining the human bladder using a funnel-shaped metal tube, with a concave mirror and a candle light source. In 1853, Desormeaus in France developed the first instrument of clinical value, primarily for diagnosis and treatment of urological disease, and called it the “endoscope”.

The endoscope comprised a viewing tube and a light source unit, a “gazogene” lamp lit by a mixture of alcohol and turpentine. The viewing tube, at its junction with the light source, had an angled mirror with a small hole in the centre.

Drawback of modern commercial colonoscope system

Even though commercial colonoscope system has long time history of development and improvement on its performance until now, endeavourers to the more convenient and easy to operate system is still going on. In recent days, one of main trends on the direction of development of the colonoscope system is automation and application of robotics technology. Commercial colonoscope system has a lot of function which can detect inflated lesion and make suitable operation in case of necessity. All the things such as manipulation are carried out by the physician. In other to reduce physical work and concentrate on the mental and medical work

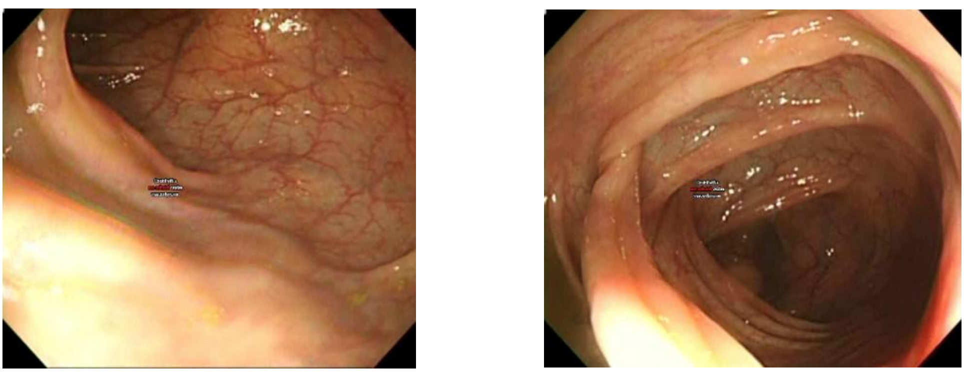

Figure 1.3 colon viewed by the colonoscope

1.2 Previous Research on the colonoscopy robot

Until now we has long time been focusing ourselves to the realization of new concept of colonoscopy in which our robot technology is melted down to be autonomous colonoscopy robot[37]. Autonomy of colonoscopy by using robot and related technology is key essenc e in our research[38-44]. In the automation of colonoscopy, one of the important and maj or trends is the introduction of robotics technology to increase the performance of the col onoscopy. This trend is going to the various directions. The major issues are as follows.

- The biomechanical model of the colon
- Automatic locomotion in the colon
- The sensing system in the colon
- Detection of lesion which has decease such as tumor or infection.
- Simulator for training of novice doctor in medical education[33-35]

Each of the above subjects is ones which have broad spectrum of issues. In the following, each of the suggested issues are investigated and discussed.

The biomechanical model of the colon

In robotics points of view, environment is something important to think. Robot always inte racts with environments. Robot makes an influence on the environment and receives influe nces from environments. Interaction is the main framework to consider when we design ro bot system[36].

Colon is special medium in the view point that this has unique characteristics compared to the industrial or real world. It is flexible and it has long thin and has small diameter jus t like tunnel. It is not fixed but hanged on the body cavity of human by the string. So it can move when it received force. When robot is inserted in the colon and start to move, the weight and thrust force will make colon move in its way.

In this situation, if we design the robot and test it to move in it, the performance of robo t will not be guaranteed. As parameters making effects to robotics behavior, interaction bet ween robot and colon should be researched ahead of the start of the regular design.

Biomechanical Modeling on the interaction

Figure 1.4 shows the biomechanical model which depicts the colon and robot by the sprin g damper components. In many situations, this model can simulates realistic world well wi th some discrepancy. Spring-damper model is a kind of lumped model. Assumption on "L umpedness" is not realistic. But we can avoid difficulty coming from complexity of real world.

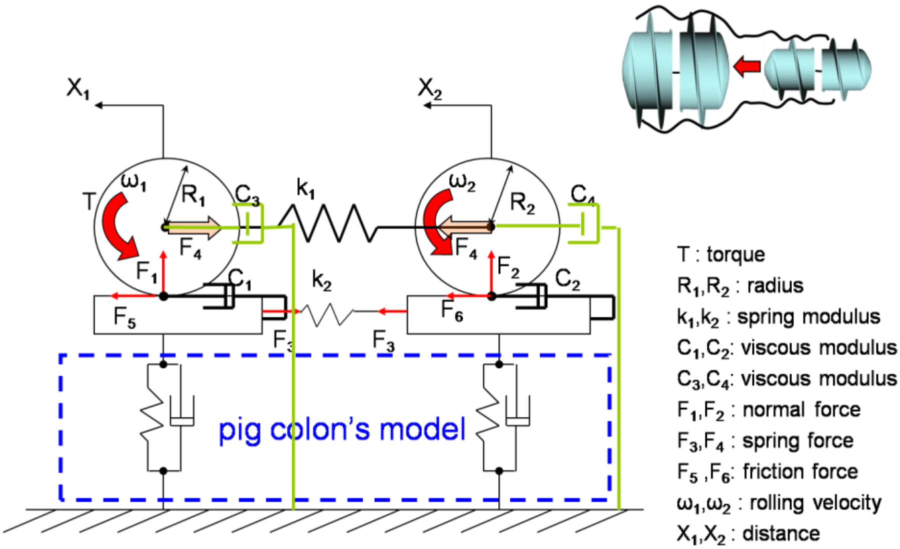

Figure 1.4 Biomechanical Model of interaction between robot and colon

In figure 1.4, two wheels means forward and rear moving part as is shown in the up per right part of figure. Pig's colon is also modeled by spring damper elements. Between them, there is interaction model expounding friction on the surface of robots. This simulati on model describes as a whole that colonoscope robot is made up of forward and rear rot ating parts and it interacts with colon and receives effect from colon wall by the amount of friction force which is important components in this biomechanical model.

Determination of Model parameters

The model parameters are determined through a number of experiments and analysis. In figure 1.5, colon wall is modeled by one spring and one viscous damper. The force re acting on the robot when robot is inserted and moved is then sum of friction force and v iscous force. These forces are basically nonlinear.

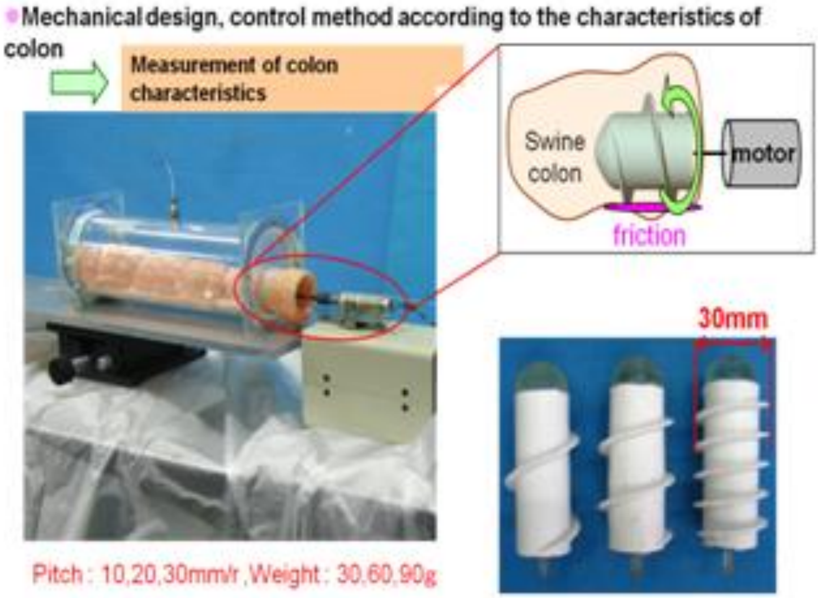

Figure 1.5 Test of characteristics of colon ; the friction property and radial elasticity of colon was measured

In figure 1.6, the device which can measure the friction force acting on the colon as a result of robot motion is shown. Dc motor is attached, which can control the input for ce and velocity to be uniform or any other specified periodic motion. The load cell that i s set on the tip of probe can measure the magnitude of force acting on the probe.

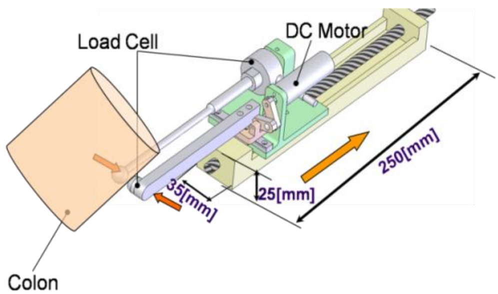

Figure 1.6 Experimental Device which can masure friction force in the colon (top) and in vivo experiment in Kyushu university hospital (bottom)

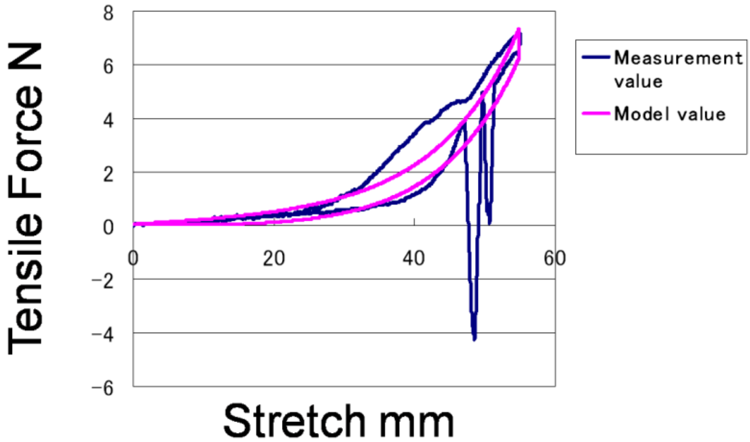

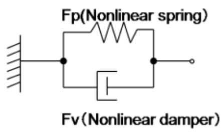

$$F = Fp + Fv$$

F_0 = 7[N]

a = 5

b = 0.01

Lmax = 55[mm]

Figure 1.7 Biomechanical Model of Pig colon; this model uses spring mass element to de scribe the biomechanical behavior of colon. The parameters are determined through a num ber of experimentations.

This force is recorded in the computer. Based on the experiment with live and dead swine, empirical friction force equations are used to estimate the parameters used in the bi omechanical models as shown in figure 1.7.

Model parameter is deduced from the measurement of tensile force and its stretch dat a such as figure 1.7. In this figure, model of the characteristics of colon when it receives tensile force is established using nonlinear spring element and nonlinear damping element. This is typically lumped model which thinks of objectives as concentrated mass. This ass umption of lumpedness can be different in detail.

With this model and experimentation results, parameters controlling the model are dete rmined. The final results showing comparison between simulation and in vitro experimentat ion are shown in figure 1.8 (a), (b). In figure 1.9(a) and (b), resulting distance is shown.

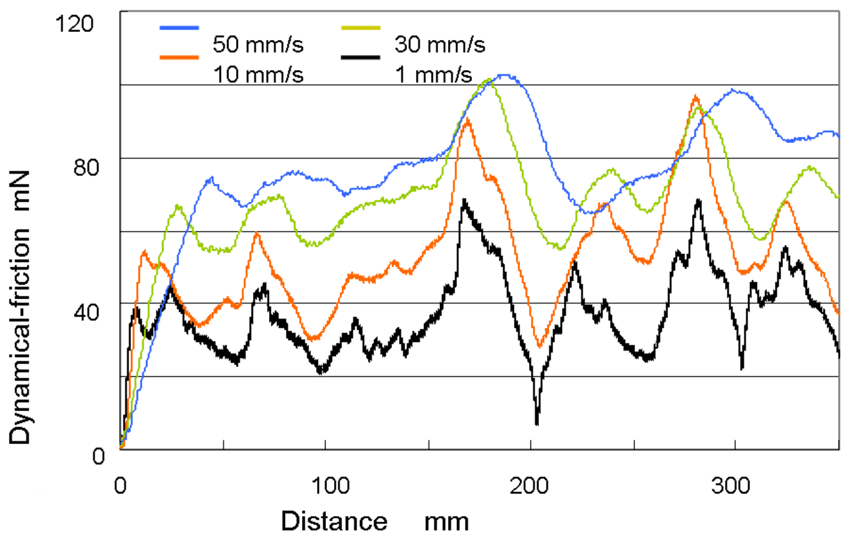

Figure 1.8 Dynamic frictions acting on the robot when rotating with different speed. This diagram shows the dynamic frictions are changing as the robot is moved in the colon wit h speed of 1, 10, 30 and 50 mm/s

The important index to movement in the colon is the distance with time. This means that as we are developing robot which can move well as a goal of research, performance on how to move well is most important.

The comparison of two results in the figure of 1.9(a) and (b) shows that this simulati on model coincides with the result of experimental results on the dead swine. Thus this al so implies that biomechanical modeling and estimation of parameters by experiments can p redict the interaction between robot and colon. Of course, simulation model cannot cover a ll real problems which can arise in the colon and robot interaction.

As it is simplified model, main issue would be the magnitude of error between two c ases. If the allowance of error is assumed which comes from experiences, accuracy of mo del would be updated

Mechanism of Colonoscopy robot

We had made mainly 2 types of mechanism: reverse screw type and crawling type. Rever se type adopts principle of screw in mechanics as a locomotion mechanism. Crawling type uses grasp and pull motion with hook like leg.

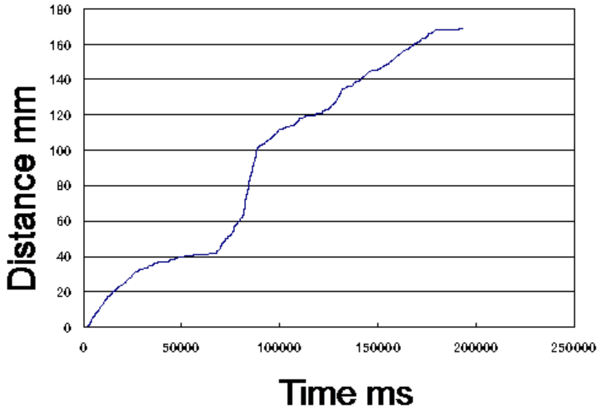

Figure 1.9(a) Distance – Time relation of dead pig case

Reverse Screw Type

Colon is flexible, long and thin organ, inside of which is sloppy. The colon is not securel y fixed to the human body [7][16]. It is more reasonable to say that it is hanged in the human body.

J. Zuo proposed micro creeping colonoscopy robot which has locomotion mechanism of ea rthworm. This robot uses several extensor units making locomotion possible by contracting and extending its body. This robot has 7.5mm diameter and 120mm length and 12.5g of weight. They have tested it in the rubber tube [16]. In [23], multi slider linkage mechanis m for endoscopic forceps manipulator was developed. Active tubular polyarticulated micro system was too implemented for flexible endoscope [24].

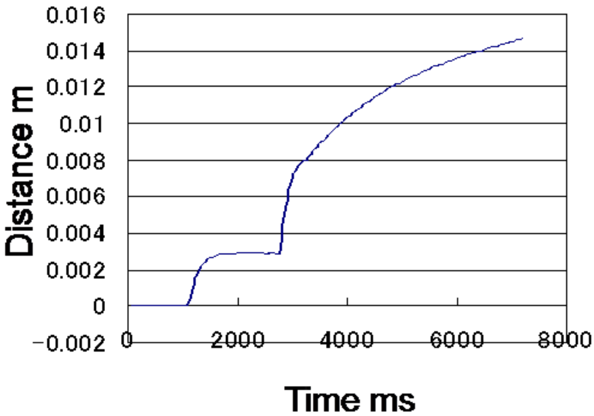

Figure 1.9(b) Distance – Time relation of simulation Model

Crawling type

As an alternative mechanism to the rotational locomotion, crawling type of mechanism was researched in recent days. In mechanical point of view, this has benefit compared to the r otation type. First of all, complex modeling concerning on the interaction between robot a nd colon is not needed. In this mechanism, robot can grasp inner wall of colon by mecha nical legs. So it can avoid slipping which usually becomes one of cause which lowers the running performance of robot in the colon.

Figure 1.10 Reverse screw type of robot

Figure 1.11 shows the crawling type of robot. This robot has legs on its own. Using this leg which is wire controlled by motors, robot can grasp the protruded part of colon such as mucosal ring of colon and move by pushing this part as the power point.

Control of Colonoscopy Robot

In order to control the robot, velocity feedback controller was developed and reinforcement algorithm was applied to meet unpredictable change of situation in the movement.

Velocity feedback Motor Controller

In the view point of control strategy, the minimum requirement which is demanded to the system is to ensure ability to meet varying situation of surroundings. With this demand i n mind, the implementation of reinforcement learning technique had been made. This meth od allows some degree of flexibility of uncertainty on the design of controller performance, which is inevitably induced when we try to evaluate the noise contaminated sensor data.

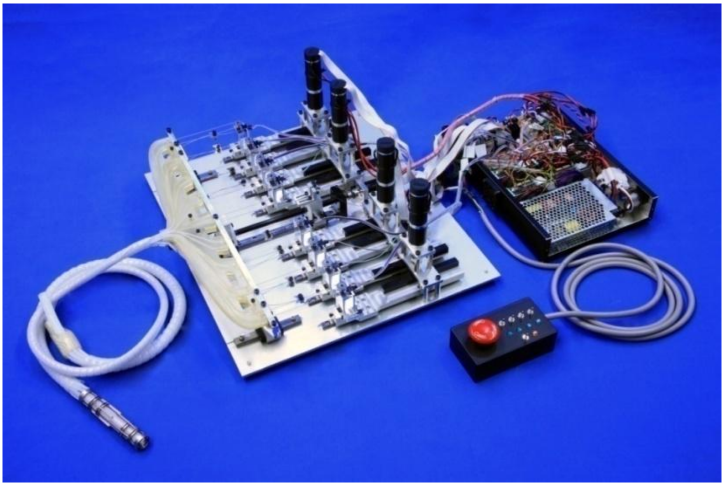

Figure 1.11 Colonoscope robot which have crawling mechanism.

Figure 1.12 shows the appearance of analog type of velocity feedback controller. Thi s board uses analog type of power amp at the motor current supply source. This power a mp can seamlessly supply current and have broad bandwidth compared to the digital-analo g chip type of amplifier. In order to remove the heat from the amplifier, the heat sink th at is made of aluminum plate is attached beneath the amplifier. The wide area of heat si nk dissipates heat effectively.

The main circuit is made of operational amplifier. Current detection is also made usi ng shunt resistor which measures the change of current by the voltage drop. The white pa rt on the figure is the shunt resistor, which can dissipate heat which comes from current f low.

Figure 1.12 Robot Controller for driving motors by using velocity feedback.

It uses operational amplifier and power amplifier to protect noise contamination. Digital control often happens to make trouble in case long distance line is needed for control. Thi s control board can prevent this kind of trouble and confirm secure and robust control. Th is concept is important specials in biomechanical system.

In figure 1.13 the system configuration for movement is shown. As shown on the figure, the robot can move in the colon by the mechanism of reverse screw type of driving syst em. Hiromasa *et al* [23] developed multi-slider linkage mechanism for endoscopic forceps manipulator. This mechanism was devised to give ability to bend flexibly in the colon.

Reinforcement Learning Control

As a control method, reinforcement learning was used. This method has different str ucture compared with classical control method [20][21]. It stresses on the interaction betwe en surroundings and robot. Here, if we say using terminology which is popular in this dis cipline, robot is called as agent and colon is named as surrounding or environment.

Programmer usually suggests agent (here, robot) the list of options agent can select. Agent usually makes logical decision based on the expectation maximization of objective f unction. Total summation of expected return is usually objective to agent. Within this term inology, return is a kind of benefit or goal robot pursues. Action is the name of robot’s l ogical endeavor to improve current situation and obtain maximum expected return.

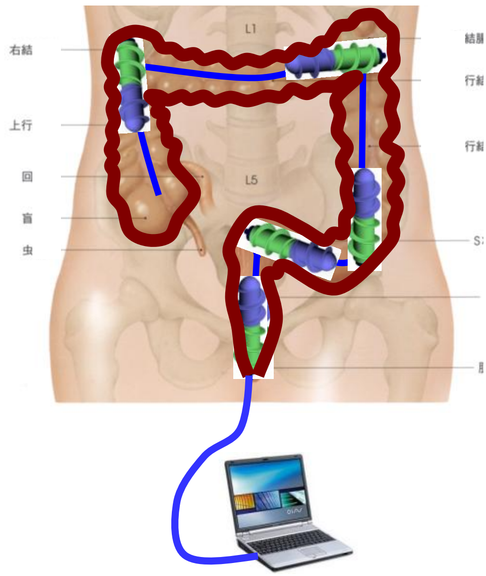

Figure 1.13 colon control: control is carried out through program which runs on the PC. I t applies reinforcement learning algorithm in order to understand situation based on the co ming signals through sensors installed on the robot and make suitable decision on the var ying situation.

Most important and distinct characteristics of this method are to use value function and action value function. Value function is defined based on the expectation of state. This is generally defined by the expected value of maximum return when agent starts from curren t state to possible state following given policy. Action value function is expected value of action state pair, when agent is in a certain state and under certain policy it selects actio n in order to move new state. This is also called as Q value. There are several methods on computing Q value;

Generally, number of state is finite. State transition from one state to another state i s assumed to follow Markov process. Thus proposition of the Markov discrete process is used.

Maximum return can be changed due to policy that agent carries out during control. There are several modifications of algorithm to implement this strategy. Figure 1.11 show s the configuration diagram of control system and relation between agent and environment.

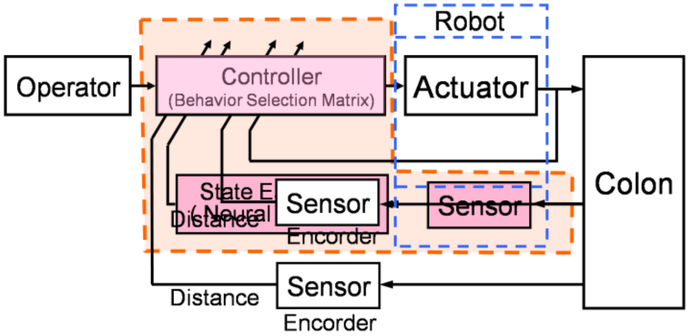

Figure 1.14 control strategy which was implemented on the robot

Figure 1.14 explains why reinforcement learning method is available in this kind of ti me varying situation. From the figure, we can know that RL based control is more efficie nt compared to the classical control. The main index to the performance is distance that r obot can move in the colon.

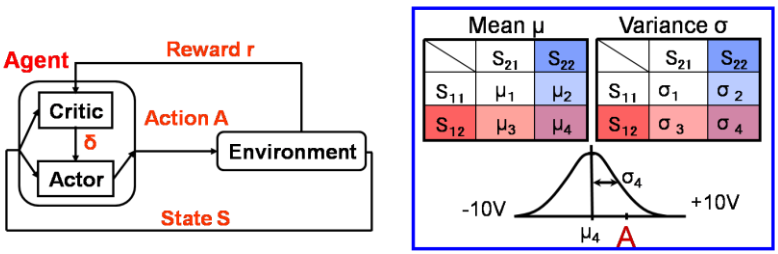

Figure 1.15 Reinforcement learning algorithm : agent(the robot in this example) predicts t he plausible state in the near future and through optimization process such as maximizing objective function (here, total reward $\sum \boldsymbol{r}(\boldsymbol{t})$) action is selected

Figure 1.15 explains actor-critic algorithm which is widely used.

Figure 1.16 is the result of measurement of performance on robot locomotion on the colon. Experiment was made on two cases; one is without RL and the other is wit h reinforcement learning control scheme. As can be seen in the figure 1.13, we can under stand that reinforcement learning algorithm improves system performance.

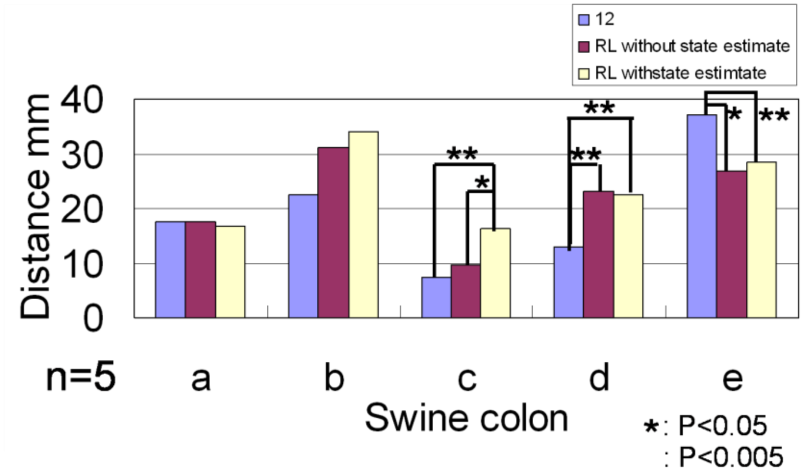

Figure 1.16 performance of robot: the experiment was carried out with live and dead swin e.

Sensing methods of shape of robot endoscope

Shape Estimation method using orientation sensors is carried out in this paper. From next chapter, this method is expounded in detail.

Medical Imaging

Medical imaging is the one of final option, say, detecting inflamed lesion and treatment and cure, in the medical robotics area [19]. In medical field, noncontact inspection is pop ular because it doesn't give damage to the human body. It has enormous spectrum in its application. There are several commercialized medical scanner such as CT, MRI, X-ray an d PET-CT. colonoscopy.

Issues relating to the colonoscopy come as the following.

1) Recognition where we are as navigation point of view of robot.

2) Detection of tumor or polyps in the colon, specially hidden tumors or polyps can be one of major issues.

Autonomous technology on where we are in the colon is essential in robotics. This agai n includes sophisticated and several sub-issues such as lumen detection or muscle wrinkles inside wall of colon or blood vessel which can be seen on the surface of colon. Lumen is the darkest area when colon is seen through camera attached on the distal tip of colono scopy. It is deeply related to the center of cross section of the colon. With various region s growing methods can be applied as seen in the figure 17 (b). Recently pixel based stoc hastic process is introduced to analyze the image.

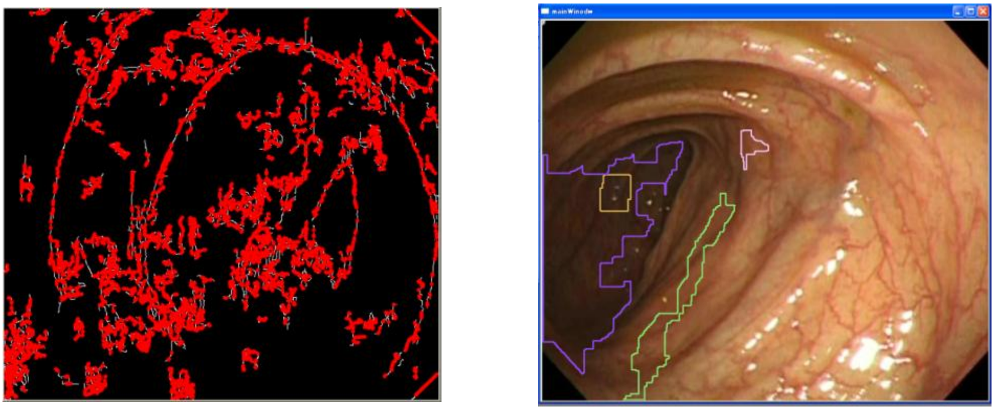

Figure 1.17 Medical Image processing: processed image (a) by hough transform line detect ion. Short lines on the boundary of wrinkles should be seperated with searching algorithm such as perceptual grouping.
(b) the lumen detection; rigion growing methods are used to detect the darkest area in the image. Histogram based detection is generally used but some degree of uncertainty exists on each method.

In the figure 1.18, the active contour algorithm is implemented to find the ring on the surface of colon. Active contour algorithm is also called as snake algorithm. It uses seeds points around the target. The objective function is made by the linear combination of sev eral type of defined energy. Here internal energy is defined by the curvature of curve whi ch comes from the extraction of edges. Image energy is also defined by the intensity of p ixels. The objective function is minimized using the differentiation of function.

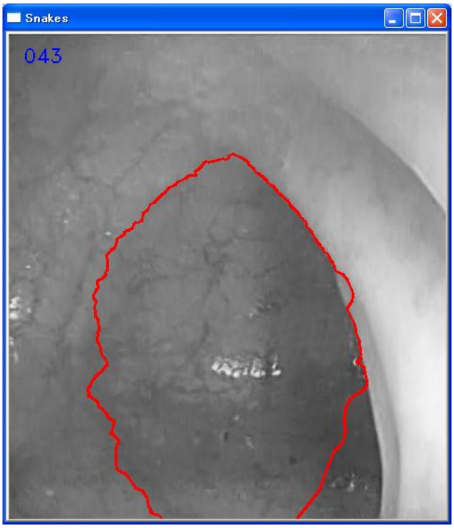

Figure 1.18 colon boundary evaluation using active contour algorithm. This method uses o ptimization technique in which Energy that object boundary has is formulated and is recur sively evaluated toward the minimization to detect the object boundary. Iteration loop is u sed. Digit on the Left upper of the image shows its iteration number.

1.3 Motivation and Objective of the research

Motivation

Colonoscope is the medical device with which physicians investigates suspicious lesions of patient’s lower intestinal bowel and makes operation for removing polyps or deceased lesion. After it was developed in 1950, it had been used and improved with many people since that time. At present days in the clinic, it became prerequisite medical device in detecting decease of the digestive system of human being.

Modern commercialized colonoscope has various functions as a medical device. Commercia l endoscope has two major functions; one is function for detecting deceased lesions in the digestive system. Another major one is function for making operation such as removing p olyps, suturing. For the purpose of the detection of decease, it has camera at the distal tip, light source to brighten the object. For the purpose of making operation, it has various t ype of forceps, snare. Besides, it has water and air ways for cleansing and ballooning.

Although its function is reliable and convenient to handle, the main demerit of endosco pe is that it requires elaborate skill to handle smoothly and it takes long time and abunda nt experiences to get skilled with endoscope. The time to take endoscopy is inversely prop ortional to the inconvenience of patients and physician himself/herself together.
Fig.1 shows in detail the time that endoscope is arrived at the appendix. In this experime nt, physicians were grouped to several levels according to their experience and skill level. Times from inserting endoscope through anus to arrival at the appendix were measured.

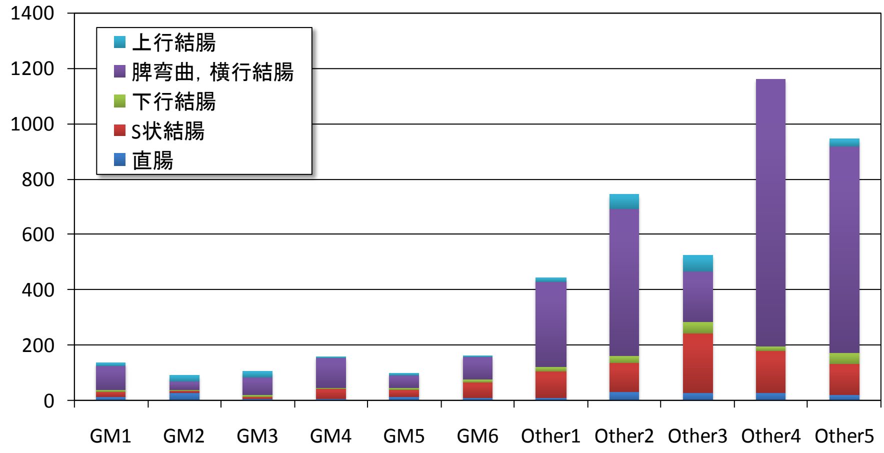

Figure 1.19 Time to go from the anus to appendix.

In the Fig.1, GM1, GM2… means groups of skillful physician. We can know from the Fig.1 that in case of skillful physician, handling time were around 20.0minutes, meanwhil e times of other groups have various distribution from around 40.0minutes to 1hours or so. The long training time is caused from the demand of the dexterity and complexity of ski ll to handle endoscope while investigating medical information. If the complexity of operat ion in endoscopy can be reduced to the reasonable level, the time will be also decreased.

The complexity of skill comes from the characteristic of the intestine. Upper intestine h as the form of long thin flexible and multiply bended tube. Specially, lower intestine is se verely folded. In order to make endoscope forward in the lower intestine, the stretching be havior of folded section is needed to go smoothly. With this reason, flexibility of endosco pe is prerequisite characteristics. But this flexibility of material of endoscope also becomes a cause of increases of complexity in skill in handling the endoscope. Physician carries o ut behaviors such as pushes, pulls or twists with grasping body of endoscope at the entran ce such as mouse or anus. In some case, even pushing endoscope, it doesn't move forwar d. This phenomenon is called "looping".

Once loop is formed, the endoscope is not moved forward inward the lower intestine, even though physician pushes it at the entrance. This complexity can be reduced when the shape of the endoscope in the colon is provided.

The shape of the endoscope is not informed to the physician in the commercial endosc ope system. At present, commercial endoscope in the market generally don't have such fu nction except the product of Olympus Co., ltd. But in the laboratory, systems which can provide information of the shape of endoscope to the physician in operation are developed and related researches on the technique to estimate the shape are carried out.

Figure 1.20 Appearance view of the magnet ic sensing system of shape of colonoscopy in the colon. This system uses ferrous coil string. This coil string is inserted through t he pass way of colonoscopy which is used for forceps. Then transmitter and receiver w hich is shown on the figure radiates magnet ic field on the patient. The coils in the col on reflect the magnetic wave. The receiver detects the coil and computer calculates the shape of the colonoscopy.

Objective of this Research

The purpose of this research is to develop the methodology which can visualize the vivid shape of the colonoscope that is moving in the colon by the manipulation of physician an d to provide the physician the suitable information which is processed optimally to the ph ysician.

1.4 Organization of the Paper

This paper consists of 6 chapters; hardware and methodology and experimental result and analysis.

In chapter 1, simplified introduction on the history of development of colonoscope is made. In chapter 2, hardware which is used in this research is explained. Accelerometer, g yroscope and magnetometer are introduced. Then noise filtering is introduced. Finally, in o rder to improve the state of inaccuracy of precision of sensor, fusion of several compleme ntary sensors is approached. Kalman and Extended Kalman filtering is introduced and com pared with the particle filtering which can be adapted even on the situation that the proce ss is not linear and non Gaussian.

In chapter 3, orientation interpolation is introduced. Orientation interpolation is different to the one of position interpolation as the orientation is not closed to the domain of mat rix multiplication.

Also the distance between interpolated points is uniformly recalculated through Arc len gth reparametrization. Numerical method is suggested as an approximate method solving pr oblem

In chapter 4, the location of the interpolated points in the Euclidian space is estimated using approximate kinematic chain model.

Chapter 5 discusses the results which were obtained from the implementation of the metho dology to the restricted experimental environment.

In the figure 1.21, the final goal of hardware is conceptually displayed.

1.5 Concluding Remarks

In this chapter, history of colonoscopy was explained. Process adding various functions to become up to the current system had been explained, which allows it to make state of the art precise inspection. Motivation on what sparked the development of this paper was prov ided and what was carried out and is going on in the laboratory was in detail introduced, specifically on the issues spanning locomotion, control and navigation.

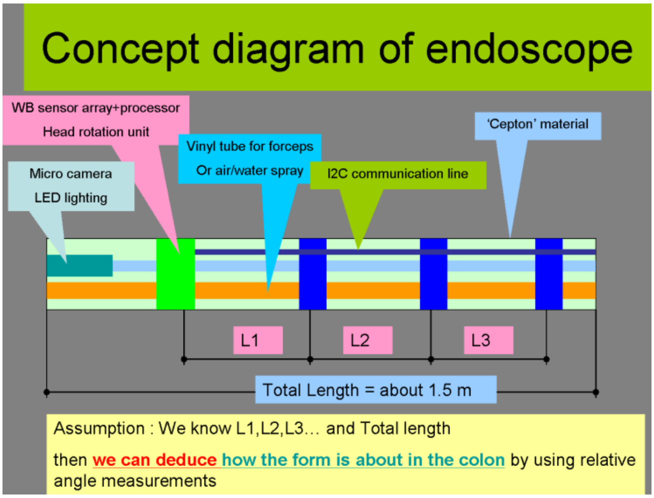

Figure 1.21 Conceptual Sketch of the New Colonoscope Tube

I. Hardware

Chapter 2

Orientation Sensor & Sensor Network

In this chapter, orientation sensor and network which consists of a number of orientation sensors are described in detail. Orientation sensor is a sensor that can detect the orientation of object. Although there are several type of orientation sensors in the market, combination of accelerometer, gyroscope and magnetometer is elucidated.

In order to express the orientation of object, inertial measurement units are widely used [17] [18]. Originally this type was used to detect the orientation of aerospace vehicles in aeronautics field. Recently, due to the rapid development of MEMS (micro electro mechanical system), low cost miniature type of orientation sensor chips had emerged in the market. With these technology, accelerometer, gyroscope and magnetometer together was able to be packaged into one or small circuit board. This type of sensor also has merit of low cost compared to the mechanically produced product. Recently board range of researches are made all around the world in the fields such as human motion capture[29], unmanned aerial vehicles, underwater vehicles, medical device and weapon control system.
According to these trends, Takanishi lab had developed inertial measurement unit called WB series.

Previous work

Cho [22] studied pedestrian navigation system using magnetometer signal. Magnetometer signal was compensated by the accelerometer signal. Then by using neural network, the walking pattern was extracted from the signals. Martin *et al* made Gesture recognition syst em using Inertial Measurement Unit [8]. Indoor positioning system was also approached wi th this sensor technique [9]. Mainly used area was human motion capture field [10]. In [1 4], detection of gestures occurring when eating and drinking arm was approached. Pedestri an navigation system is another research area [22].

2.1 Orientation Sensor Hardware

In the figure 2.1, inertial measurement unit which was developed by the bioinstrumentati on group at Waseda University are shown. Its name of model is WB-3[11].

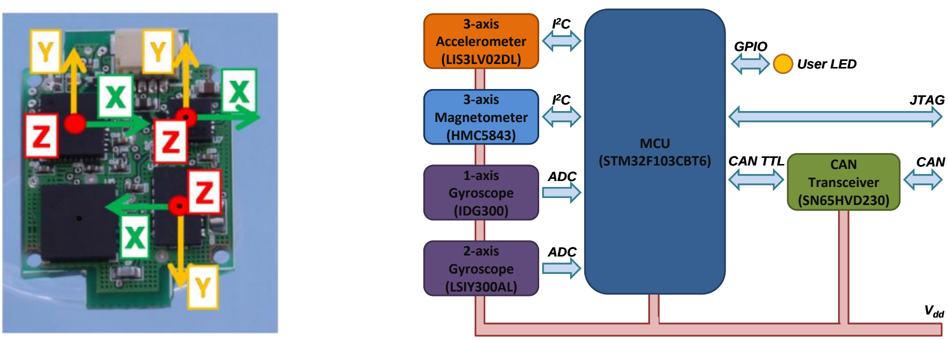

(a) (b)

Figure 2.1 WB-3: (a) the appearance of board which embodies triads of accelerometers, tri ad of gyroscope and triad of magnetometer. The other side of board has 32bit microproces sor which can communicates with CAN (control area network) protocol. (b) Configuration of board: As can be seen, MCU is in the center of configuration diagram.

From the left of figure 2.1, MCU communicates with several chips including accelerome ter, magnetometer and two rate gyros. They use I2C and AD converter for data input. On the right of figure, there is CAN transceiver which can talk with another MCU chip with high speed.

WB-3 sensor

First of all, this is made up of miniature board configuration. This embodies triads of a ccelerometer, triads of magnetometer and triad of rate gyroscope. In addition, microprocess or of 32bit controls the data communication with the outside world. Thus this is completel y accomplished appearance [2].

Table 2.1 IMU characteristics [2]

	WB-3	WB-2R	InertiaCube-3 (InvenSense)	MTx 3DoF Orientation Tracker (Xsense)
Price($)	550	650	2,295	2,265
Size[mm]	20x26x8	30x30x15	26x39x15	48x33x15
Weight[g]	2.9	5	17	11

The LIS3LV02DL (STMicroelectronics) is a 3 axis accelerometer, the small size (4.4 x 7.5 x 1[mm]), the high performance characteristics (see table 1) are suitable to the applica tion such as a wearable and precise measurement system for the rehabilitation [11]. The a ccelerometer has a user selectable full scale of ±2[g], ±6[g] and it is capable of measurin g acceleration over a bandwidth of 640[Hz] for all axes. The resolution is 2[mg] with a f ull scale ±2[g] and bandwidth 160[Hz] internally limited.

The LISY300AL (STMicroelectronics) is a miniaturized 7.0 x 7.0 x1.9 [mm] single axis gyro sensor. The LISY300AL has full scale of ±300 [deg/sec], Bandwidth of 88 [Hz] an d sensitivity of 3.3 [mV/deg/sec].

In order to measure 3 axes angular velocities, we also used a bi-axial gyro IDG300 (In venSense). This configuration, LISY300AL + IDG300, allows a one layer compact design. The IDG300 size is 6.0 x 6.0 1.5 [mm], the measurement range is ± 4.0 [gauss] and the Bandwidth is 20 [Hz] internally limited.

The sensor’s bandwidth is significantly higher than the body movement and physiologica l tremor [17 – 18] (max. frequency 15 [Hz]). The module also contains a 32 bit microcon troller STM32 Cortex (STMicroelectronics) for embedded signal elaboration. The communic ation between the PC and the IMU is performed using a Controller Area Network (CAN) Bus at 1 Mbps.

Let’s investigate chips on the board in detail. On the right side of Figure 2.1 IDG-300 is the integrated dual axis gyro chip. This chip has full scale range of ±500°/sec and has integrated low pass filter. It operates 3V single supply operation. LISY300AL is a single axis yaw rate gyroscope which outputs analog signals in the range of ±300°/sec. LIS3LV02DL is the 3 axis accelerometer chip which can measure acceleration in the range of ±2g/±6g by the form of digital output. It uses 2.16 to 3.6V single supply voltage. These chips can communicate with CPU by the I^2C/SPI protocol.

Table 2.2 Sensors characteristics

	LIS3LV02DL	IDG300	LSIY300AL	HMC5843
Range	±G	±500deg/sec	±300deg/sec	±4Gauss
Sensitivity	12±1bit	12±1bit	12±1bit	12±3bit
Bandwidth	40Hz	140Hz	88Hz	20Hz
Sample Rate	160Hz	500Hz	500Hz	50Hz
Linearity	±2%	<1%	±8%	±0.1%

Another Alternative - Electronic Compass Chip LSM303DLH

This chip embodies 3 axes of accelerometer and 3 axes of magnetometer and can be used as an electronic compass of UAV. This chip has small size of 5mm x 5mm x 1mm and packaged as a SMD chip. In the situation that motion is not severe or quasi static, measurement of tilting angle is possible.

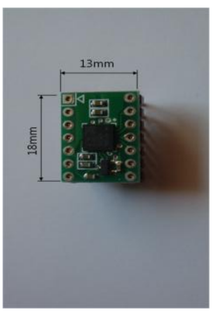

(a)

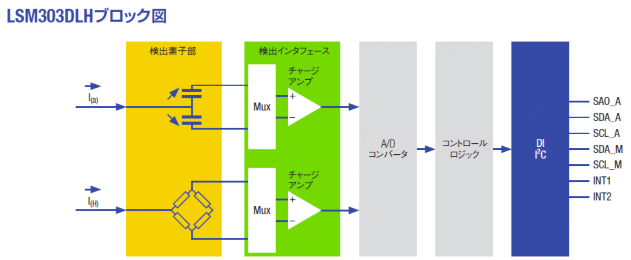

(b)

Figure 2.2 single chip packages of accelerometer and magnetometer pair. This chip has 3 axis of accelerometer and 3 axis of magnetometer. (a) The appearance of chip mounted sample board (b) its schematic diagram elucidating inner configuration of chip.

Filter Design for Noise filtering

The accelerometer signals are commonly contaminated by the noises. The sources of noise are coming on from several kinds of sources. In order to reduce the level of noise, suitable filtering should be applied before further processing. In case of human motion or colonoscopy movement in the operation of hospital, the frequency of movement is not high. This kind of motion has the frequency range of at most less than 10Hz. Therefore, low pass filter is suitable to purify the high frequency noise. The general digital filter can be expressed as the following transfer function.

According to help document of Matlab, Butterworth filter has the following merit. Butterworth filter provides the best Taylor Series approximation to the ideal low pass filter response at analogue frequencies $\omega = 0$ and $\omega = \infty$: For any order N, the magnitude squared response has 2N-1 zero derivatives at these locations (maximally flat at $\omega = 0$. and $\omega = \infty$. Response is monotonic overall, decreasing smoothly from $\omega = 0$ to $\omega = \infty$. The cut-off frequency is the frequency at which the noise and signal can be clearly separated.

2.2 Shape Sensing System

With unit sensor, we can measure Euler angles along the time step. In order to evaluate the shape of the colonoscope in the colon, we need sensor array with specified distance between them. Moreover, synchronization between sensors is important in view point of data acquisition. Here, we investigate what kind of problem can occur when sensor network is constructed.

When we make sensor network with a number of sensors, the following problem could be thought.

Sensing Element

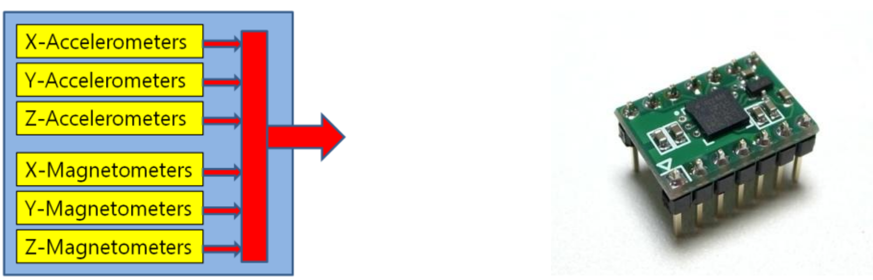

Figure 2.3 Schematic diagram of the Orientation Sensor Unit

As in figure 2.3, the sensing unit embodies accelerometer and magnetometer. This module can calculate the roll pitch and yaw angle by the following equation.

Orientation Representation

In the following figure, structure of estimation is shown by the diagram. Let's explain step by step for grasping how the system is constructed for estimation of shape.

Convention of coordinate framework

X, Y, Z reference systems are clockwise for all the sensors. Z axis is always directed out of the screen, towards the reader. Y axis of magnetometer and gyroscope are directed towards the JTAG connector (UP in Figure 2.4(a)).

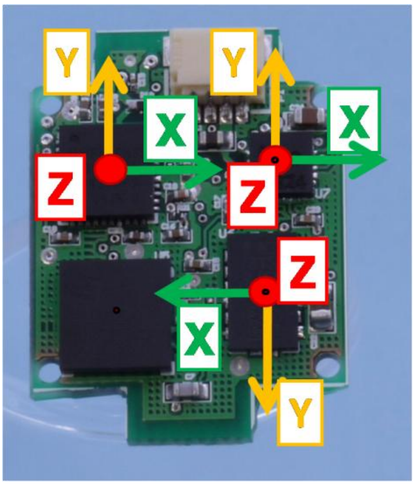

(a) Appearance of board
(JTAG connector is upward)

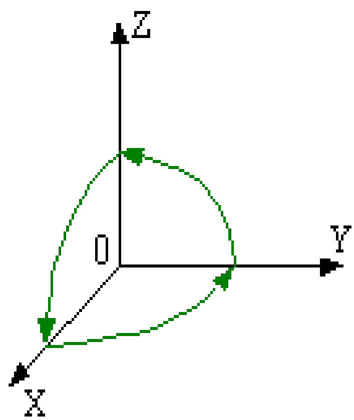

(b) board coordinate frame

Figure2.4 Oorientation coordinate frame of the sensor; in (a) the arrows show the direction of the positive value of each axis on the chip.

Accelerometer's direction is down on the board. X axis are consequently oriented: right for gyroscope and magnetometer; left for accelerometer. All rotations are clockwise around the axis [3].

Specifically, the right hand rule is utilized which specifies that positive rotation is in the direction in which the fingers of one's right hand curl when the thumb is oriented alon

g the positive axis of rotation (away from the origin).
With this convention in mind, let's check the coordinate frame of the sensor. As we can see from the symbol marked on the board, two gyros together constitutes 3 orthonormal c oordinates. The red filled circle means that the direction of the arrow showing z axis goes upwards from the board. In the Figure 2.4(a), there are 4 chips on the board. Two chips on the left side are the rate gyro chips. Among them, upper one is the 2 axis gyro and lower one is the 1 axis gyro. Accelerometer is on the top right side on the board. This c hip is 3 axis accelerometer which produces by the STMicroelectronics, co., ltd. 3 axis ma gnetometer is on the bottom right of the board. The same convention is also applied to th e accelerometer and magnetometer. As we know from the magnetometer coordinate frame, the direction of y axis is reversed, say, positive y direction go towards downward of the figure.

In Figure 2.3(b), roll, pitch and yaw angle are shown in terms of the absolute coordinat e frame. Absolute coordinate frame in this case means coordinate frame that is fixed on t he earth.

Angle representation method

There is several kind of method to describe orientation. Orientation is essentially angle or rotation about axis. The followings are popular method to express this orientation.

Axis angle method

Suppose we consider one object is rotated around fixed axis. Or we may think of axis on its own. Then we can express rotation around the axis as follows. Euler theorem also sta tes that any orientation can be expressed as a single rotation about an axis.

Euler Angle and Rotation matrix method

Euler angle is widely used. It is easy and intuitive method of expression. Twelve comp onents in the matrix exist according to the Euler theorem. Rotation matrix uses 3x3 matrix es for representing orientation. Therefore 9 components of angle are needed to represent or ientation.

Quaternion method

In order to avoid Gimbal lock or singularity which occurs when Euler angle system is used, 4-dimensional quantity called quaternion is used [31]. Quaternion was created by the William Rowan Hamilton is 1893. This representation is suitable to express smoothly the orientation without singularity problem coming from reduction of degree of freedom of ro tation in space [84].

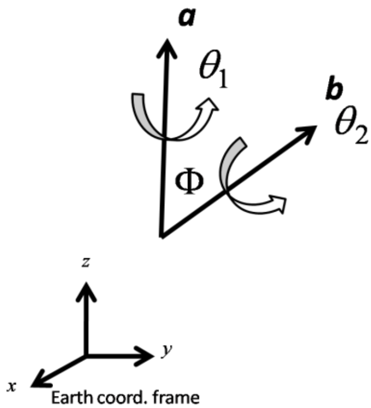

Figure 2.5 Rotation expression by Axis angle representation: angle is expressed by the rot ation around the axis. In this expression, the axis of rotation from the 1st line a to 2nd lin e b can be expressed by the cross product **a** x **b.** then the angle between lines becomes dot product$|\boldsymbol{a}||\boldsymbol{b}|\, \boldsymbol{cos}\, \emptyset$**.** Finally, $\emptyset = \mathbf{acos}(\mathbf{a} \cdot \frac{\mathbf{b}}{|\mathbf{a}||\mathbf{b}|})$

Dual Quaternion method [84]

Recently, Geometric Algebra began to use as a tool to deal with translation and rotation together among the researchers. Dual quaternion was created by the Windrow Clifford [8 6] [90] [92] [93] in 1890. Hestense and Dorst [95] in Cambridge and Amsterdam had big c ontribution on implementation to the computer science and robotics area. Using this tool, s crew motion can be completely handled with consistent framework. We will introduce this theory in detail on chapter 5.

Assumption of the quasi-static situation

The principle of measurement of tilt angle using accelerometer is simple. Suppose senso r is in the space and inclined towards the specified orientation. This means that coordinate frame of sensor is inclined to the coordinate frame of earth. Accelerometer can measure gravity force acting on the sensor body and from this gravity force, we can calculate tilt angle which the sensor body rotate from the coordinate frame of earth.

But there is one limitation in this calculation. The accelerometer should measure pure gr avity force. That is to say, there should be no other acceleration except gravity. Let's call all the other acceleration is external acceleration. Then existence of external acceleration i s important when we think of precision of measurement of tilt angle. Figure 5.1 shows th e experimental results. In this experiment, sensors are attached on the colonoscopy. It mov es slowly with similar speed the colonoscopist handles. We can notice from Figure 5.1 tha t external acceleration is dominant in the initial handling phase and disappears as time pas ses. We say this situation as "quasi-static" situation concerning on the acceleration.

The accelerometer signal has noise which comes from the several cause of source. It m ainly comes from the drift of temperature, common mode noise. Here we assume the stati c state when we apply accelerometer on the endoscope in the colon. Generally, the acceler ometer signal means summation of external acceleration and gravitational acceleration.

$$a = a_{external} + a_{gravity} \tag{2.1}$$

Endoscope is constrained by the colon when physician operates endoscope in the colon. The motion is slow and almost constant, so the accelerometer can be assumed in the "qua si" state. In this situation, we can assume as below.

$$a_{external} = 0 \quad \text{and} \quad a = a_{gravity} \tag{2.2}$$

Figure 2.5 shows that the accelerometer signal approaches to the 1,000 $bits$. This means it is nearly 1g which is the unit of 9.8 m/s^2. This value shows our assumption is suitabl e to the practical situation which sensor is working on.

We can estimate the synthesized accelerometer signal by using equation (2.3)

$$a = \sqrt{a_x^2 + a_y^2 + a_z^2} \tag{2.3}$$

, where a_x, a_y, a_z is x-, y-, z- axis accelerometer signal.

As we can see in figure 2.5, the residual of the synthesized signal of the accelerometer is very small compared to the total one.

Whole Structure of Shape Sensing System

Stage I

At this stage, raw data is filtered by the digital low pass filter. As can be seen from th e signals, high frequency noise is overloaded on the accelerometer signals. In reality, 9^{th} B utterworth filter was used to remove noise.

Stage II

At stage II, orientation is calculated based on the filtered signals. The signals are as fol lows.

Roll angle

Roll angle is calculated from the accelerometer signals.

$$\theta = \arcsin\left(\frac{a_x}{g}\right) \tag{2.4}$$

Where θ is roll angle, a_x is x component of accelerometer signal, g is gravitational accele ration.

Pitch angle

Pitch angle is also calculated from the accelerometer signals.

$$\emptyset = \arcsin\left(\frac{a_y}{g}\right) \tag{2.5}$$

Where ∅ is pitch angle, a_y is y component of accelerometer signal, g is gravitational acce leration.

Yaw angle

Before calculating yaw angle based on the magnetometer signals, measurement plane hav e to be corrected using the roll and pitch angle.

$$\begin{bmatrix} M_{xH} \\ M_{yH} \end{bmatrix} = \begin{bmatrix} \cos\theta & \sin\theta\sin\emptyset & -\cos\emptyset\sin\theta \\ 0 & \cos\emptyset & \sin\emptyset \end{bmatrix} \begin{bmatrix} M_x \\ M_y \\ M_z \end{bmatrix} \tag{2.6}$$

With this modification for the horizontal plane, yaw angle can be calculated by the follo wing.

$$\psi = \tan^{-1}\left(\frac{M_{xH}}{M_{yH}}\right) \tag{2.7}$$

Stage III

At this stage, positions of sensors and its interpolants in space are determined using the forward kinematics which is used in robotics. Homogeneous transformation matrix is calc ulated at each point on the curve.

Stage IV

In this stage, the interpolant is determined. As orientation is not commutative about the multiplication, interpolation is carried out on the unit quaternion sphere. This is a 4 dimen sional space. In this space, Spherical linear interpolation is applied instead of linear interp olation between start and end point.

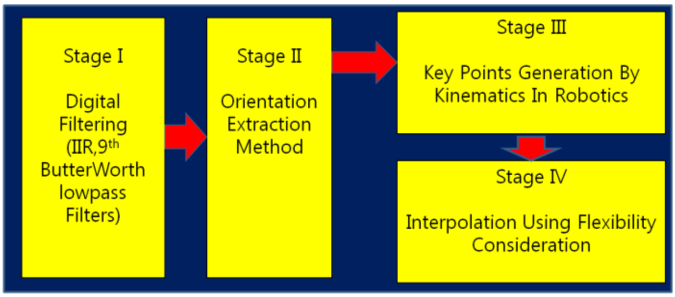

Figure 2.6 Structure of the sensor network

Miscellaneous problem

When network is connected to the PC, we use CAN to USB converter. With this devic e (this is made by type of “dongle”), Data collected from the sensor network are converte d to the format of USB communication. Libraries are prepared for C++ interface. Users can use these libraries to make communication program. This interface uses RS232C interf ace.

There might be latent problem which result from synchronization between CAN bus syst em and RS 232 communication system. Figure 2.7 shows connection diagram.

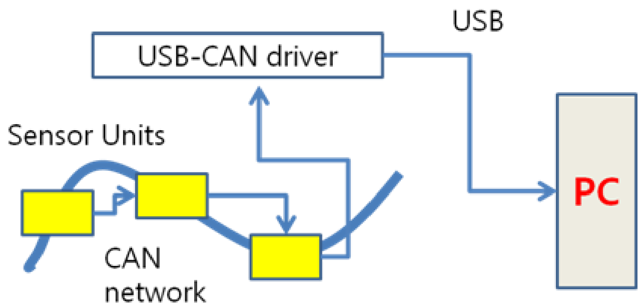

Figure 2.7 Configurations of the communication method in the figure: the sensors are arra nged along the body of the colonoscope. They are connected each other by the CAN net work. The final connection with the PC uses USB through USB-CAN converter. Synchron ization between chips is under 5 micro seconds. So the whole sensors can be assumed to send and receive data with the same time.

As in figure 2.7, CAN-USB converter might be a cause of mismatch of synchronization. In figure 2.8, the entire configuration of the system hardware and software is displayed a s a form of diagram. The sensors are conceptualized and arranged along the line of colon oscope tube. In reality, the size of chip is not so small compared to the diameter of com mercial colonoscope. It cannot be inserted into the system.

The other part is at present time implemented on the personal computer by using Matla b code. This should be converted to the C++/C type. The filtering part can be inserted int o the microprocessor. In order to realize for the commercialization in the future, all softw are part should be implemented as a code of microcontroller.

2.3 Improvement of precision by the Kalman filtering

Gyro sensor signal suffers from drift and shows severe bias due to the integration according to time [12] [13]. In order to make gyro signal to modify, accelerometer and magnetometer signals are used as compensators of error. As accelerometer and magnetometer don’t suffer from drift, it can be said to be robust in time. But basically, the accuracy is not good compared to the gyro.

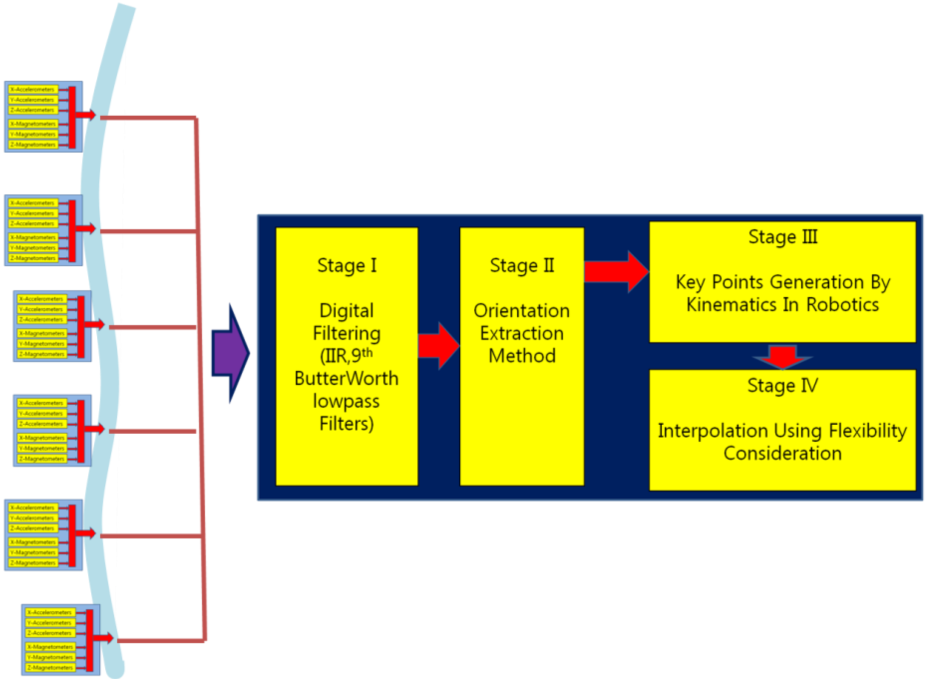

Figure 2.8 Configuration of whole data flow between the sensor network and algorithm

Besides, if motion is engaged, accelerometer does not show correct tilt angle. When tilt angles such as roll and pitch angle are measured by the accelerometer, assumption of static condition is made. Under static condition, when accelerometer is inclined from the vertical direction, say, gravitational direction of earth, tilt angles can be measured precisely.

In addition, magnetic field is not the same if place of measurement is different. Magnetometer measures magnetic field of earth. Earth magnetic field is vertical only at the arctic and Antarctic point. Magnetic field is not vertical to the ground at the other place on the earth. At another place, magnetic field makes inclination with the ground by the amount of difference of tilt angle. So in order to measure the magnetic field strength correctly at any place, this amount of inclination should be corrected ahead of calculation. As inclination angle is measured by the accelerometer, yaw angle measured by the magnetometer might also have wrong value. So when we use magnetometer and accelerometer pair to for measuring Euler angle, existence of motion is important.

By the way, aaccelerometer and magnetometer can measure body orientation. But in case object of measurement is moving according to time step, the accuracy will decrease. In order to improve this degradation of precision of measurement, sensor fusion technique is widely used in the field. From the following, sensor fusion technique is used for a metho d to improve accuracy of time varying sequence of data.

Related Works on sensor fusion

Ji et al [17] used classical PID control estimator with least square method to reduce the error from the drift and bias of the gyro signal. They compared result with the encoder signal and showed it to be good.

Chul et al [12] used Extended Kalman filter to compensate the error caused by the drift and bias of gyro signal. They updated Kalman parameters through the fuzzy adaptation w hich receives gyro signal and accelerometer signal. Veltink and Luinge [18] also have rese arched on the Kalman filtering on position tracking [25] [53] [59]. In [27], particle filtering algorithm was used to avoid assumption of linear Gaussian model on the process and me asurement. This theory is well described on the book in [28] [32].

Structure of improvement on degradation of sensors

In usual, Kalman filtering technique is widely used in the field. Kalman filtering has be en long time applied to the many fields and especially, this technique has earned success in tracking problem.

The Kalman filter has state and measurement model of process in the structure. We can say that Kalman filter is a recursive version of Bayesian filter. This has two stages to re fresh gains based on the prior and measurements: Prediction and Update. At the prediction stage, estimation of state based on the previous state is 'predicted'. At the update stage, predicted estimation of state is corrected based on the current measurement.

In our case, we can make process model as follows.

$$x_{t+1} = f(x_t) \tag{2.8}$$

Where f is a function of current state x_t, $x_{t+1}$is a one step ahead state, which we want to know.

Here state variable is constructed as follows

$$x_t = \begin{pmatrix} \theta \\ \emptyset \\ \varphi \end{pmatrix} \tag{2.9}$$

Where θ, $\emptyset$, φ means roll, pitch and yaw angle each.

As well known, Kalman filter uses assumption of linearity of process model. It also hypothesize that Gaussian distributed noise is added to the process model. This means that uncertainty of process can be modelled by the Gaussian distribution.

$$x_{t+1} = Ax_t + Q \tag{2.10}$$

Where A is transition matrix from state x_t to x_{t+1}, Q is process noise. Linear Kalman filter approximates Q as Gaussian distribution as following

$$Q := \mathcal{N}(\mu, \sigma^2) \tag{2.11}$$

Linearity assumption on the process model makes the mathematical manipulation be easy to deal with. But practical cases are rarely approximated by the linearity. In the Extended version of Kalman filter, this assumption is relaxed. In Extended Kalman filter, nonlinear format of process model is used. Nonlinear function is linearized at the point where we want to know the state. Derivative of function is used instead of linear function. Jacobian is used in Matrix.

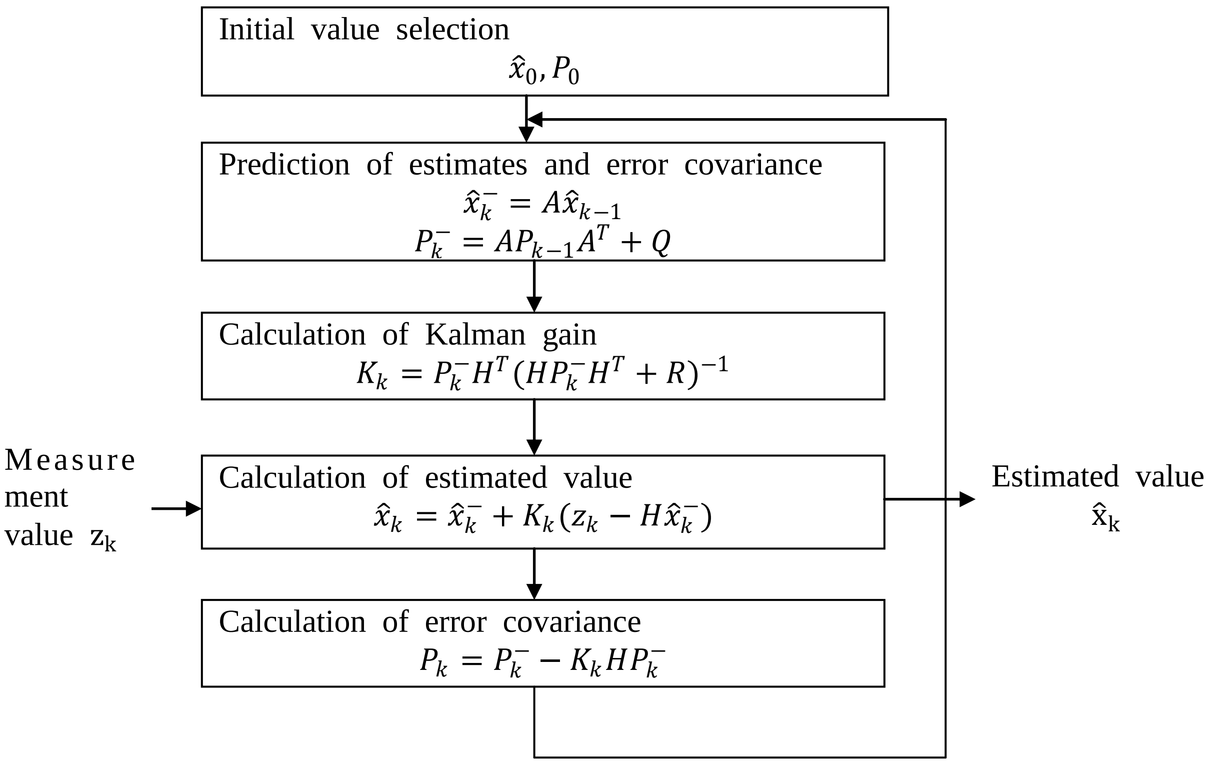

Figure 2.9 Structure of Kalman filtering algorithm

2.4 Concluding Remarks

In this chapter, hardware which can acquire orientation data was introduced. Due to the micro-electro-mechanical technology, it was clearly understand that compact system even though complex in its structure and functionality could be possible.

Specification on the hardware which is used for detecting orientation was suggested and explained in chip level in section 1. As we understand from the specification, commercial chips which state of the art technology such as high speed LAN network and 32-bit micro processor function are applied were implemented. As can be seen from this specification, we should wait until more powerful and small sized package or chip comes in the market.

In section 2.2, pre-requisite knowledge for understanding the hierarchical structure estimating shape was developed. With diagram that shows the sequence of processing, entire hierarchy on the method could be revealed clearly. Coordinate system, expression conventions on 3 dimensional rotations were also added for deep understanding. Networking method for expressing orientations of several sensors simultaneously was introduced in the last of this section.

Section 2.3 is one that concerns with dynamic situation, which occurs during sequence of time steps. Kalman filter is a powerful and popular tool to find solution in this case. By using this filtering technique, errors occurring from the deterioration of measuring accuracy could be reduced to the safe level. This technique is popular in the field of motion capture community.

Chapter 2 orients its main interest to the detailed description of hardware. From the following chapter, methodology needed to estimate and visualize shape will be suggested in earnest.

II. Methodology

Chapter 3

Orientation Interpolation & Arclength Reparametrization

In this chapter, I discuss how to interpolate orientation. In the previous chapter, we c ould see the Euler angles can be generated from the sensor units attached on the colonosc ope body. But there are practical problem in this approach: the size of sensor. The smalle st size of sensor that uses in the commercial market is about 13x13mm per one package, practically; too big to arrange enough number of sensors to guarantee the precision as a s hape sensing system which makes it possible to estimate the shape of the colonoscope. If we are in a bad situation enough to increase the number of sensors along the colonoscope, then as a second hand alternative, we can think of interpolation.

3.1 Orientation Interpolation

As the sensor outputs angles by which it expounds its orientation in space, we cannot d irectly introduce the concept of interpolation which is used in the Euclidian space. As was explained in the appendix, angles are not similar to the position in the Euclidian space. I ts space constitutes special orthogonal group (abbreviated as *SO* (3)). In this space, compo sition such as multiplication is not commutative [4] [5] [6].

First of all, what we should know on the interpolation between sensors is that we are not trying to interpolate position in Euclidean space but we want to handle orientation as immediate points to interpolate. As well known, when we deal with consecutive rotation i n the rotation space, we use rotation multiplication as an operator. Unfortunately, the rotati on multiplication is not closed to the set of rotation group. That is to say, it means that when we pick up two elements from the set of the orientation set, the result of multiplica tion is not included in the original set. So basically, it is difficult to use Euler angle repr esentation in order to deal with consecutive rotation.

In this chapter, orientation interpolation method is described and implemented for deter mining the intermediate points between orientations of sensors in the sensor network. Orie ntation interpolation technique is widely studied in the field of Computer Aided Graphics Design community. Its main application area is finding in-betweens when some intermediat e points in the orientation of snippet are given.

3.1.1 Orientation Interpolation Theory

Background of Theory

As a problem of both practical value and theoretical value, rotation interpolation has b een studied for years [45-48]. Related applications include computer graphics and animatio n [54] [72], machine vision, computer aided design (CAGD), human motion tracking [49] [5 5] [57] [58] [70-71] and robot motion planning [64] [65]. Specially, rotation interpolation is widely used in the computer animation field. As an example, imagine the scene that solid bodies roll and tumble through space. In computer animation, so do cameras. This is also a problem of rigid body motion [51]. The rotations of these objects are best described us ing a four coordinate system, quaternion [56], as we will describe hereafter. Of all quatern ion, those on the unit sphere are most suitable for animation. The first research introducin g quaternion interpolation into the animation society was famous paper by Ken Shuemake in 1985 [5].

Ken Shuemake suggests using quaternion interpolation for consecutive rotation interpolat ion, which was the start point of using quaternion in the animation field. As well known in the field, representation of rotation by the Euler angles and rotation matrix cannot avoi d problem of singularity, which is caused by the cycle of angles in the periods of 360 de gree. In aerospace field, terminology of Gimbal rock is used, where the two axes among t he three axes of elevation, heading and banking comes to be parallel on the same directio n. We can prevent this trouble by using quaternion representation [48], as Ken Shoemake in his paper also makes emphasis on.

As a modern application to the robotics area, when we want to know the trajectory in the space of the object which is grasped by the endeffector of serial link robot and desi gn suitable controller to follow the trajectory [66] [67] [68] [75], we will try to tackle this orientation interpolation in *SO* (3), where interpolation is different to the one in the Euclid ian space.

3.1.2 Orientation representation method

Orientation is expressed by several methods. Most popular is the Euler angle representation. Euler angle is easy to understand. But this representation suffers from uncertainty due to singularity. Direction cosine is another method. There is angle axis representation. In comp uter animation community, quaternion is widely used to find in-betweens between key fra mes. Recently dual quaternion is also increasing in usage. This is suitable to describe scre w motion of rigid body in space.

(1) Euler angles

Rotation is in the special orthogonal group, which is abbreviated as *SO* (3). This is the su bspace of Lie group [66-68]. There are generally 3 ways of expression for rotation in mat hematics. What is most popular is Euler angle representation. The following theorem says that Euler's theorem is suitable to the description of rotation.

(Euler's theorem)

Let $O, O' \in \mathbb{R}^3$ be two orientations. Then there exists an axis $l \in \mathbb{R}^3$ and an angle of rotat ion $\theta \in]-\pi, \pi]$ such that O yields O' when rotated θ about l. (This is different in this c hapter. It does not mean roll angle but general rotation angle in this chapter.)

Euler's theorem gives a simple definition of rotations. In most of the literature, Euler angl es are used to define rotation. The space of orientations can be parameterized by Euler an gles. When Euler angles are used, a general orientation is written as a series of rotations about three mutually orthogonal axes in space. Usually, the *x*, *y* and *z* axes in a Euclidian coordinate framework are used. The rotations are also called roll, pitch and yaw.

(2) Rotation Matrices

Rotation Matrices are the typical choice for implementing Euler angles For roll, pitch and yaw angles, there are a corresponding rotation matrix, i.e. an *x* rotation matrix, a y rotation matrix, a *z* rotation matrix. The matrices rotate by multiplying them to the position vector for a point in space, and the result is the position vector for the rotated point. A rotation matrix is a 3x3 matrix but usually homogenous 4x4 matrices are used instead.

A general rotation [63] is obtained by multiplying the three rotation matrices corresponding to the three Euler angles. The resulting matrix embodies the general rotation and can be applied to the points that are to be rotated.

Matrix multiplication is not generally commutative. This fits well with the fact that rotations in space do not commute.

Finally it should be noted that using homogeneous transformation matrices gives the only implementation that effectively embodies all standard transformations: translation, scaling, shearing and various projection transformations.

(3) Quaternion

Quaternion were invented by Sir William Rowan Hamilton (1809-1865). Quaternion based. The detailed description is shown in the appendix. Like in [60] [61] [62] [69], quaternion is widely used as a description language of rotation [65].

(4) Dual Quaternion

As our problem can be expressed as visualization of spatial curve which one sensor draws in the space, the suitable language for this purpose is dual quaternion. Dual quaternion is suitable to exploit the spatial screw motion of rigid body as were explained. As was seen before, Quaternion are best on describing rotation of vector. But our problem is including translation together.

So let’s think of mathematics of dual quaternion in more simplicity. Dual quaternion was invented by Clifford in 1890.

The algebra of dual quaternion is shortly introduced in the appendix.

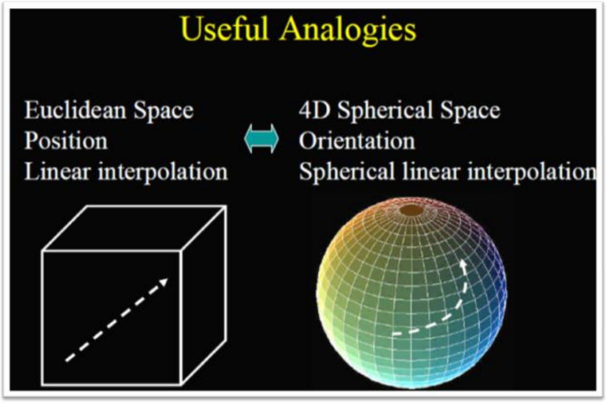

Figure 3.1 Analogies between quaternion space and Euclidean space of position

Visualization of Rotations

Suppose we want to view rotations as points lying on an n-D sphere. Then interpolating rotation means points moving on n-D sphere. Let us think of the case of 3 angle rotation. This can be represented easily as quaternion. Quaternion is a point on a 4D unit sphere [71]. That is to say, rotations satisfy (3.1).

$$q = (s, x, y, z), \|q\| = 1 \tag{3.1}$$

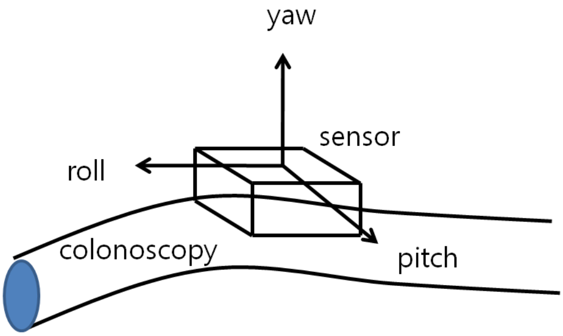

Figure 3.2 Sensor coordinate framework on the colonoscopy

3.1.3 Interpolation in quaternion sphere

Notice that unit quaternion means amount of rotation that scalar value represent around sp ecified axis by vector. (See appendix in A.3). If we think of the sphere consisting of unit quaternion, we know that this sphere is a collection of unit quaternion which has differen t rotation [77].

Then again suppose that we are watching rigid body moves [75] along the path tumbli ng. In this case, orientation of the rigid body changes continuously along the time. If we choose the two fixed scene of the moving rigid body as the starting point and ending poi nt, intermediate scenes between starting and ending scenes can be expressed by two points on the unit quaternion sphere. From this discussion, we can understand interpolation betw een orientations is the same as interpolation between two points on the unit quaternion sp here. Unit quaternion sphere is 4D space. Therefore orientation interpolation means interpol ation on the 4D quaternion sphere. Then let's think what could be the problem when we think of interpolation on the 4D sphere. We can imagine linear interpolation like one in t he Euclidian space.

Linear Interpolation

Linear interpolation is the method which linearly divides start and ending points of orienta tion. Linear interpolation is simple and easy to calculate. But here we have to notice deali ng with quaternion. The path from the starting point and ending point has curvature. If w e divide angle between two points linearly along the path (see the green square in Figure 3.4), resulting divided angles are not uniform (see the yellow circle in the figure).

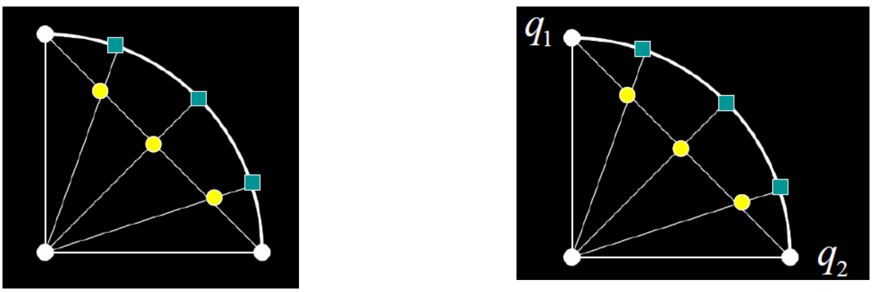

(a) linear interpolation (b) spherical linear interpolation

Figure 3.3 Linear interpolations between starting point and ending point in quaternion sphe re.

This trouble comes from the fact that the path has curvature as is different from the lin ear interpolation in the Euclidian space. Euclidian space is made of zero curvature. We ca n solve this problem by including curvature when interpolating. Spherical linear interpolatio n is the solution that can linearly interpolate between two points on the quaternion sphere.

Spherical linear interpolation (SLERP)

When we want equal increment along arc connecting two Quaternions on the spherical sur face of the quaternion sphere [50][73-74], equation (3.2) is used

$$slerp(q_1, q_2, u) = \frac{sin(1-u)\theta}{sin\theta} q_1 + \frac{sinu\theta}{sin\theta} q_2 \quad (3.2)$$

, where q_1, q_2 are two points on the quaternion sphere and u is the parameter in the rang e between 0 and 1. As we can see in the figure 3.4, the blue points on the arc does not maintain uniformity any more but the yellow circle has uniform angle.

Although angle was divided uniformly along the arc, there are still more problem in th is method. See the figure 3.3. As we are dealing with sphere, there is always two ways f rom one point to another point.

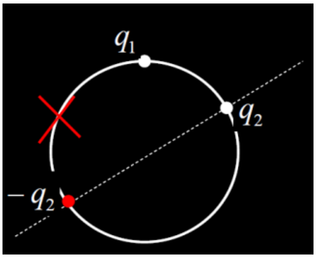

Figure 3.4 q_1, q_2 are two points on the sphere. Recall that q and $-q$ represent same rotatio n. SLERP can go the long way on the sphere. We have to have shorter way; $q_1 \cdot q_2 > 0$

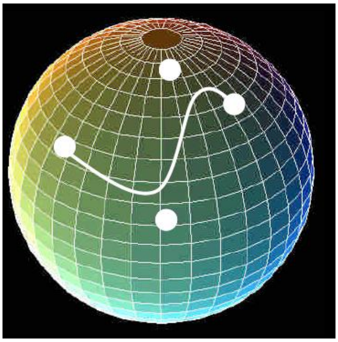

Figure 3.5 Bezier interpolation on 4D unit quaternion sphere

3.1.4 Orientation Interpolation between sensors

Let's think of our problem for orientation interpolation based on the previous section on o rientation interpolation theory. We have 10 sets of sensors in the network to describe the shape of the colonoscopy. Because the sensor outputs accelerometer and magnetometer sign als, Euler angles based on these signals will be calculated first of all. Then quaternion for each Euler angles is calculated.

$$slerp(q_1, q_2, u) = \frac{sin(1-u)\theta}{sin\theta} q_1 + \frac{sinu\theta}{sin\theta} q_2 \qquad (3.3)$$

Bezier Interpolation on 4D Sphere [80]

With this concept in mind, let's go into the practical situation. As we are using several sensors in the network, the best one will be the smooth interpolation between first and la st sensor including intermediate sensors. Ken Shuemake [5] described interpolation using B ezier curve between several points. This method used SLERP repeatedly on the points.

3.2 Arclength Parameterization

In the previous chapter we have derived interpolated points between orientations of sens ors by using orientation interpolation[26][76][78][79][82][83]. Orientations of sensors are n aturally expressed in the coordinate frame along the colonoscope. It is because sensors are arranged along the colonoscopy. In addition, sensor is arranged with equidistance along th e colonoscopy.

Here we can consider centerline of colonoscope as a curve in the space. Then this curv e is described by the coordinate of Arclength. Arclength is terminology which expresses li ne of colonoscopy. Position of sensors in the curve can be defined by the distance from o rigin to its position along the curve, say, Arclength. If arc length is s, then orientation is expressed as

$$\Phi = \Phi(s) = < \phi_r(s), \phi_p(s), \phi_y(s) > \qquad (3.4)$$

Sensor position is fixed on the curve, which has equal distance between sensors. These po sitions can be expressed as

$$s = s_1, s_2, \dots, s_n \qquad (3.5)$$

Where $s_1 = (i)th\ sensor\ position, s_n = (i+1)th\ sensor\ position$

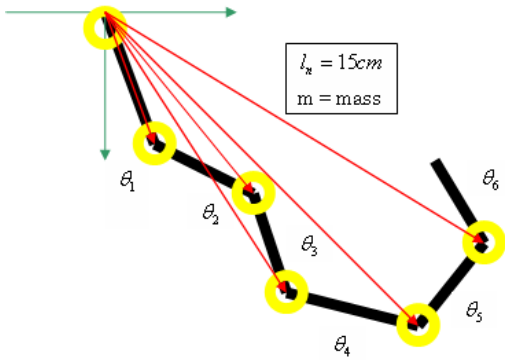

Figure 3.6 Joint Link pairs showing how to calculate the position vector; in order to calc ulate the position being seen by the red line vector, we should know length of line segm ent between interpolated points.

So orientation is represented by Arclength coordinate. But when we apply orienta tion interpolation to find intermediate points between sensor orientations, this situation is c hanged. Because we use parametric form of any parameter *t*, it has to be transformed to t he arc length parameter *s* again.

3.2.1 Introduction

In order to apply kinematic chain model, we should know the length of the line segment as shown in figure 3.8. If we make interpolation between the sensor positions, then the le ngth of line segment between interpolated points should also be known. Generally, we des cribe the curve by a parametric form

$$Q(u) = (Q_x(u), Q_y(u)) \qquad (3.6)$$

, where u is the parameter controlling relative position between start and end points and $Q_x(u), Q_y(u)$ are the x position and y position being represented by the parametric form.

The range of u is in the range of [0, 1]. If we uniformly divide range of [0, 1] by m, each subdivision will be $0, 1 * l, 2 * l, \cdots, m * l$, where $l = 1/m$. Let's think a particle is on the 0 position. When a particle is moving from 0 to m along the curve, we can mark its position on the curve. The result is shown on the figure 3.8 (a). As we can see from the figure, every length between the points is not uniform as is different to our intuition.

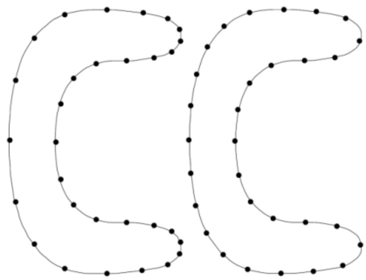

(a) (b)

Figure 3.7 Two parametric curves. The dots in curve (a) are at equal parametric intervals. The dots in curve (b) are at equal arc length intervals. As we can see from comparison of point's interval, when we make interpolation with equal parametric intervals on the curve, the final curve does not maintain uniform distance between points (this figure is from the paper [26]).

These interpolated points have flaw as it is to the calculation of position with kinematic chain model. Interpolated points are not uniform to the arc-length even though we interpolate with uniform parameter values as in figure 3.7. If the distance between the points is not uniform, then position of interpolated points between sensor positions can be determined with kinematic chain model of chapter 5. In this chapter we deal with method on how to make interpolated points be uniform to be able to calculate the positions with kinematic equation.

3.2.2 Table building method

Analytically, arc length is defined as:

$$L = \int_{u_1}^{u_2} \left| \frac{dP}{du} \right| du \tag{3.7}$$

Where P is the curve and u is the parameter. L is the arc length corresponding to the range between u_1 and u_2.

In numerical analysis, a quadrature rule is an approximation of the definite integral of a function, usually stated as a weighted sum of function values at specified points within t he domain of integration. An n point Gaussian quadrature rule, named after Carl Friedrich Gauss, is a quadrature rule constructed to yield an exact result for polynomials of degree 2n – 1 or less by a suitable choice of the points x_i and weights w_i for $i = 1, \ldots, n$. The Dodoma of integration for such a rule is conventionally taken as [-1 , 1], so the rule is stated as

$$\int_{-1}^{1} f(x)dx \cong \sum_{i=1}^{n} w_i f(x_i) \qquad (3.8)$$

If we use Gaussian quadrature to express the curve P, equation (4.3) is reduced to:

$$L = \sum_{i=1}^{n} w_i f(u_i) \qquad (3.9)$$

Where n is the number of sample points, w_i are the weight values and u_i are the sampled values. The u's can be normalized to the range zero to one and tables of weights and sa mple values can be found in tables.

As most of the time, the curves that arise in computer animation applications are not a nalytically reparameterizable by arc length. Therefore they should be reparameterized numer ically. But simpler and often more efficient method is making lookup table. This method can be somewhat inaccurate approach. It computes in advance a table of values which rela tes the original parameter with an arc length parameter.

Table 3.1 Look-Up table for parameter and its Arclength

Index	Parametric Entry	Arclength	Index	Parametric Entry	Arclength
0	0.00	0.000	11	0.55	0.900
1	0.05	0.008	12	0.60	0.920
2	0.10	0.150	13	0.65	0.932
3	0.15	0.230	14	0.70	0.944
4	0.20	0.320	15	0.75	0.959
5	0.25	0.400	16	0.80	0.972
6	0.30	0.500	17	0.85	0.984
7	0.35	0.600	18	0.90	0.994
8	0.40	0.720	19	0.95	0.998
9	0.45	0.800	20	1.00	1.000
10	0.50	0.860			

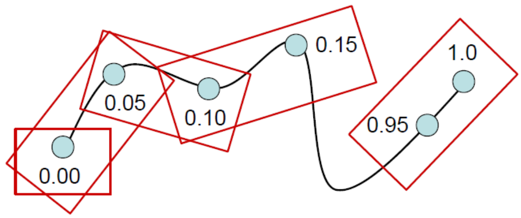

Figure 3.8 Method to build look up table between arc length and parameter values: as the number of samples in the range, so increase the accuracy of table.

The number of entries in the table depends on the accuracy with which the arc lengt h should be computed. This is determined by the application. The function is evaluated at n equidistant parameter values. Let's think of these ones as t = 0.00, 0.01, 0.02, 0.03 etc. the number of samples n should be sufficiently large to ensure that the resulting arc leng ths are within tolerance, this will become clear as the technique is described.

Suppose we divide range between 0 and 1 with 0.05 units. Then number of samples in this case will be 20.

$$u = 0.00,\ 0.05,\ 0.10,\ 0.15, \ldots,\ 1.0$$

Let's see figure 3.10. If we interpolate between *0.00* and *0.05* the curve will be deter mined. Interpolated curve is *P(u)*. Then at *u = 0.00* and *0.05*, *P(0.00) and P(0.05)* can be determined. Suppose arc length is *G(u)*. Then *G(0.05)* is like the following.

$$\begin{aligned} G(0.05) &= distance\ between\ P(0.00)\ and\ P(0.05) \\ G(0.10) &= G(0.05) +\ dist.\ between\ P(0.05)\ and\ P(0.10) \\ G(0.15) &= G(0.10) +\ dist.\ between\ P(0.10)\ and\ P(0.15) \qquad (3.10) \\ &\ldots \end{aligned}$$

$$G(1.00) = G(0.95) + \ dist.\ between\ P(0.95)\ and\ P(1.00)$$

3.2.3 Approximate Integration by Newton-Raphson

When we apply orientation interpolation using quaternion space, which is the unit sphere, we can express the interpolation curve (here, interpolant) using the parameter *t*. then para metric curve takes the following form:

$$F(t) = (X(t), Y(t), Z(t)) \tag{3.11}$$

Then the arc length between two points on a parametric curve is given by:

Where

t_{ref} = *the value of the parameter corresponding to the point of reference on the curve*

t = *the value of the parameter corresponding to some general point on th e curve*

In generating an arc length parameterization the problem then becomes one of finding the value of *t* for a given arc length *L*. thus we have to solve the non linear algebraic integ ral equation , shown in equation (3.14) for *t*.

By rearranging (3.14) we obtain:

$$M(t) = \int_{t_{ref}}^{t} (X'(t)^2 + Y'(t)^2 + Z'(t)^2)^{\frac{1}{2}}\, dt - L = 0.0 \tag{3.12}$$

A very efficient technique for finding the value of the parameter which satisfies *M*(*t*) is to apply the Newton-Raphson technique. This non linear equation solving technique converge s quadratically, provided a good initial point is used to start the algorithm.

The Newton Raphson method generates a sequence of successively improved approximatio ns to the solution of the equation *M*(*t*) = *0* using the relation:

$$t_{n+1} = t_n M(t_n) M'(t_n) \tag{3.13}$$

Thus to solve the equation (3.16), we have to first compute *M'*(*t*). in this case, *M'*(*t*) is :

$$M'(t) = \ (X'(t)^2 + Y'(t)^2 + Z'(t)^2)^{\frac{1}{2}} \tag{3.14}$$

By substituting (3.15) and (3.16) into (3.17), an iteration equation is obtained which will a llow successively improved approximation to the parameter *t* to be found.

$$t_{n+1} = t_n - [\int_{t_{ref}}^{t_n} G(t)dt - L]/M'(t_n) \tag{3.15}$$

Where

$$G(t_n) = (X'(t)^2 + Y'(t)^2 + Z'(t)^2)^{\frac{1}{2}}$$

Once a final t is found, it can then be substituted back into the original parametric equati on of the curve to find the coordinates of the point.

$$X = X(t_{final})$$
$$Y = Y(t_{final}) \tag{3.16}$$
$$Z = Z(t_{final})$$

A complication in applying the iteration equation is the evaluation of the integral. This integral cannot, in general, be solved analytically. A numerical integration technique has to therefore be applied.

Romberg technique [81] can be a good solution as the numerical method. This techniqu e required less time to converge than the trapezoidal rule or Simpson's rule.

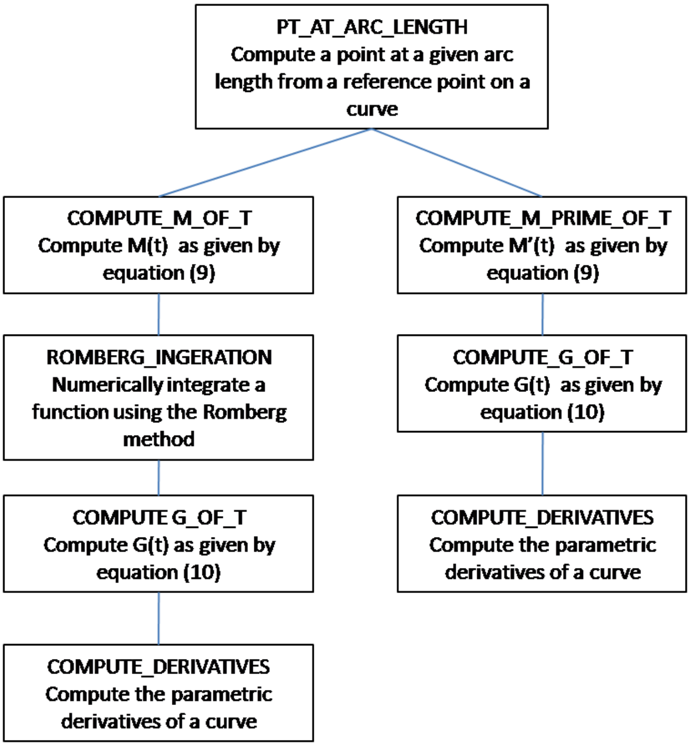

Figure 3.9 Algorithm to calculate the arc length by Newton – Raphson.

In figure 3.9, each module has the following meaning.

Input Arguments	
CURVE_DATA	A data structure which contains data defining the curve primitive and a flag indicating the curve type (eg, parametric cubic, Bezier etc)
T_REF	The parameter value of the reference point on the curve
T_ZERO	The parameter value of an initial guess point on the curve. This guess point is used to start the Newton Raphson solution and to provide a direction
Output Arguments	
T_FINAL	The parameter value of the computed point
POINT_FINAL(3)	The Cartesian coordinates of the computed point

The calling program has to provide an initial guess point to start the Newton Raphson iteration. This guess point also indicates the direction along the curve to place the computed point. The guess point in this case is computed using equation (3.17)

$$t_0 = t_{ref} + \left(\frac{\Delta t}{\Delta L}\right) L \qquad (3.17)$$

Where $\Delta t = 0.1$

$\Delta L =$ the arc length from t_{ref} to $t = t_{ref} + 0.1$

L = the arc length at which to place

The sign of L determines whether the computed point will be placed at a value of $t < t_{ref}$ (negative L) or at a value of $t > t_{ref}$ (positive L).

The basis for the above equation is that although parameter value is not exactly proportional to arc length it is approximately proportional to most curve types.

Chevyshev approximation

A Chevyshev polynomial $T_i(u)$ is defined as:

$$T_i(u) = \cos(i \arccos u) \tag{3.18}$$

For small values of i, $T_i(u)$ are:

$$\begin{aligned} T_0(u) &= 1 \\ T_1(u) &= u \\ T_2(u) &= 2u^2 - 1 \\ T_3(u) &= 4u^3 - 3u \end{aligned} \tag{3.19}$$

To approximate a function f(u) with a K order Chevyshev polynomial, we compute a set of coefficients c_i:

$$c_i = \frac{2}{K}\sum_{j=1}^{K}\left[\cos\left(\frac{\pi\left(j-\frac{1}{2}\right)}{K}\right)\right]\cos\left(\frac{\pi\left(j-\frac{1}{2}\right)}{K}\right) \tag{3.20}$$

So that:

$$f(u) \approx \left[\sum_{i=0}^{K-1} c_i T_i(u)\right] - \frac{1}{2}c_0 \tag{3.21}$$

Giving a polynomial in terms of $T_i(u)$ that approximates$f(u)$. In the case of computing a n approximation to the reparametrization function, $f(u)$ is set to $L^{-1}(u)$, where L^{-1} is the "inverse arc length" function.

For very large values of K, the Chevyshev approximation is very accurate.

3.3 Concluding Remarks

In this chapter, interpolation of orientation was dealt with on the SO(3). As a languag e to represent the spatial orientation, rotation matrix, Euler angle, Axis-Angle and quatern ion were reviewed in short. Among them, quaternion was adapted as a language to repre sent the orientation of spatial body. The Unit Quaternion was used to describe the orient ation. Interpolation theory was introduced from the Ken Shoemake paper. De Casteljeu al gorithm was used to find interpolating points between two points. Bezier curve are gener ally used and here also used for interpolating multiple points. This curve had property of continuity. Sensor points were considered as key points in this chapter.

Even though orientation scheme used uniform division between key-points, the resulting interpolating points were not equidistant. In order to solve this problem, reparametrizatio n was carried out on the Arclength parameter. Table look-up method was explored in det ail. Other method such as Newton-Raphson and Chevyshev method were also explained.

Chapter 4

Kinematic Chain Model

In this chapter, the kinematic model for describing shape of the colonoscope is sug gested. As we arranged sensors along the colonoscopy and colonoscopy has generally bend ed or arc shape when it operates in the colon, each Euler angle which were calculated ba sed on the sensor signals is represented as a function of arc length *s*. still now, we don't know how these sensors are arranged in the Euclidian space. Mapping from arc length co ordinate frame to Euclidian coordinate frame is carried out through kinematic chain model. This model evaluates the position vector of the interpolated points in the Euclidian space using the Euler angles which was determined by the sensor's Euler angles and their interp olated angle.

4.1 Introduction

In order to represent the shape of the colonoscope, mathematical modeling is necessar y. In the previous chapter, we introduced the sensor network and how to extract the orien tation and how to interpolate in case the number of sensor is limited in the network. So hereafter, we assume that the distance between the interpolated points are short enough to use approximate method to describe the shape of the colonoscopy. If enough points exist on the shape, then we can think that the shape of colonoscopy is smooth enough to think that it is “continuous and smooth curve”. *Smoothness* and *continuity* are important concept in the mathematics of curve. If the curve can be *smooth* and *continuous,* it can be *differe ntiated* at any points on the curve. This means that we can use *differential geometry* to d escribe the mathematical model to express the shape of the colonoscope. But at this point, it is meaningful

4.2 Coordinate Framework for Shape Description

Frenet-Serret coordinate frame

Figure 4.1 shows the Frenet - Serret Coordinate frame [52]. This coordinate fram e can describe the trajectory of moving body. If we imagine one sensor moves in the 3D space along the colonoscope, we can easily understand that sensor draws trajectory in the Euclidian space. Like this case, the Frenet – Serret coordinate frame can be used to desc ribe the trajectory of moving sensor.

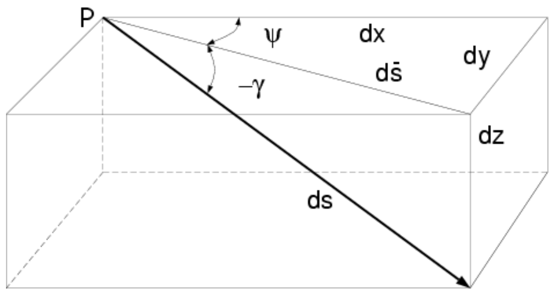

Figure 4.1 Relationship between Arclength framework and Euler angle in the Frenet-Serret coordinate framework. This coordinate framework is suitable to describe the trajectory of moving object.

Framework for colonoscope

Here we use kinematic chain for serial robot. We assume that the shape can be app roximated by the joint link pair as shown in figure 4.2. In the figure, one sensor is attach ed on the center of one link. If we can obtain the link length and its orientation, then the position of the end of each link can be calculated based on the well defined equation of forward kinematics which is widely used in the robotics field.

This is approximation model. If the length of link is small enough to obtain accurac y of the shape estimation, this model can be used to represent the real shape. It concerns with the number of joint link pair. But sense has certain size; too many sensors cannot be arranged on the colonoscope. Thus instead of many sensors, interpolation was applied i n the previous chapter.

As in figure 4.3 serial link robot has similar mechanism if joint link pair is used.

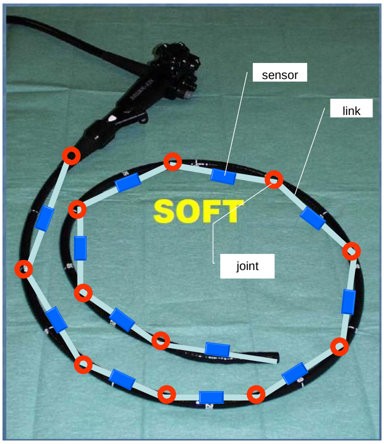

(a) approximation of shape by joint link pai r in colonoscopy

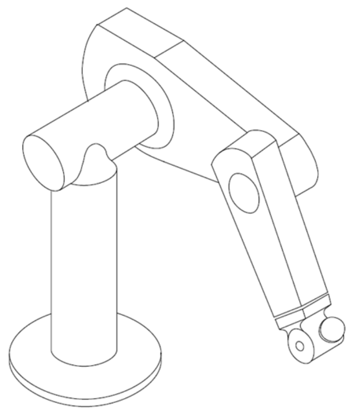

(b) six-degrees of freedom industrial articula ted serial link type robot

Figure 4.2 Sensor arrangement on the colonoscope: blue one is the sensor. Red circle mea ns joint. Line segment between joints is the link. If line segment is small compared to th e diameter of colonoscope, then error arising from the approximation could be small.

4.3 Kinematic Chain Model in Classical Robotics Theory

The most popular method is the representation by the Denavit – Hartenberg method [8 7] [89]. This method is used widely in the robotics fields. This is introduced in the Appe ndix. Here, more simple and easy to access description method for consecutive link expres sion by the Exponential expression is introduced and used.

The manipulator in robotics is assumed to be composed of joints and links. Suppose we have manipulator as in Figure 4.4. Joints are assumed to be all revolute joints with 3 de grees of freedom on the rotation in each joint. Joints which constitute manipulator are nu mbered as$P_i, i = 1 \sim n$. If the manipulator has n joints, the number of joints is $n+2$, that is to say, the joints become $P_0 \sim P_{n+1}$. Among these, P_0 represents base of the manipulator. It is also called point O. P_{n+1} depicts the point on the end-effector at the end of the manipulator, which is called as P_r. P_i is used to represent joint having one degree of freedom, this describes one set of actuator.

In case of universal joint which has 2 degrees of freedom, two joints are assumed to be connected in parallels with zero length, when we show, link is not shown in the figure. The location of the point P_i is defined on the axis of rotation. But the detailed location on the axis of rotation is not specified.

The vector of the link ($j = 1 \sim n$) is generally defined as vector from joint P_j to joint P_{j+1}. Rotation vector s_i ($i = 1 \sim n$) is set up as vector whose start point is P_i and length is unit length.

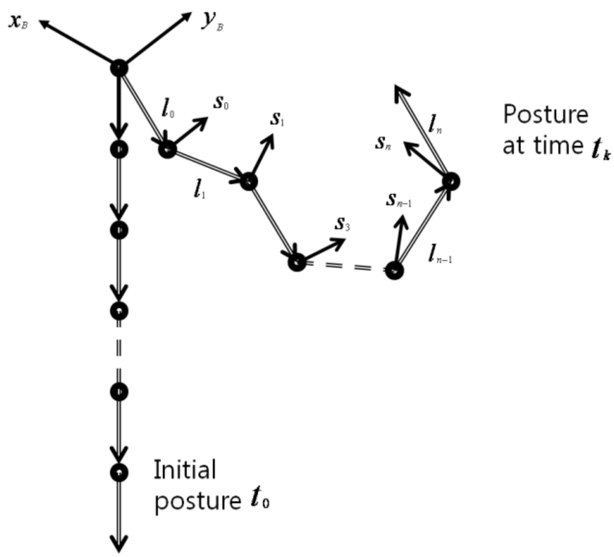

Figure 4.3 Kinematic chain model of the colonoscopy with sensor. At time step t_k, the shape of the colonoscope is approximated by the transformation matrix operation.

4.4 Kinematic Model in the Clifford Algebra [105]

Kinematics is essential in serial link robotics. There are generally two kinds of kinematics: forward kinematics and inverse kinematics. Forward kinematics problem is concerned with the relationship between the individual joints of the robot manipulator and the position and orientation of the tool or end-effectors. Stated more formally, the forward kinematics problem is to determine the position and orientation of the end effectors, given the values for the joint variables of the robot. The joint variables are the angles between the links in the case of revolute or rotational joints, and the link extension in the case of prismatic or sliding joints. The forward kinematics problem is to be contrasted with the inverse kinematics problem, which is concerned with determining values for joint variables that achieve a desired position and orientation for the end effector of the robot.

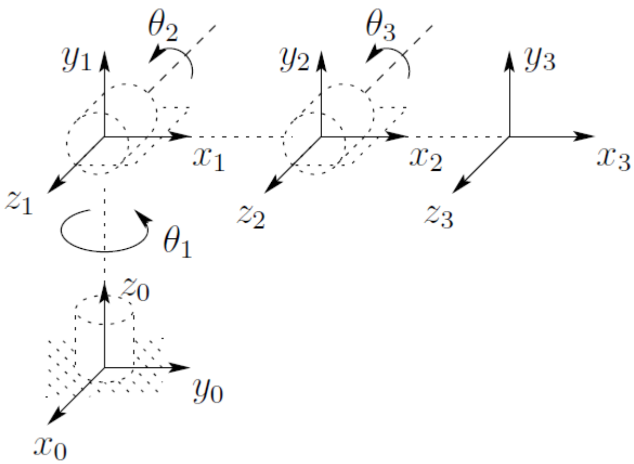

Figure 4.4 Kinematic Chain[105]

Generally stated, a robot manipulator is composed of a set of links connected together by various joints. The joints can either be very simple, such as a revolute joint or a prismatic joint, or else they can be more complex, such as a ball and socket joint.

The difference between the two situations is that, in the first instance, the joint has only a single degree of freedom of motion: the angle of rotation in the case of a revolute joint, and the amount of linear displacement in the case of a prismatic joint. In contrast, a ball and socket joint has two degrees of freedom. In his paper, it is assumed throughout that all joints have only a single degree of freedom. Note that the assumption does not involve any real loss of generality, since joints such as a ball and socket joint, in this case, two degrees of freedom – or a spherical joint, three degrees of freedom - can always be thought of as a succession of single degree of freedom joints with links of length zero in between.

With the assumption that each joint has a single degree of freedom, the action of eac h joint can be described by a single real number: the angle of rotation in the case of a r evolute joint or the displacement in the case of prismatic joint. Here we will develop a se t of conventions that provide a systematic procedure.

A robot manipulator with n joints will have n+1 links, since each joint connects two l inks. We number the joints from 1 to n, and we number the links from 0 to n, stating fr om the base. By this convention, joint *i* connects link *i-1* to link *i*. we will consider the l ocation of joint *i* to be fixed with respect to link *i-1*. When joint *i* is actuated, link *i* mo ves. Therefore, link 0 (the first link) is fixed, and does not move when the joints are actu ated.

4.5 Spherical Joints [105]

In this section, we examine spherical linkages. These linkages have the property that ev ery link in the system rotates about the same fixed point. Thus, trajectories of points in e ach link lie on concentric spheres with this point as the center. Only the revolute joint is compatible with this rotational movement and its axis must pass through the fixed points. We study the spherical RR and 3R open chains and determine their configuration as a fun ction of the joint variables and the dimensions of the links.

Coordinate rotations

A revolute joint in a spherical linkage allows spatial rotation about its axis. To define this rotation, we introduce a fixed frame F and a moving frame M attached to the moving li nk. The coordinate transformation between these frames defines the rotation of the link.

Consider a link connected to ground by one revolute joint. Let the O be directed alon g the axis of this joint and choose A to define the other end of the link. Both O and A are unit vectors that originate at the center c. the angle α between these vectors defines t he size of this link.

Choose an initial configuration and locate the fixed frame F so its origin is at c, its z-axi s directed along O, and its y-axis directed along the vector $\boldsymbol{O} \times \boldsymbol{A}$**.** This convention ensure s that A has sinα as its positive *x* component. Attach the moving frame M to **OA** so tha t in the initial configuration it is aligned with F. as the crank rotates, the angle θ measur ed counterclockwise about $\boldsymbol{O}$ from the x axis of $\boldsymbol{F}$ to the x axis of $\boldsymbol{M}$ defines the rotatio n of the link.

The orientation of $\boldsymbol{OA}$ is defined by transformation between coordinates $\mathbf{x} = (\boldsymbol{x}, \boldsymbol{y}, \boldsymbol{z})^{\boldsymbol{T}}$ in M to $\mathbf{X} = (\boldsymbol{X}, \boldsymbol{Y}, \boldsymbol{Z})^{\boldsymbol{T}}$ in $\boldsymbol{F}$, given by the matrix equation.

$$\begin{Bmatrix} X \\ Y \\ Z \end{Bmatrix} = \begin{bmatrix} cos\theta & -sin\theta & 0 \\ sin\,\theta & cos\,\theta & 0 \\ 0 & 0 & 1 \end{bmatrix} \begin{Bmatrix} x \\ y \\ z \end{Bmatrix}, \tag{4.1}$$

Or

$$\mathbf{X} = [\mathbf{Z}(\boldsymbol{\theta})]\mathbf{x} \tag{4.2}$$

The notation **[Z(.)]** represents a rotation about the z axis.

We can define similar matrices **[X(.)] and [Y(.)] to represent about the x- axis and y-axis, given by**

$$[\boldsymbol{X}(\boldsymbol{\alpha})] = \begin{bmatrix} cos\theta & -sin\theta & 0 \\ sin\,\theta & cos\,\theta & 0 \\ 0 & 0 & 1 \end{bmatrix},$$

$$\textbf{and}\ \ [\boldsymbol{Y}(\boldsymbol{\alpha})] = \begin{bmatrix} cos\theta & -sin\theta & 0 \\ sin\,\theta & cos\,\theta & 0 \\ 0 & 0 & 1 \end{bmatrix} \tag{4.3}$$

Shape description by Clifford Algebra

In this section we formulate design equations for a spatial serial chain using the matrix exponential form of its kinematics equations. These equations define the position and orientation of the end effector in terms of rotations about the joint axes of the chain. Because the coordinates of these axes appear explicitly, we can specify a set of task positions, and solve these equations to determine the location of the joints. At the same time, we are free to specify joint parameters or certain dimensions to ensure that the resulting robotic system has certain features. The structure of these design equations can be simplified by using the even Clifford algebra $C^{+}(P^{3})$, known as dual quaternions.

The product of exponentials Form of the kinematics equations

The synthesis equations for a spatial serial chain are obtained from the matrix exponential form of its kinematics equations. This form of the kinematics equations replaces the Denavit Hartenberg parameters with the coordinates of the n joint axes$\mathrm{S_i}, \mathrm{i} = 1, \dots, \mathrm{n}$. It is the coordinates of these axes that are the unknowns of the design problem.

Consider a displacement defined such that the moving body rotates the angle $\emptyset$ and slides the distance k around and along the screw axis $\mathbf{J} = (\mathbf{S}, \mathbf{V}) = (\mathbf{S}, \mathbf{C} \times \mathbf{S} + \mu\mathbf{S})$**,** where μ is called the pitch of the screw. The components of J define the 4 x 4 twist matrix.

$$J = \begin{bmatrix} 0 & -s_z & s_y & \nu_x \\ s_z & 0 & -s_x & \nu_y \\ -s_y & s_x & 0 & \nu_z \\ 0 & 0 & 0 & 0 \end{bmatrix}, \tag{4.4}$$

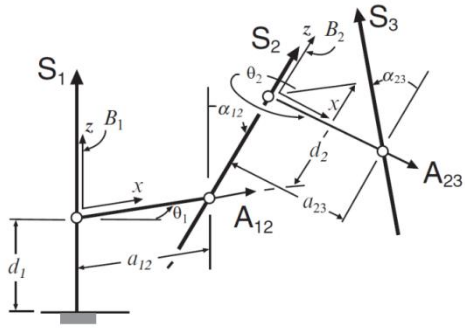

Figure 4.5 Local coordinates for serial chains[105]

And we find that the 4 x 4 homogeneous transform representing a rotation ∅ and a trans lation k about and along an axis $S, [T(\phi, k, S)]$, is defined as the matrix exponential

$$[T(\phi, k, S)] = e^{\phi J} \tag{4.5}$$

The matrix exponential takes a simple form for the matrices $Z(\theta_i, d_i)$ and $X(\alpha_{i,i+1}, a_{i,i+1})]$. The screws defined for these two transformations are $K = (\vec{k}, \nu\vec{k})$ and $L = (\vec{l}, \lambda\vec{l})$. Thus we have

And the kinematics equations become

$$[Z(\theta_i, d_i)] = e^{\theta_i K}$$
$$[X(\alpha_{i,i+1}, a_{i,i+1})] = e^{\alpha_{i,i+1} I} \tag{4.6}$$

$$[D] = [G] e^{\theta_1 K} e^{\alpha_{12} I} e^{\theta_2 K} \ldots e^{\alpha_{n-1,n} I} e^{\theta_n K} [H] \tag{4.7}$$

This is one way to write the product of exponentials from of the kinematics equations.

The Even Clifford Algebra $C^+(P^3)$

The Clifford algebra[85][86][88][90-104] of the projective three-space P^3 is a sixteen dime nsional vector space with a product operation that is defined in terms of a scalar product. The elements of even rank form an eight dimensional subalgebra $C^+(P^3)$ that can be ide ntified with the set of 4 x 4 homogeneous transforms.

The typical element of $C^{+}(P^{3})$ can be written as the eight dimensional vector given by

$$\widehat{A} = a_0 + a_1 i + a_2 j + a_3 k + a_4 \varepsilon + a_5 i\varepsilon + a_6 j\varepsilon + a_7 k\varepsilon \tag{4.8}$$

Where the basis elements I, j and k are the well known quaternion units, and ε is called the dual unit. The quaternion units satisfy the multiplication relations

$$\begin{gathered} i^2 = j^2 = k^2 = -1 \\ ij = k, jk = i, ki = j, \\ ijk = -1 \end{gathered} \tag{4.9}$$

The dual number ε commutes with i, j and k and multiplies by the rule $\varepsilon^2 = 0$.

In our calculations, it is convenient to consider the linear combination of quaternion units to be a vector in three dimensions, so we use the notation $A = a_0 + a_1 i + a_2 j + a_3 k$ and $A^o = a_0 + a_5 i + a_6 j + a_7 k$; the small circle superscript is often used to distinguish coeffici ents of the dual unit. This allows us to write the Clifford algebra element (5.8) as

$$\widehat{A} = a_0 + \mathbf{A} + a_4 \varepsilon + \mathbf{A^o} \varepsilon \tag{4.10}$$

Now collect the scalar and vector terms so that this element takes the form

$$\widehat{A} = (a_0 + a_4 \varepsilon) + (\mathbf{A} + A^o \varepsilon) = \hat{a} + \mathbf{A} \tag{4.11}$$

The dual vector $A = \mathbf{A} + \mathbf{A}^o \varepsilon$ can be identified with the pairs of vectors that define lines and screws.

Using this notation, the Clifford algebra product of elements

$\widehat{A} = \hat{a} + \mathbf{A}$ and $\widehat{B} = \hat{b} + \mathbf{B}$ takes the form

$$\hat{C} = (\hat{b} + B)(\hat{a} + A) = (\hat{b}\hat{a} - B \cdot A) + (\hat{a}B + \hat{b}A + BxA) \tag{4.12}$$

Where the usual vector dot and cross products are extended linearly to dual vectors.

Exponential of a Vector

The product operation in the Clifford algebra allows us to compute the exponential of a v ector $\theta\mathbf{S}$, where $|\mathbf{S}| = 1$,as

$$e^{\theta \boldsymbol{S}} = 1 + \theta \mathbf{S} + \frac{\theta^2}{2}\mathbf{S}^2 + \frac{\theta^3}{3!}\mathbf{S}^3 + \cdots \tag{4.13}$$

Using (5.11) we can write $\mathbf{S} = \mathbf{0} + \mathbf{S}$ and compute

$$S^2 = (0 + S)(0 + S) = -1, S^3 = -S, S^4 = 1, S^5 = S \tag{4.14}$$

Which means we have

$$e^{\theta \boldsymbol{S}} = \left(1 + \frac{\theta^2}{2}\mathbf{S}^2 + \cdots\right) + \left(\theta \mathbf{S} + \frac{\theta^3}{3!}\mathbf{S}^3 + \cdots\right)\mathbf{S} \tag{4.15}$$

$$= \cos\theta + \sin\theta\,\mathbf{S}$$

This is well known unit quaternion that represents a rotation around the axis S by the an gle $\emptyset = 2\theta$. The rotation angle $\emptyset$ is double that given in the quaternion because Clifford algebra form of a rotation requires multiplication by both $Q = \cos\theta + \sin\theta\,\mathbf{S}$

And its conjugate $Q^* = \cos\theta - \sin\theta\,\mathbf{S}$. In particular, if x and X are the coordinates of a point before and after the rotation, then we have the quaternion coordinate transformation equation

$$X = QxQ^* \tag{4.16}$$

For this reason the quaternion is often written in terms of one half the rotation angle, that is , $Q = \cos(\frac{\emptyset}{2}) + \sin(\frac{\emptyset}{2})\,\mathbf{S}$

Exponential of a Screw

The Plücker coordinates $S = (\mathbf{S}, \mathbf{C} \times \mathbf{S})$ of a line can be identified with the Clifford algebra element $S = \mathbf{S} + \varepsilon\mathbf{C} \times \mathbf{S}$. Similarly, the screw $J = (\mathbf{S}, \mathbf{V}) = (\mathbf{S}, \mathbf{C} \times \mathbf{S} + \mu\mathbf{S})$ becomes the ele ment $J = \mathbf{S} + \varepsilon\mathbf{V} = (1 + \mu\varepsilon)S$. Using the Clifford product we can compute the exponential of the screw θ J.

$$e^{\theta \mathbf{J}} = 1 + J + \frac{\theta^2}{2}J^2 + \frac{\theta^3}{3!}J^3 + \cdots \tag{4.17}$$

Notice that $S^2 = -1$; therefore

$$J^2 = -(1 + \mu\varepsilon)^2 = -(1 + 2\mu\varepsilon), J^3 = -(1 + 3\mu\varepsilon)S,$$
$$J^4 = 1 + 4\mu\varepsilon, \text{and } J^5 = (1 + 5\mu\varepsilon)S$$

We obtain

$$\begin{aligned} e^{\theta \mathbf{J}} &= \left(1 - \frac{\theta^2}{2} + \frac{\theta^4}{4!} + \cdot\cdot\cdot\right) + \left(\theta - \frac{\theta^3}{3} + \frac{\theta^5}{5!} + \cdots\right)S \\ &-\theta\mu\varepsilon\left(\theta - \frac{\theta^3}{3!} + \cdots\right) + \theta\mu\varepsilon\left(1 - \frac{\theta^2}{2} + \cdots\right)S \\ &= (\cos\theta - d\sin\theta\varepsilon) + (\sin\theta + d\cos\theta\,\varepsilon)S \end{aligned} \tag{4.18}$$

Let $d = \theta\mu$ the slide along the screw axis associated with the angle θ. At this point it is convenient to introduce the dual angle $\hat{\theta} = \theta + d\varepsilon$, so we have the identities

$$\sin\hat{\theta} = \sin\theta + d\cos\theta\,\varepsilon \text{ and } \cos\hat{\theta} = \cos\theta - d\sin\theta\,\varepsilon \tag{4.19}$$

Which are derived using the series expansions of sine and cosine.

Equation (5.12) introduces the unit dual quaternion, which is identified with spatial dis placements. To see the relationship we factor out the rotation term to obtain

$$\widehat{Q} = \cos\hat{\theta} + \sin\hat{\theta}\,S = (1 + \mathbf{t}\varepsilon)(\cos\theta + \sin\theta\,S), \tag{4.20}$$

Where

$$\mathbf{t} = dS + \sin\theta\cos\theta\,\mathbf{C}\times\mathbf{S} = -\sin^2\theta\,(\mathbf{C}\times\mathbf{S})\times\mathbf{S} \tag{4.21}$$

This vector is one half the translation $\mathbf{d} = 2\mathbf{t}$ of the spatial displacement associated with t his dual quaternion in the same way that we saw that the rotation angle is $\emptyset = 2\theta$. This is because the transformation of line coordinates x to X by the rotation $\emptyset$ around an axis S with the translation d involves multiplication by both the Clifford algebra element $\widehat{Q} = \cos\hat{\theta} + \sin\hat{\theta}\,S$ and its conjugate $\widehat{Q}^* = \cos\hat{\theta} - \sin\hat{\theta}\,S$, given by

$$X = \widehat{Q}x\widehat{Q}^* \tag{4.22}$$

For this reason the unit dual quaternion is usually written in terms of the half rotation an gle and half displacement vector,

$$\widehat{Q} = \cos\frac{\widehat{\emptyset}}{2} + \sin\frac{\widehat{\emptyset}}{2}S = \left(1 + \frac{1}{2}\mathbf{d}\varepsilon\right)\left(\cos\frac{\emptyset}{2} + \sin\frac{\emptyset}{2}\mathbf{S}\right), \tag{4.23}$$

Where

$$\mathbf{d} = 2\left(\frac{k}{2}\mathbf{S} + \sin\frac{\emptyset}{2}\cos\frac{\emptyset}{2}\mathbf{C}\times\mathbf{S} - \sin^2\frac{\emptyset}{2}(\mathbf{C}\times\mathbf{S})\times\mathbf{S}\right) \tag{4.24}$$

Here we notice that we introduced the slide along S given by $k = \emptyset\mu$, so we have the du al angle $\widehat{\emptyset} = \emptyset + k\varepsilon$

Clifford Algebra Kinematics Equations

The exponential of a screw defines a relative displacement from an initial position to a fi nal position in terms of a rotation around and slide along an axis. This means that the co mposition of Clifford algebra elements defines the relative kinematics equations for a serial chain.

Consider the nC serial chain in which each joint can rotate through an angle θ_i around, a nd slide the distance d_i along, the axis S_i for $i = 1, \ldots, n$. Let $\vec{\theta}_0$ and $\vec{d}_0$ be the joint param eters of this chain when in the reference configuration, so we have

$$\Delta\vec{\hat{\theta}} = \left(\vec{\theta} + \vec{d}\varepsilon\right) - \left(\vec{\theta}_0 + \vec{d}_0\varepsilon\right) = (\Delta\hat{\theta}_1, \Delta\hat{\theta}_2, \ldots, \Delta\hat{\theta}_n) \tag{4.25}$$

Then, the movement from this reference configuration is defined by the kinematics equatio ns

$$\widehat{D}\left(\Delta\widehat{\vec{\theta}}\right) = e^{\frac{\Delta\theta_1}{2}S_1} e^{\frac{\Delta\theta_1}{2}S_1} \dots e^{\frac{\Delta\theta_1}{2}S_1},$$
$$= \left(c\frac{\Delta\hat{\theta}_1}{2} + s\frac{\Delta\hat{\theta}_1}{2}S_1\right)\left(c\frac{\Delta\hat{\theta}_2}{2} + s\frac{\Delta\hat{\theta}_2}{2}S_2\right)\dots\left(c\frac{\Delta\hat{\theta}_n}{2} + s\frac{\Delta\hat{\theta}_n}{2}S_n\right) \quad (4.26)$$

Here, s and c denote the sine and cosine functions, respectively.

Design Equations for a Serial Chain

The goal of design problem is to determine the dimensions of a spatial serial chain that c an position a tool held by its end effector in a given set of task positions. The location o f the base of the robot, the position of the tool frame, as well as the link dimensions and joint angles are considered to be design variables.

Specified Joint Positions

Identify a set of joint positions $[P_j], j = 1, \dots, m$. Then the physical dimensions of the chai n are defined by the requirement that for each position $[P_j]$ there be a joint parameter vec tor$\hat{\theta}_j$ such that the kinematics equations of the chain satisfy the relations

$$[P_j] = [D(\vec{\theta}_j)], i = 1, \dots, m \quad (4.27)$$

Now choose $[P_1]$as the reference position and compute the relative displacements $[P_j][P_1]^{-1} = [P_{1j}], j = 2, \dots, m$.

For each of these relative displacements $[P_{1j}]$ we can determine the dual unit quaternion $\widehat{P}_{1j} = \cos\frac{\Delta\widehat{\emptyset}_{1j}}{2}P_{1j}, j = 2, \dots, m$. The dual angle $\Delta\widehat{\emptyset}_{1j}$defines the rotation about and slide along the axis P_{1j} that defines the displacement from the first to the *j*th position. Now writing equation (5.17) for the m-1 relative displacements, we obtain

$$\widehat{P}_{1j} = e^{\frac{\Delta\hat{\theta}_{1j}}{2}S_1} e^{\frac{\Delta\hat{\theta}_{2j}}{2}S_2} \dots e^{\frac{\Delta\hat{\theta}_{nj}}{2}S_n}, j = 2, \dots, m \quad (4.28)$$

The result is 8(m-1) design equations. The unknowns are the n joint axes $S_i i = 1, \dots, n$ an d the $n(m-1)$ pairs of joint parameters $\Delta\hat{\theta}_{ij} = \Delta\hat{\theta}_{ij} + \Delta d_{ij}\,\varepsilon$.

T Joint

Consider the RR chain formed by axes S_i and S_{i+1}. suppose these axes to intersect in a r ight angle, and denote by a T. this geometric constraint is defined by the dual vector equ ation

$$\mathrm{T}: \mathrm{S_i} \cdot \mathrm{S_{i+1}} = 0 \tag{4.29}$$

Which expands to define the two constraints.

$$\mathrm{T}: \mathbf{S}_\mathrm{i} \cdot \mathbf{S}_\mathrm{i+1} = 0 \text{ and } \mathbf{S}_\mathrm{i} \cdot \mathbf{S}^\mathrm{o}_\mathrm{i+1} + \mathbf{S}^\mathrm{o}_\mathrm{i} \cdot \mathbf{S}_\mathrm{i+1} = 0 \tag{4.30}$$

The design equations for the RRR chain for instance are easily transformed into design eq uations for th TR chain by including these two constraint equations with the appropriate i ndices.

The S Joint

In the same way, a sequence of three revolute joints and RRR chain, can be constrained such that they intersect in a point, and the pairs in sequence are perpendicular. This is a common construction for an active spherical joint, denoted by S, which allows full orientat ion freedom around the intersection point. However, for synthesis applications it can be sh own that any three axes create the same spherical joint.

Label three axes $\mathrm{S_i}, \mathrm{S_{i+1}}$ and $\mathrm{S_{i+2}}$. Then the equations that define this joint consist of th e dual vector constraints

$$\mathrm{S}: \mathrm{S_i} \cdot \mathrm{S_{i+1}} = 0,\ \ \mathrm{S_i} \cdot \mathrm{S_{i+2}} = 0 \quad \text{and} \quad \mathrm{S_{i+1}} \cdot \mathrm{S_{i+2}} = 0 \tag{4.31}$$

If we write the spherical joint as the dual quaternion product of these individual axes,

$$\hat{\mathrm{S}}(\theta_1, \theta_2, \theta_3) = \hat{\mathrm{S}}_1(\theta_1)\hat{\mathrm{S}}_2(\theta_2)\hat{\mathrm{S}}_3(\theta_3) \tag{4.32}$$

When expanded, we obtain

$$\hat{\mathrm{S}}(\theta_1, \theta_2, \theta_3) = \alpha_4 + \alpha_1 \mathrm{S}_1 + \alpha_2 \mathrm{S}_2 + \alpha_3 \mathrm{S}_3 \tag{4.33}$$

Where each α_i appears as combinations of the joint variables,

$$\begin{aligned}
\alpha_1 &= \sin\frac{\theta_1}{2}\cos\frac{\theta_2}{2}\cos\frac{\theta_3}{2} + \cos\frac{\theta_1}{2}\sin\frac{\theta_2}{2}\sin\frac{\theta_3}{2} \\
\alpha_2 &= \cos\frac{\theta_1}{2}\sin\frac{\theta_2}{2}\cos\frac{\theta_3}{2} - \sin\frac{\theta_1}{2}\cos\frac{\theta_2}{2}\sin\frac{\theta_3}{2} \\
\alpha_3 &= \sin\frac{\theta_1}{2}\sin\frac{\theta_2}{2}\cos\frac{\theta_3}{2} + \cos\frac{\theta_1}{2}\cos\frac{\theta_2}{2}\sin\frac{\theta_3}{2} \\
\alpha_4 &= \cos\frac{\theta_1}{2}\cos\frac{\theta_2}{2}\cos\frac{\theta_3}{2} + \sin\frac{\theta_1}{2}\sin\frac{\theta_2}{2}\sin\frac{\theta_3}{2}
\end{aligned} \tag{4.34}$$

Now we show any directions $\mathbf{S_1}, \mathbf{S_2}, \mathbf{S_3}$ can be used to define the spherical joint. Equate (5. 23) to a goal displacement $\hat{P} = (p_w + \varepsilon p_w^o) + (\mathbf{P} + \varepsilon \mathbf{P}^\mathrm{o})$,

$$\hat{\mathrm{S}}(\theta_1, \theta_2, \theta_3) = \hat{P} \tag{4.35}$$

And solve linearly for the combinations of joint variables in the α_i factors using the real part of the dual quaternion equation,

$$\begin{bmatrix} \mathbf{S}_1 \mathbf{S}_2 \mathbf{S}_3 \vec{0} \\ 0 \;\; 0 \;\; 0 \;\; 0 \end{bmatrix} \begin{Bmatrix} \alpha_1 \\ \alpha_2 \\ \alpha_3 \\ \alpha_4 \end{Bmatrix} = \begin{Bmatrix} \mathbf{P} \\ p_w \end{Bmatrix} \tag{4.36}$$

Where we write the scalar term as the fourth row. The values obtained for the joint angle s,

$$\alpha_1 = \mathbf{S_1} \cdot \mathbf{P}, \qquad \alpha_2 = \mathbf{S_2} \cdot \mathbf{P}, \quad \alpha_3 = \mathbf{S_3} \cdot \mathbf{P}, \qquad \alpha_4 = p_w \tag{4.37}$$

Are related by the following expression,

4.6 Concluding Remarks

This chapter introduced serial kinematic chain model to be able to evaluate the shape of the colonoscopy. Classical transformation matrix was substituted by the Clifford Algebra. Clifford Algebra gave us the method to consolidate rotation and translation in consistent framework.

In section 4.2, coordinate system for describing shape in space was introduced and exp lained in detail. Section 4.3 deals with classical point of view in handling kinematic chain model. Section 4.4 shows well that Serial Kinematic chain model can also expressed in t erms of Clifford Algebra. This method is more compact and can maintain consistency with quaternion interpolation.

Section 4.5 is for the Spherical Joint, which we are concerned with deeply related to the joint-link model of colonoscopy. With this development, the shape of colonoscopy is finall y expressed by the kinematics equation.

III. Evidences, Discussions & Conclusions

Chapter 5

Experiments & Results

In this chapter, we will show experimental devices, experimental procedures and results on the theories developed until now. Main points to show is the fact that precedin g theories are valid. We will try to prove it through several evidences including graphics, pictures and tables.

Section 5.1 and 5.2 is for the hardware related evidences. As I started this resea rch with some underdeveloped devices, I will show that signal processing techniques that are needed can produce orientation in the sensor network. Section 5.3, 5.4 and Section 5.5 are concerned with simulation tests for validating theories which were introduced. Integrat ed results are shown from Section 5.6 to Section 5.7.

5.1 Check of the Quasi-state condition

Purpose of experiment

In this section, test was carried out for checking stability of accelerometer signals by exter nal acceleration. Normally, accelerometer signals are processed to evaluate the pitch and ro ll angle based on the gravity components on the body framework. So other components ex cept gravity should not be included in the signals.

Test procedure

In order to check the stability from effect of external acceleration, accelerometer signal wa s measured while moving. WB-3 Sensor accelerometer was used for checking external acc eleration. Moving velocity was 50mm/sec.

Result and Discussion

Gravity line is displayed as can be seen in the following figure. We can see how big the effect of external acceleration.

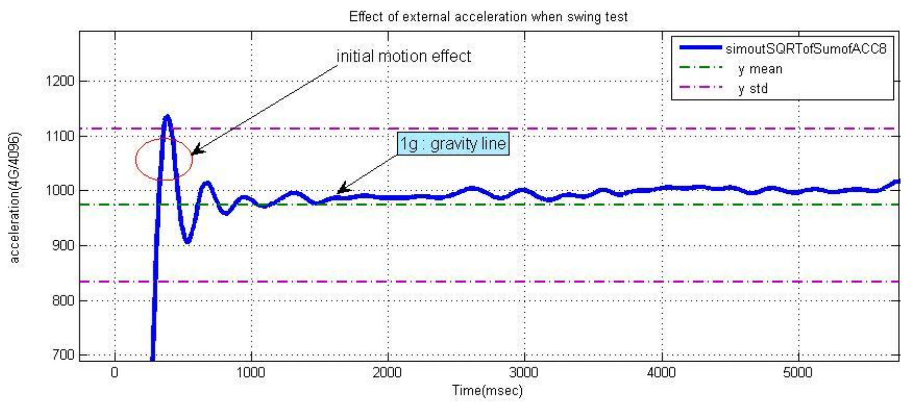

Figure 5.1 Effect of the external acceleration: this experiment was carried out to confirm whether the external acceleration is plausible to make measurement contamination. As can be seen in the figure, effect of motion is rapidly disappeared as time passes.

We think that external acceleration is not big compared to gravity in this range of velocit y. As we assumed quasi-static movement for evaluating roll and pitch angle by using acce lerometer, confirmation on the stability is meaningful.

5.2 Noise reduction and Improvements by filtering

Purpose of experiment

Motion is low speed, meanwhile accelerometer signals have the wave form which incurs from low and high frequency. So low pass filter was needed to reduce the noise as a pre step of the calculation of orientation from the signals.

Experiment Procedure

Digital Butterworth filter was designed. We carried out design with the function library in the Matlab. The filter designed is infinite impulse response (IIR) digital filter. it has 9^{th} order polynomial transfer function. Cutoff frequency and Nyquist frequeny is 70mHz and 150mHz each. We compared noisy measurement values and its counterpart: filtered signals on figure 5.2.

Noise reduction by low-pass filtering

The test on the accelerometer was good. The high frequency part was clearly removed as can be seen in figure 5.2.

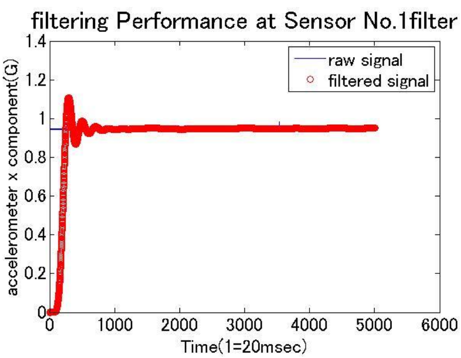

(1) Sensor No.1

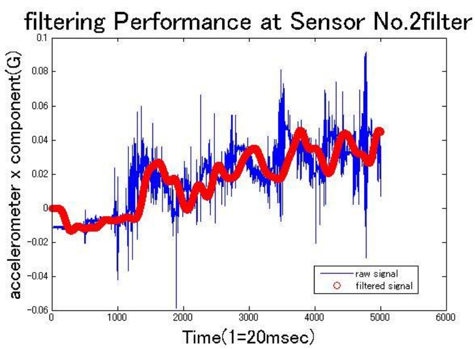

(2) Sensor No.2

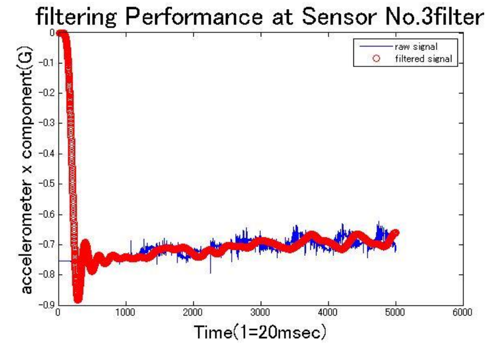

(3) Sensor No.3

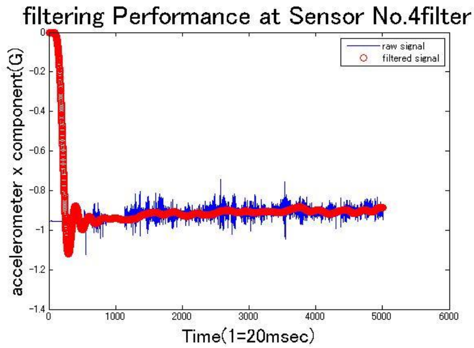

(4) Sensor No.4

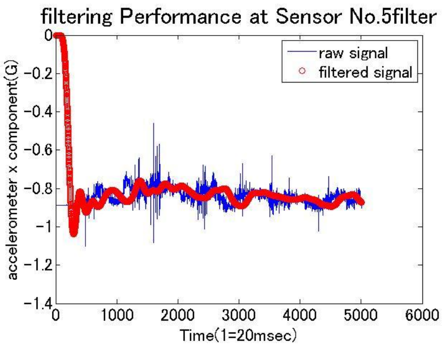

(5) Sensor No.5

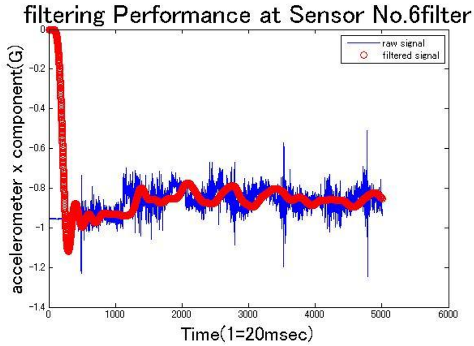

(6) Sensor No.6

Figure 5.2 Filtering Performance of *x* component of Accelerometer Signals: 9^{th} Butterworth IIR digital Filter was used. Cut off Freq. = 0.002Hz

Order of filter function = 9

With this design, we applied it to the signal and evaluated the Euler angles from the filt ered signal.

In Figure 5.3, each picture from top to down is calculated posture of the sensor body, which is changed with regard to the time-varying motion. If we consider at certain sample, we can extract 6sets of roll, pitch and yaw angles. This constitutes the shape of colonosc ope at that instant.

Improvements Effects by Kalman filtering

Purpose of Experiment

We think that 5 degrees of inaccuracy always exist on the evaluated Euler angles as the noise and instability of sensor itself might affect final result.

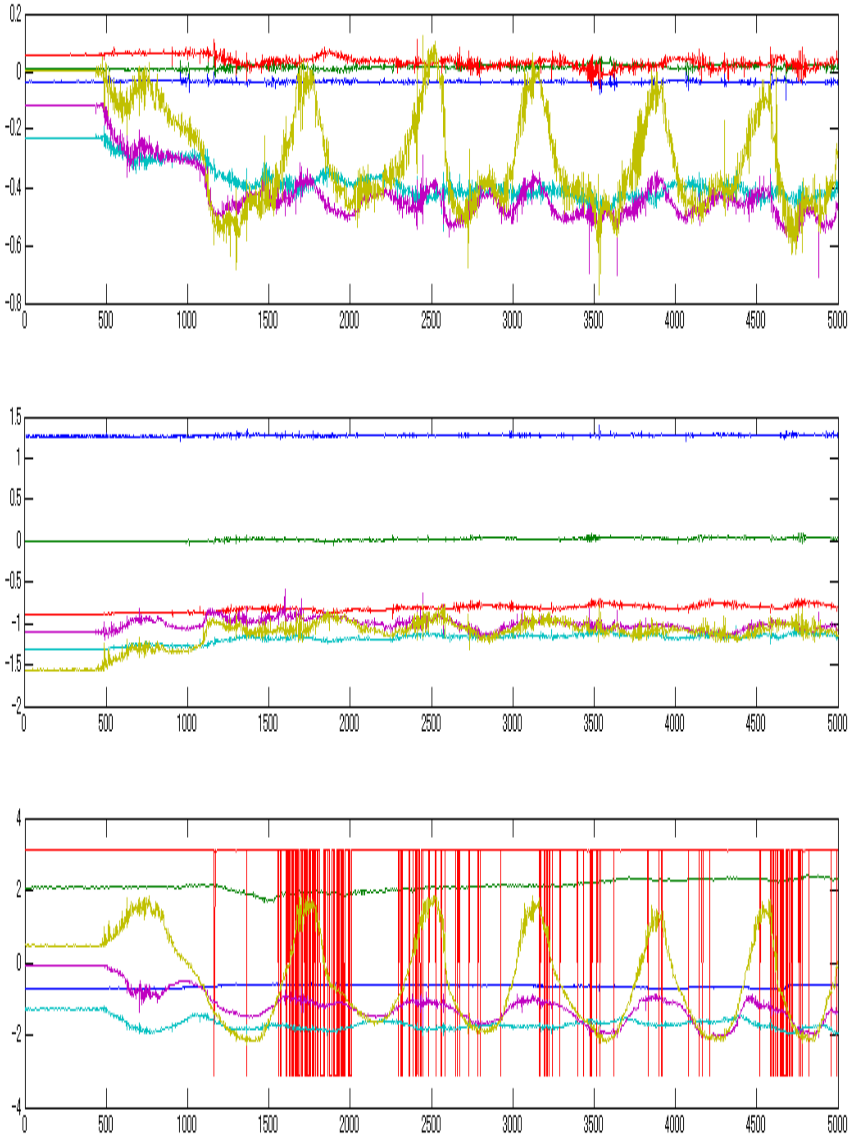

Figure 5.3(a) Roll Pitch and Yaw angle estimation with without filtering

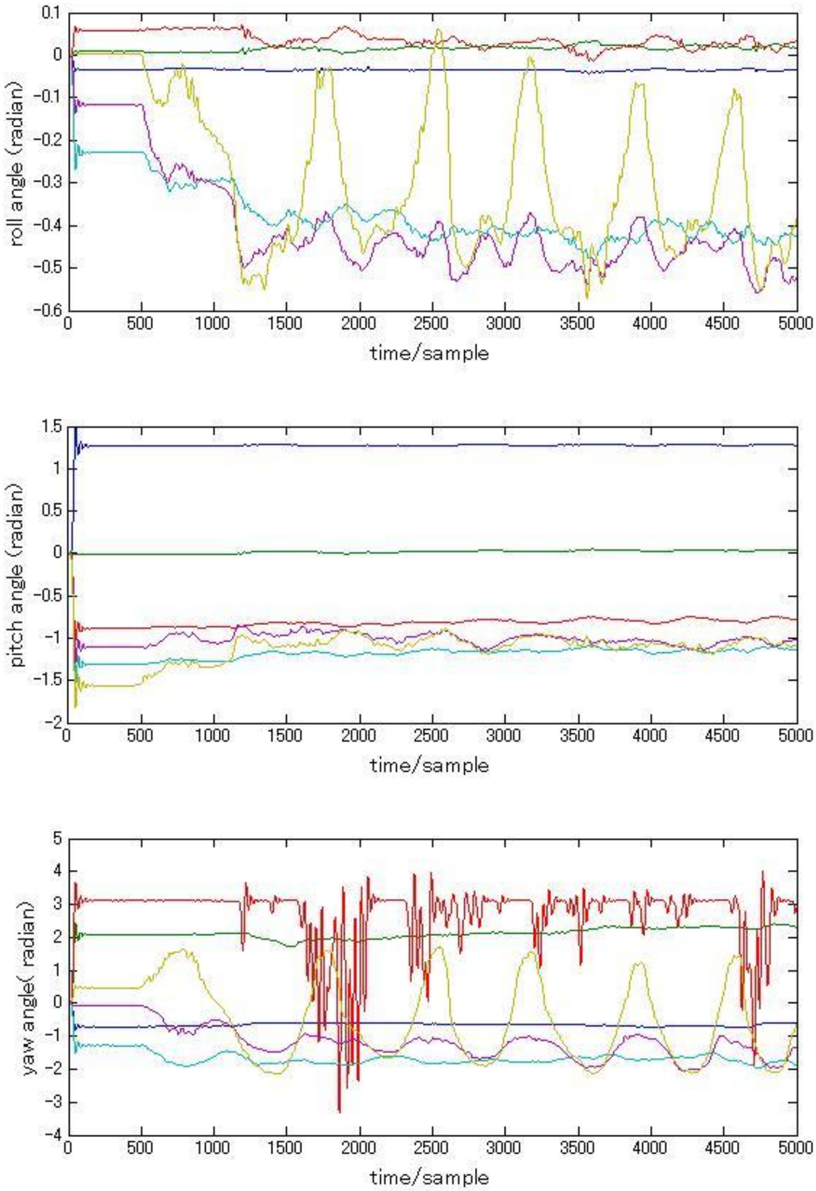

Figure 5.3(b) Roll Pitch and Yaw angle estimation with noise filtering

Figure 5.3(a) is the Euler angle with time evaluated by using raw data and figure 5.3(b) is the result evaluated by the filtered signal.

Experimental Procedure

Extended Kalman filter was used. This program was coded by Matlab and was developed by the Bioinstrumentation group of Takanishi Lab. Input to function is Euler angles and results are filtered Euler angles.

Results and Discussion

Based on the signal, Euler angles were calculated. In this procedure, the filtered signal was used in previous stage. Figure 5.2 shows the calculated Euler angles. 6sets of sensors were arranged along the tube which was prepared as a substitute of colonoscopy sheath. Orientation information was extracted from the sensor network. Then experiment for checking accuracy of methods was made and finally, the visualization result was suggested.

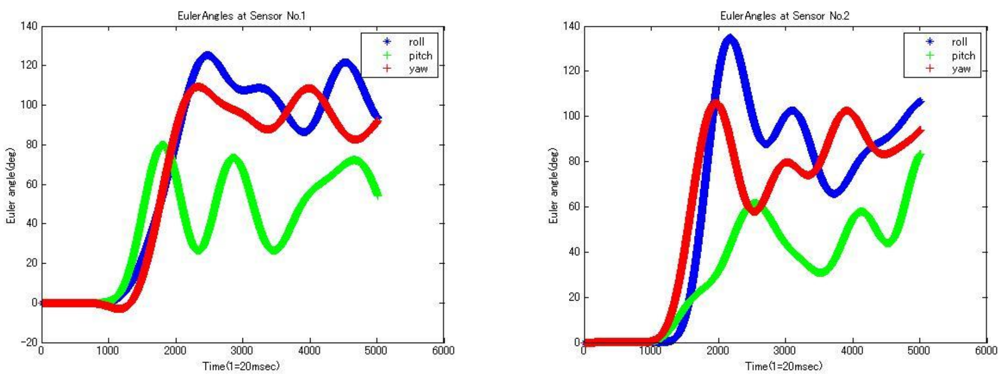

(a) Sensor No.1 (b) Sensor No.2

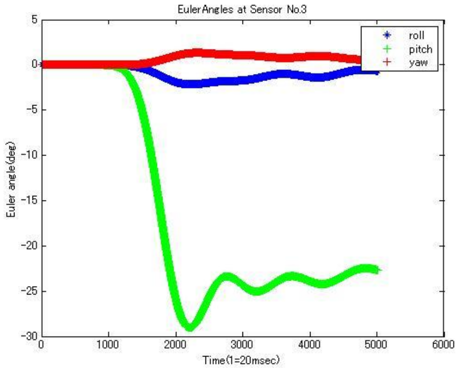

(c) Sensor No.3

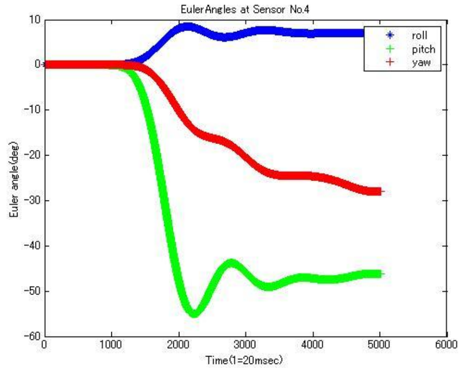

(d) Sensor No.4

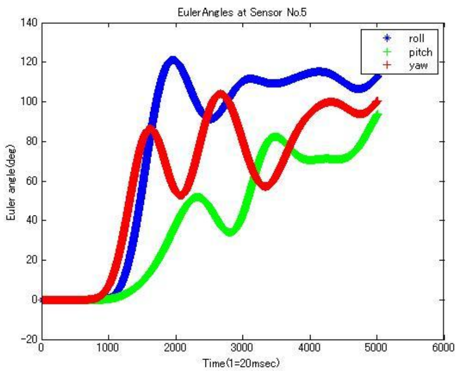

(e) Sensor No.5

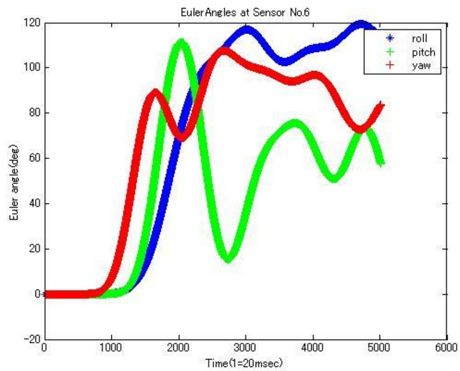

(f) Sensor No.6

Figure 5.4 Euler Angle (roll pitch yaw) change with time and sensor No. after Extended Kalman filter implementation

The Kalman filtering technique was implemented on calculation of orientation. In figure 5. 4, motion is well represented on each sensor. At the initial stage, filtered results are in th e zero state. This means that the initial value of the Gyroscope angle starts with zero. As time passes, the signals are recovered rapidly. Until 2000 sample times (here, 1 sampling time is 20msec), signals are recovered by the complementary signal from accelerometers and magnetometers. As can be known from the figure, the drift of gyro along the time do es not happen as the complementary function of Kalman filter updates current state recursi vely based on the measurement.

5.3 Orientation Interpolation

In this section, orientation interpolation is tested with computer simulation. Computer simul ation program was implemented in Matlab. We implement 2 different algorithms; one is S pherical Linear Interpolation other is Bezier interpolation. Final objective of orientation inte rpolation is to obtain the curve which has natural and similar properties to the curve in th e nature.

Simulation Test for SLERP (Spherical Linear Interpolation)

Purpose of Simulation

We check whether the performance of SLERP algorithm is good to us. Although this met hod uses simplest curve as interpolating curve, it can give us simplicity and high speed c omputation.

Test Procedure

We wrote SLERP code with Matlab for test. This is simply small code. Key point angles were given in manual format as arguments. Interpolation parameter is changed within ran ge 0 and 1. Euler angles were changed to quaternion values and on the 4D hyper sphere, it was interpolated.

Results and Discussion

In figure 5.5, the first and last points are key points and the other points are interpolated points. Although the spherical linear interpolation is effective in computation time, it appr oximates the curve by linearized line segments. In our case, the approximation error does not make big trouble. This algorithm also has limitation on its precision: curve used in int erpolation is first order polynomial, say, line. It does not guarantee continuity and smoothn ess, which makes curve be more natural.

Table 5.1 condition of simulation test

Start orientation	Final orientation
-18 degree	70degree

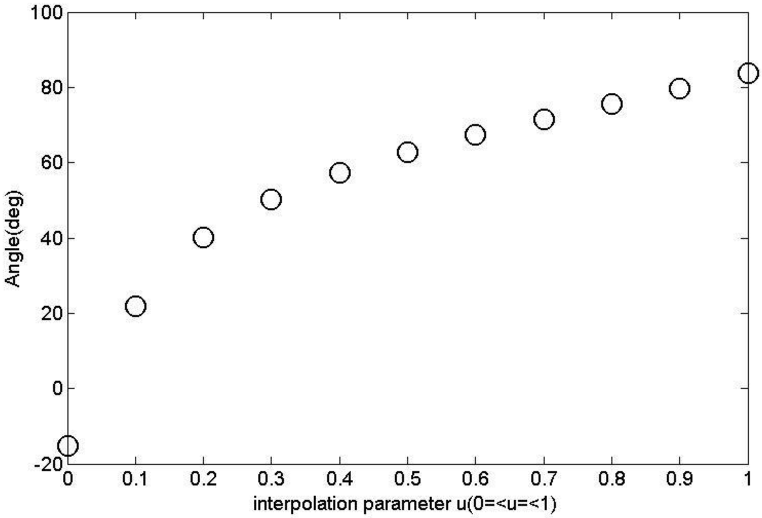

Figure 5.5 Result of rotation interpolation. We can see from the figure that the distance b etween points are not uniform in Arclength. In this figure, red lines mean interpolated cur ve. As can be seen, this method uses line as interpolating curve. Continuity and smoothne ss are not guaranteed as continuity and smoothness are generally defined by the first order and second order derivative.

Simulation Test for Bezier Curve interpolation

Bezier curve is widely used as good interpolating curve. We try to implement this one as interpolating curve.

Purpose of Test

There are several methods to guarantee smoothness and continuity. We implement the Bezi er curve to make curve more natural to the original curve that colonoscopy have.

Test procedure

5 points were suggested and tried to interpolate between them using Bezier Curve interpol ation method. Bezier curve confirm continuity and smoothness.

Table 5.2 Key-Points on the interpolating Curve

Points on the sphere
Q1=1+0i+0j+0k+e(0+0.5i+0j+0.5k)

Q2=1+0i+0j+0k+e(0+3i-1j+1k)
Q3=1+0i+0j+0k+e(0+3i+1j+1k)
Q4=1+0i+0j+0k+e(0+4i+1j+1k)
Q5=1+0i+0j+0k+e(0+5i+1j+4k)

Results and Discussion

As can be seen in figure 5.6, the curve interpolates between points with high order natura lness. Naturalness comes from continuity and smoothness. If we apply curve which has 1^{st} order derivative and 2^{nd} order derivative in 4D hyper sphere as interpolating curve, we c an get naturalness from the resulting curve.

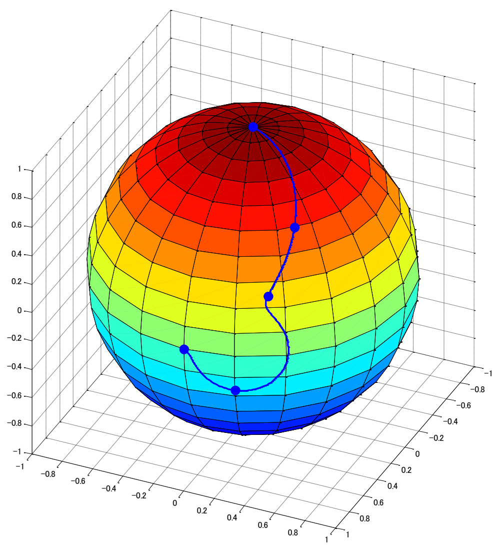

Figure 5.6 orientation interpolations on the unit quaternion sphere. Unit quaternion sphere is 4-dimensional hyperspace. Blue points are key points, say, break points which will be i nterpolated. Unit is dimensionless and ranges are between 0 and 1.

As can be seen in the figure, the curve shows its smoothness without cusps in its shape. Naturalness is important subject in the curve interpolation field.

5.4 Arclength Reparametrization

We demonstrate how to calculate Arclength Reparametrization by showing simple numerica l calculation

Simple Numerical Example

(a) From parameter value to Arclength

With this table finished, we can determine arc length at arbitrary points on the curve. Sup pose we want to know the distance (arc length) from the beginning of the curve (u = 0.0 0) to the point (u = 0.73).

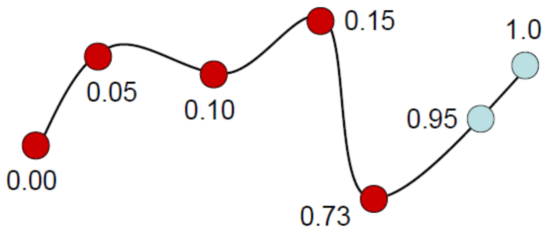

Figure 5.7 Numerical examples on how to use this table.

Then we can calculate arc length by the following simple calculation as given by equatio n (5.1) and (5.2).

$$\mathrm{i} = (\mathrm{int})\left(\frac{\text{given parameter value}}{\text{distance between entries}}\right) = (\mathrm{int})\left(\frac{0.73}{0.05}\right) = 14 \tag{5.1}$$

$$\begin{aligned} \mathrm{L} &= \mathrm{ArcLength[i]} \\ &+ \frac{(\text{Given Value} - \mathrm{Value[i]})}{(\mathrm{Value[i+1]} - \mathrm{Value[i]})}(\mathrm{ArcLength[i+1]} \\ &\qquad - \mathrm{ArcLength[i]}) \\ &= 0.944 + \frac{0.73 - 0.70}{0.75 - 0.70}(0.959 - 0.944) \\ &= 0.953 \end{aligned} \tag{5.2}$$

(b) From Arclength to parameter value

Inversely, suppose we want to know the value of u given the arc length; for example, wh en L = 0.75, we want to know the value of u. in the figure 5.8, red circle is the point which we want to know. In table 5.3, the intermediate value for calculation is shown. In this case, calculation is as follows.

$$0.75 = 0.72 + t(0.8 - 0.72)$$
$$t = \frac{0.75 - 0.72}{0.8 - 0.72} = \frac{0.03}{0.08} = 0.375 \qquad (5.3)$$
$$u = 0.4 + t(0.45 - 0.4)$$
$$u = 0.4 + 0.375(0.45 - 0.4) = 0.41875$$

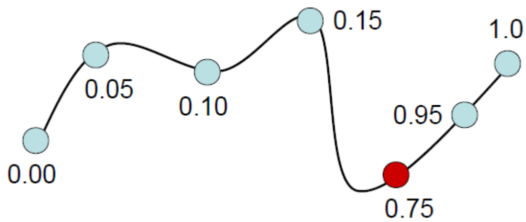

Figure 5.8 Inverse calculation from Arc length to parameter value

Curve orientation interpolated and Arclength reparameterized by Table

Purpose of test

We show that interpolated points should be equally distanced for our kinematics purpose.

Test procedure

We use circle as a reference curve. Circle is easy to think about. First of all, we use circle curve parameterized by one variable. Then we change variable between 0 and 1 and interpolate it. Next we reevaluate the interpolated points through the process of Arclength Reparametrization.

Results and Discussion

In this figure, circle is shown. The points represented by red markers represent interpolated with equal parameter values. Even if parameter was changed with equal distance, resulting orientation curve shows uneven distance between points.

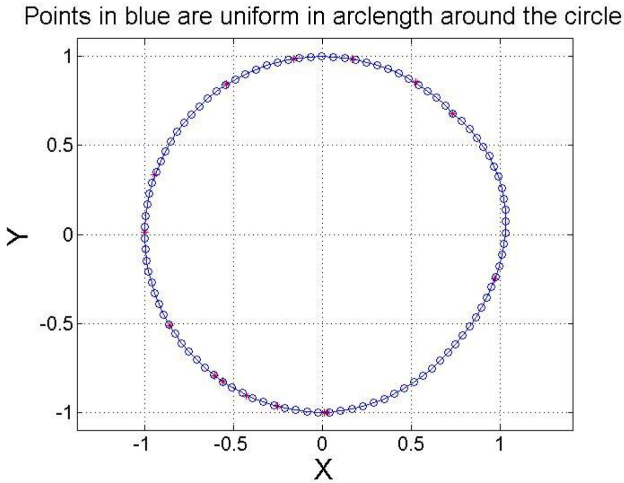

Figure 5.9 Simulation test for validating table lookup method

But in case of blue points which was reparameterized by Arclength, it shows even arrange ment along the circle.

5.5 Serial Kinematic Chain

Simple Numerical Example

Applying a rotation of point (3,4,5) by 180° around the x axis is given by:

P2 = (0 + i)*(1 + 3iε + 4jε + 5 kε)*(0 - i)

P2 = (i - 3ε -5jε + 4kε)*(0 - i)

P2 = 1 + 3iε - 4jε - 5 kε

Combined Displacement and Rotation (displace then rotation)

Starting from the previous position: (1 + 3iε + 4jε + 5 kε) and both displace by (x=4, y =2, z=6) and applying a rotation of 180° around the x axis represented by: (0 + i) Theref ore:

Q = (0 + i) (1 + 2 iε + 1 jε + 3 kε)

Q = (i -2ε -3 jε + 1 kε)

So applying the transform gives:

P2 = (i - 2ε -3 jε + 1 kε)*(1 + 3iε + 4jε + 5 kε)*(-i + 2ε -3 jε + 1 kε)

P2 = (i - 5iε - 8jε + 5 kε)*(-i + 2ε -3 jε + 1 kε)

$P2 = 1 + 7i\varepsilon - 6j\varepsilon - 11k\varepsilon$

Figure 5.10 shows that point is moved by rotation and translation.

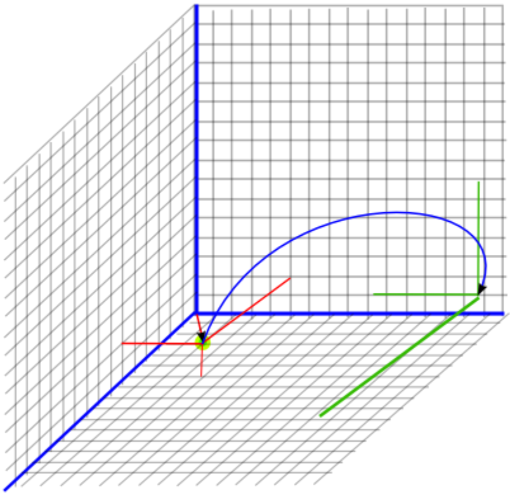

Figure 5.10 Numerical Calculation for validating dual quaternion based kinematics

5.5.1 Estimation Experiment with Sensor Network

Until now, focus was on the orientation extraction. Hereafter, shape of the colonoscopy is estimated and experiments on the shape are carried out.

Experimental Procedure

Figure 5.11 is the setup of experimental device. Grasping with hands on the fixed frame, tube was oscillated slowly about 6 times. The plane of swing was along the horizontal

6 sets of sensor unit were installed on the test body. 18 channels of accelerometer signals and another 18 channels of magnetometer signals were processed with digital filter to obtain the resulting orientation of each sensor bodies based on the fixed frame as in Figure 5.11.

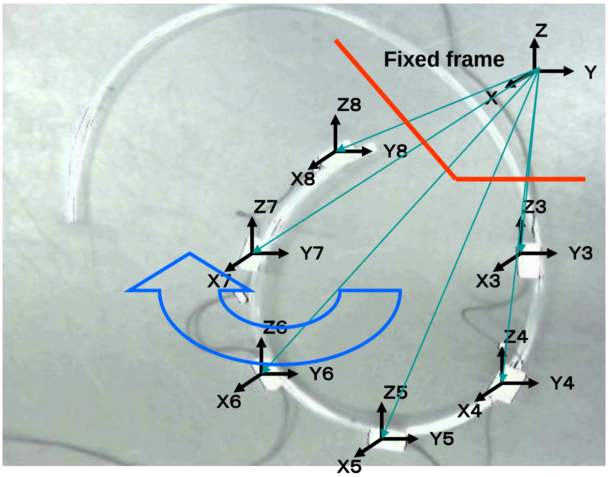

Figure 5.11 Experimental system of sensor network. This sensor network has 6 sets of IM U sensors on it. Every sensor is carefully arranged on the tube with the uniform distance between sensors along the curve.

Sensor trajectory along the time

Sensors on the colonoscope are moved as time passes. So the trajectory of each sensor also gives meaningful viewpoints in finding the right shape of entire shape. Sensors on the colonoscope will move around arc if we move colonoscope with arc trajectory.

In figure 5.12, trajectories on two sensors are displayed. No.7 sensor are far from the center of rotation compared to the No.2 sensor. Thus the arc radius is bigger than that of No.2 sensor.

In figure 5.12, the shapes of the colonoscope are shown along the time change. This is the results of estimation based on the sensor data of figure 5.5.

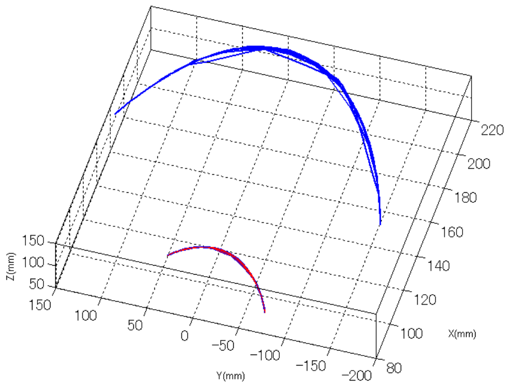

Figure 5.12 Trajectory of sensors ; No.2 and No. 7 are followed

As can be shown in the figure 5.12, the flexible shape change is also shown. This means that colonoscope is bended from hand to end point of colonoscope. This matches with intuition of bending flexible materials.

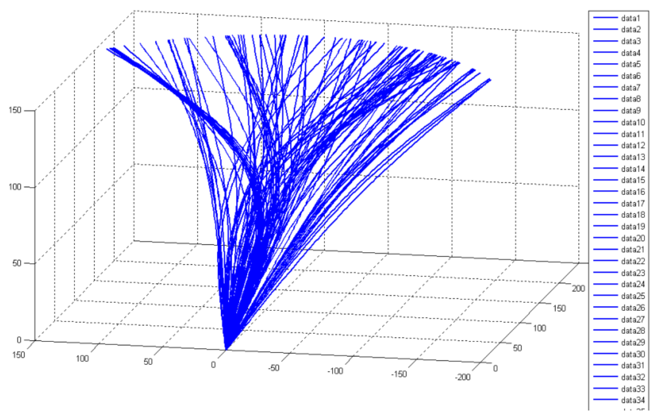

Figure 5.13 Trajectory of the sensor network along the time step.

In figure 5.13, sensors are attached on the body of flexible tube. Tube dia. 9mm, length 1 20mm. Sensors has its own clad with the white plastic boxes. Each is connected through t he CAN communication bus finally to PC. The signals are processed by PC

5.5.2 Calibration for Shape

Calibration is important in estimating shape of colonoscopy. It is because this method uses relative estimation. Thus good standard reference is prerequisite on the precise measurement. There are many devices which can play a role as a standard of shape estimation. Vicon® and Optotrack® are the usually used device for this purpose. We use Optotrack® system for measuring the initial shape of the colonoscopy.

Procedure of Experiment

In this experiment, Optotrack® System was used as a reference gauge. Optotrack® has the following specification. Markers were attached on the frontal surface of the sensor unit.

The system finds markers rotation and positions with infrared camera. Its accuracy is under 0.1 mm. In figure 5.6, the experimental device is shown. The initial posture or shape should be measured precisely.

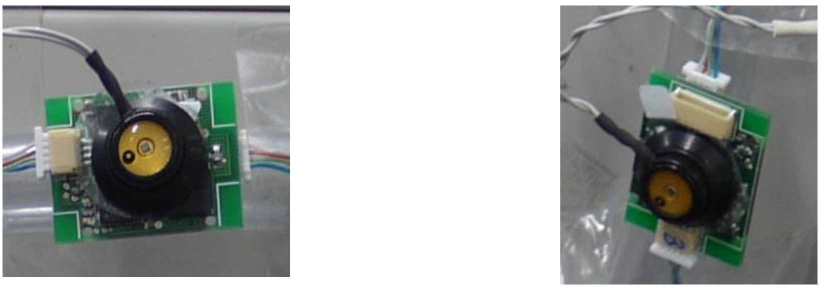

Figure 5.14 Markers on the WB sensor units

In this method, shape is estimated relative to the initial shape. As the sensor is embodied in the tube of colonoscopy, precise shape and angle at the initial state should be checked in order to predict consecutive shape recursively. Based on this shape measurement, next step of shape is estimated with the orientation angles that are calculated from the sensor signals.

In figure 5.16, simulation, estimation from measurement and real shape are compared. As can be seen from the figure, simulation and measurement results predict its real shape.

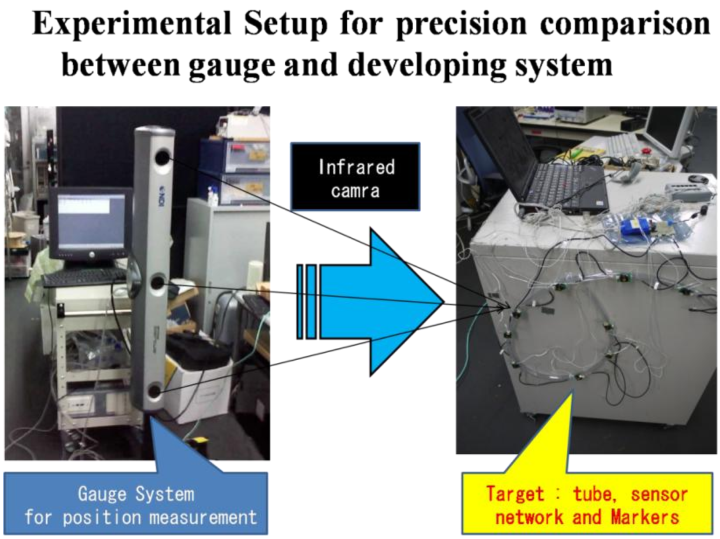

(a) Gauge System (b) Target ; markers are shown

Figure 5.15 Experimental Setup for precision comparison between gauge and developing system. Here as a gauge, Optotrack system was used

5.6 Accuracy problem

Accuracy test is checked with two viewpoints. Firstly, simulation test is made by comparing true sine curve with the estimated sine curve by this method. Secondly, the effect of number of sensor on the network on the shape accuracy is investigated.

Accuracy Test Procedure

Accuracy test compose of two phase. One is by the comparison between sine curve and estimated curve with the method proposed in the paper. The other is by the looking for the effect of the number of sensors in the net.

(1) Self accuracy test

Sine curve was used to check the self accuracy of the method. The link segment was fixed at 1.37 which came from 1/6 of total length of sine curve. The averaged value of both end of line segment was used as the orientation of the line segment. Then using this information, the simulation using suggested algorithm was made. In the simulation, sensors are assumed to be on the ground plane.

The points on which sensors are assumed to be were calculated along the sine curve.

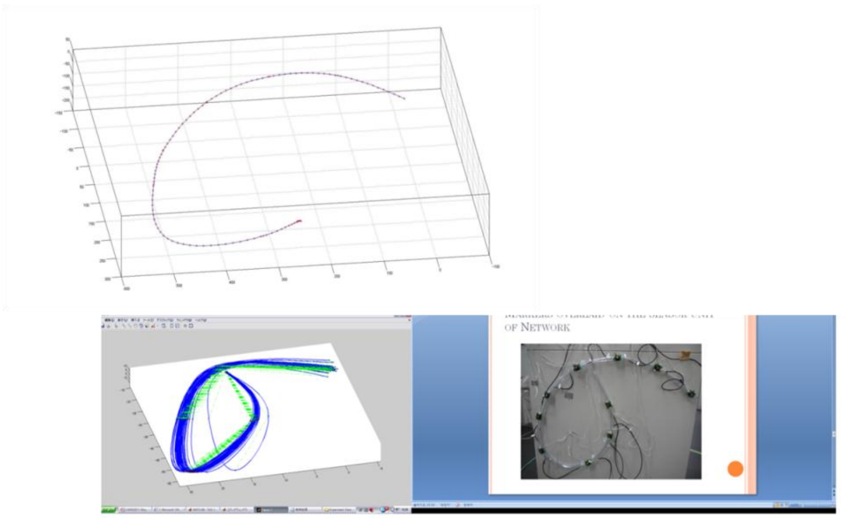

Figure 5.16 Comparison between simulation result, Optotrack estimation result and real shape

(2) Effect of number of sensor to the accuracy.

In order to look for relation between the accuracy and the number of sensor in the network, we used circle as a standard shape because circle curve is the standard geometry with curvature which can be measured easily.

Like in figure, the components are arranged on the body of tube such that the pitch angle direction is along the centreline of the tube. All components are connected by CAN bus, finally to the PC for data acquisition.

The percentage ratio of (1 - measured data / its simulated data) was used as metric of error. Test was made, decreasing the number of sensors to 6, 5 and 4 sets in the network. Then, percentage of measured data on the basis of simulated data was calculated.

Visualization Test procedure

The time trace of shape of the colonoscope was calculated while acquiring data from the sensor network. Calculation time was about 150ms per frame with Pentium 4 dual core I ntel processor

In this test, entire data was acquired with offline for validation of method. The data acq uisition from the sensor network, evaluation of orientation from the sensor signal with digi tal filtering and panoramic view for visualization was processed separately at the present r esearch.

5.7 Discussions on Accuracy problem

Accuracy comparison between True and simulated Curves

Figure 5.17 shows the comparison between the true curve and the simulated curve. The angle of pitch in the 3 kind of orientation angles was used for demonstration.

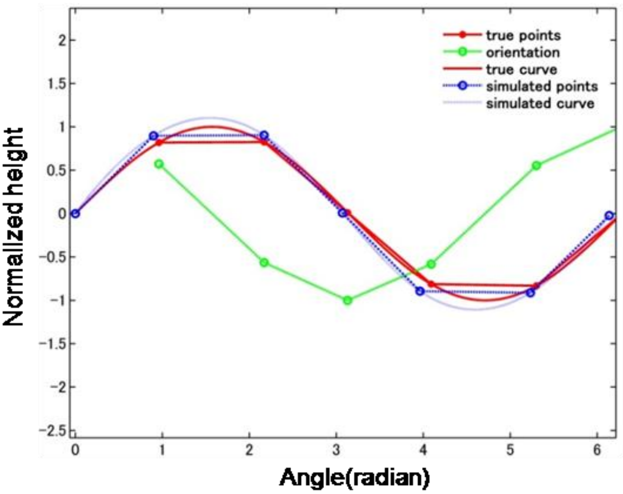

Figure 5.17 Precision test by comparison of simulated points and true points on the sine curve

Figure 5.17 shows the comparison between the true curve and the evaluated curve. Blue li nes are true sine curve and points. Red-solid line and Red-dashed line are ground truth an d blue-solid line and blue-dashed line are evaluated curve. One unit of abscissa and ordina te axes were normalized as one distance between neighboring sensors.

The angle of simulated one is slightly different compared to the ground truth. The disc repancy of position of each data points comes from angle difference between ground truth and simulated one. We have regarded the link as rigid body. So the orientation is assum ed not to be changed in one link segment. In these experiments, we used averaged value as true orientation value. The green line represents the orientation of link segment in the ground truth.

Accuracy Change according to the Number of Sensors

In figure 5.18, simulated results are compared with measured ones. As number of sensor in the network is reduced, the percentage error of (1- S/M) is also increased.

As we can guess generally, figure 5.18 shows that the error of length of linkage is reduced as the number of sensor in the network is decreased. This means that accuracy depends on the number of sensor in the network. So we can predict from the result that the number of sensors in the network should be increased to obtain more precise result. In order to reduce the error from the estimation within 1%, figure 5.18 reveals that one sensor per 13cm should be at least used, which means distance can be allowed up to about 10 times of its diameter 9m

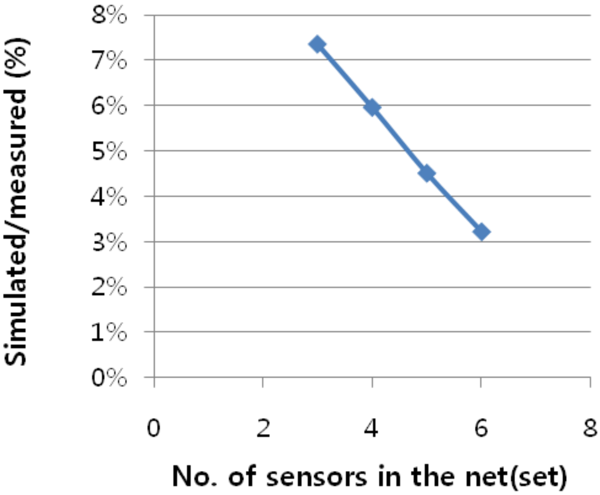

Figure 5.18 the effect of number of sensors in the network on the performance; as can be known from the figure, accuracy is degenerated as the number of sensors are decreased.

5.8 Panoramic display for physician assistance

The trajectory of the curve is evaluated with time step. In Fig.19, the green circles display the key points which were estimated by the measured sensor data. There are some noisy movements on the boundary of shape. Blue trajectories are data and green trajectories are wrong trajectory contaminated by the noises which are shown in figure 5.19

This indicates rejection of noise by low pass filter at the stages of extracting orientation is not enough and this method also needs more accurate rejection of wrong trajectories which might be caused from the limited number of sensors in the network.

Figure 5.19 shows the trajectory of colonoscope with time. Blue circle and red circle displays the sensor locations with time. Noises in the estimation seems be included – little bit of irregular location of sensors shows error in which noises results.

5.9 Accuracy Verification with real world data

Until here, verification for accuracy was performed by using computer simulation. But c omputer simulation limits its availability to the real world application. In order to confirm real world application, additional experiments using real world sensing system are needed. In this section, verification method for accuracy is explained and implemented using calib ration target.

Two kinds of elements are needed for making effective accuracy verification process. O ne is for verification method; it consists of similarity metric that can compare object quant itatively with ground truth gauge. Specially created concept which is made for comparing similarity between curves is used: Frechet distance and Hausdorf distance. These two conc epts are adequate to measuring similarity between curves.

With these concepts, comparison between ground truth curve and curve which was const ructed using data from sensor network is performed. In order to fix the distortion trouble of reconstructed curve from sensor data, SQUAD (spherical quadratic interpolation) algorith m was newly implemented. SQUAD has characteristics which can increase the smoothness of curve when piece wisely separated curve segments are used to reconstruct original sha pe of the curve. It guarantees C1- continuity on the curve since first derivatives on the co nnected points between curve segments make entire curve be smooth in mathematical C1- continuity framework.

At the stage of analysis, quantitative values are suggested using Hausdorf distance metri c. Frechet distance metric was also implemented but its performance would not be good w ith big data group. With small data points less than 1000, these two metrics displayed al most the same values.

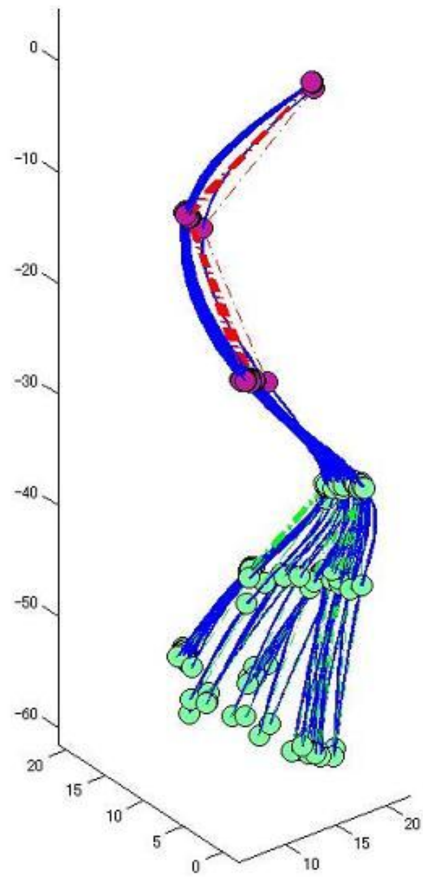

Figure 5.19 visualization of the shape of the colonoscope x,y and z are units of cm each.

5.10 Hausdorf distance

As 3 dimensional curve is treated, specially designed metric for comparisons needed. By [ ], Hausdorf distance can be defined;

Given two bounded sets A and B in Euclidean space E^m, the following can be defined:

$$d_B(A) = \sup_{a \in A} d(a, B) \qquad (5.4)$$

Where the distance from point a to set B is given by

$$d(a, B) = \inf_{b \in B} d(a, b) \qquad (5.5)$$

The point distance d(a,b) may be any distance in E^m, such as for example an ℓ_p distance.

(5.5) is referred as the *min B calculation*. In general,$d_B(A) \neq d_A(B)$. Letting $Ball_b(\epsilon)$ denote the closed ball of radius ϵ centered at point b, the *Minkowski* $\epsilon - sausage$ of B, denoted by B_ϵ is the set

$$B_\epsilon = \bigcup_{b \in B} Ball_b(\epsilon) \tag{5.6}$$

So $d_B(A)$ is equal to the smallest ϵ such that A is contained in the $\epsilon -$ sausage of B.

Sets A and B could be the graphs of curves. Then, in 2-dimensional space, $A = \{(x(t), y(t)): t \in [0,1]\}$ for some parameterized curve $\gamma: t \in [0,1] \rightarrow (x(t), y(t))$. Similarly, for B.

The Hausdorf distance between A and B will be taken as

$$h(A, B) = d(B, a) + d(a, B) \tag{5.7}$$

In figure 5.20 shows the result that Hausdorf distance metric was implemented to check the variation trend of similarity. Hausdorf distance becomes zero when two curves are completely the same. In this test, the link which is a main parameter to influence the quantitative degree of similarity.

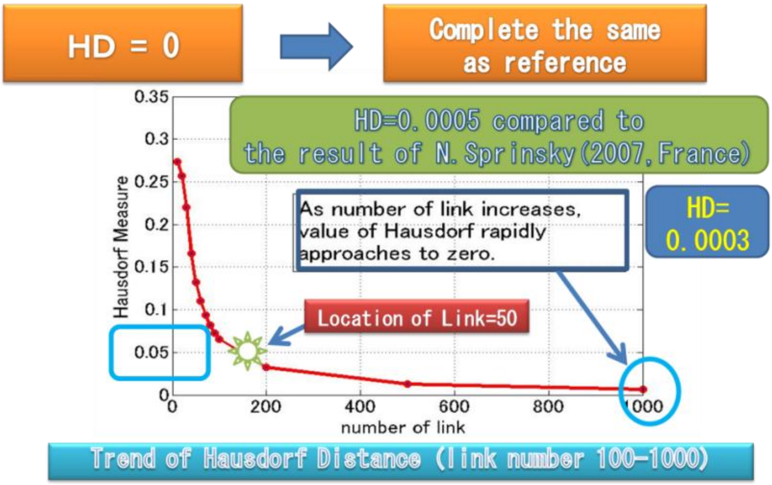

Figure 5.20 Trend of Hausdorf distance when number of link in the kinematic chain model increases; test range between 100 and 1,000

As can be seen in the figure, Hausdorf distance goes to zero as the number of link increase from 100 to 1000. At value of 1,000 in link number, practical Hausdorf distance is

0.0003; this value can be compared to the value of result by N. Sprinsky(2007, France). F rom N. Sprinsky experiments, value of Hausdorf distance was 0.005.

5.11 Calibration Target

Calibration target plays role like measure. This is treated as the ground truth in the ex periment. Target is made of aluminum profile which can guarantee specified under milli meter level of precision on straightness and stability on the structure itself. On the target, calibration paper which is made of thick cardboard is attached. Perpendicularly crossing grid is pre-printed with precision. The following figure shows the configuration of the en tire system.

Aluminum extrusion bars were used for keeping straightness and perpendicularity of de vice. Commercially used aluminum extrusion bars are generally guaranteed up to less tha n 0.1 mm straightness on the 1m length. Standard brackets and fixtures are provided for confirming the perpendicularity of structure when in assembly.

In Figure 5.20, the figure of calibration target is shown. As can be seen in the figure, sensors are located on the points which are pre-determined at the design stage of experi ment. This ensures that accuracy of location of sensor points is in the specified error ran ge.

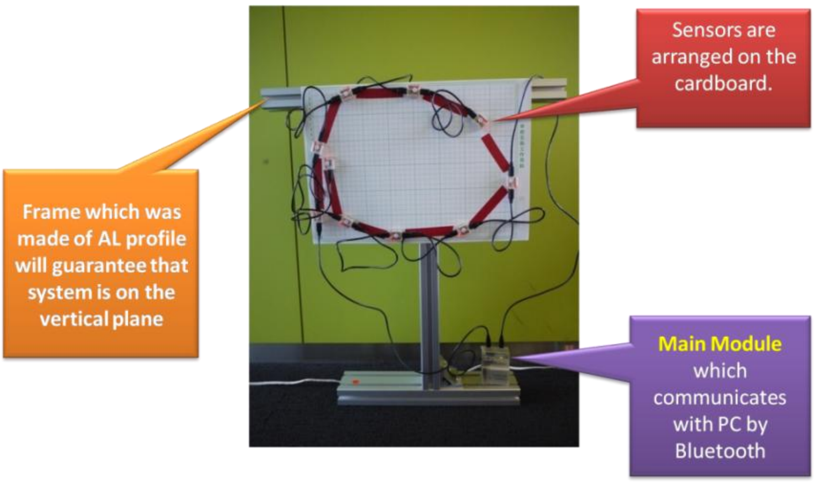

Figure 5. 21 Experimental setup for real world verification: aluminum extruded bars was used to confirm mechanical straightness and perpendicularity of device.

In this experimental setup, 10 sensors were used with serial connection for communicati on. On the lower part of the device, main station which can gather data to transmit collec ted data to the PC via Bluetooth communication.

Figure 5.21 shows the detailed configuration of experimental device, on which sensors are located on the pre-designed points with angle of inclination measured, connected via c able serially each other.

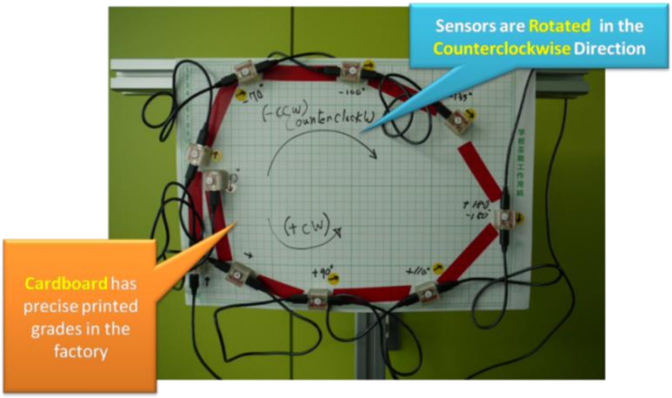

Figure 5.22 pre designed directions of sensors are marked with pen on the cardboard of ta rget.

Table 5.1 shows pre-designed location and orientation of all sensors in the network. These values were measured manually with angle measures. Unit of measurement is centimeters with counted by the number of grid from the origin. With this prior, suggested method was implemented to reconstruct the shape of a colonoscope.

Table 5.3 Test condition ; sensor location and orientation

Unit of location (grid unit = one centimeter squared)

No	X	Z	Y assumed 0	Angles(deg)
Point 1	1.5	25.5	0	-10
Point 2	2.5	11.5	0	-30
Point 3	8.5	1.5	0	-70
Point 4	20.5	1.5	0	-100
Point 5	32.5	7.5	0	-135
Point 6	39	17.5	0	-180/+180
Point 7	30.5	27.5	0	+110
Point 8	16.5	29.5	0	+90
Point 9	6.5	27.5	0	+70
Point 10	3.5	14.5	0	+85

Orientation Interpolation

Data were collected to the PC from the sensor network. Then it was processed to obtain orientation using Kalman filtering and pre designed low pass filtering. But there are still problem that should be solved. The number of sensors in the network is limited. One reason comes from the size of sensor package: their size is too big to arrange enough to use as they are. Another trouble comes from the cabling between sensors. They have two pieces of terminals for connecting each other per package. These cabling prevent distance between sensors close enough to obtain all the data that are needed without interpolation. Not enough number of sensors in the network becomes the cause of deteriorating performance of sensor network.

In order to overcome problem of performance deterioration which comes from the lack of number of sensors in the network, solution based on the computational viewpoints is suggested. Specifically, interpolation between sensor data can be one of useful options. If sufficient data points are ensured with this technique, smooth curve reconstruction using kinematics chain model can be obtained with ease.

But we are dealing with rotation, not position data: rotation is not the element of Euclidian spac e. Rotations make a group in mathematical point of view. This property makes commutative op eration between rotations be not effective.

At first, spherical linear interpolation was applied to interpolate orientations. As well kn own, linear interpolation which is used widely in the position interpolation is not adequate to the rotation interpolation.

5.12 Computer Simulation for accuracy test

Computer simulation was performed to verify whether the suggested method ensures curve reconstruction efficiently. To verify the usefulness of suggests model, analytically proven curve was generated using numerical method.

Table 5.4 simulation condition for curve reconstruction

	Equation of curve	No. of Points	range
True Curve	F(t)=(X(t),Y(t),Z(t)) X(t)=t*exp(t) Y(t)=-sin(2*pi*t) Z(t)=-t(0<=t<=1)	200 points	[0,1]is divided b y 0.05
Simulated Curve	PROPOSED METHOD (KINEMATIC CHAIN MODEL)	200 points	[0,1]is divided by 0.05

In table 5.2, equation of true curve, which was used as a gauge in this comparison, is described with its range. The number of points on the curve is 200 points, the range is [0, 1] divided by 0.05. Simulated curve is generated using kinematic chain model with the same 200 points, the same range for comparison.

Bezier Interpolation between two points

Bezier interpolation is applied to obtain intermediate points between two points. Figure 5.2 3 shows the results of the quaternion based Bezier interpolation. As can be seen in the fi gure, the smoothness of the entire curve is achieved with this algorithm. Then let us impl ement this algorithm to the multipoint interpolation, by which general case is implemented.

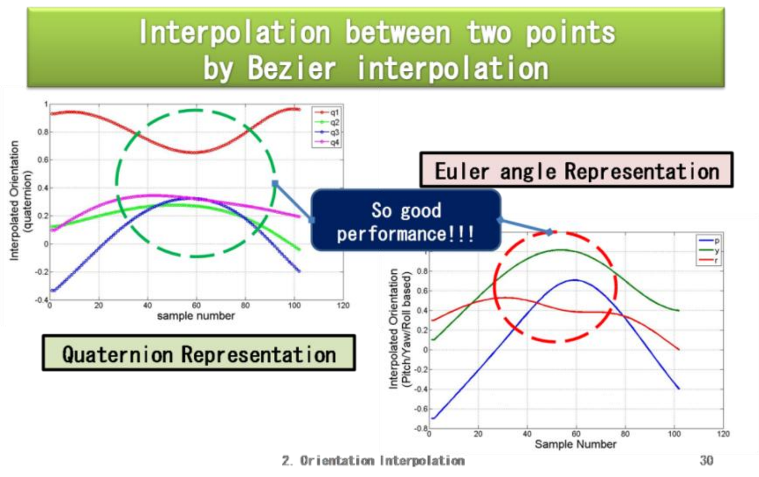

Figure 5.23 interpolation between two points by Bezier interpolation method

Figure 24 is the results of the multipoint interpolation of Bezier method. In the figure, distortion occurs in the mid of the curve. The main reason is that we didn’t consider continuity condition when we apply interpolation method between the break points. In two point case, this trouble was not revealed. But in multipoint case, distortion revealed that we need more condition between break points. Generally, smoothness of curve can be guaranteed by using C1 continuity condition between points.

Figure 5.25 is the picture at which C1 continuity condition is not applied. As we see in the figure, distortion is shown in the mid of the curve. From this investigation, we know that C1 continuity is necessary for creating smooth curve which is more natural to the original colonoscope shape.

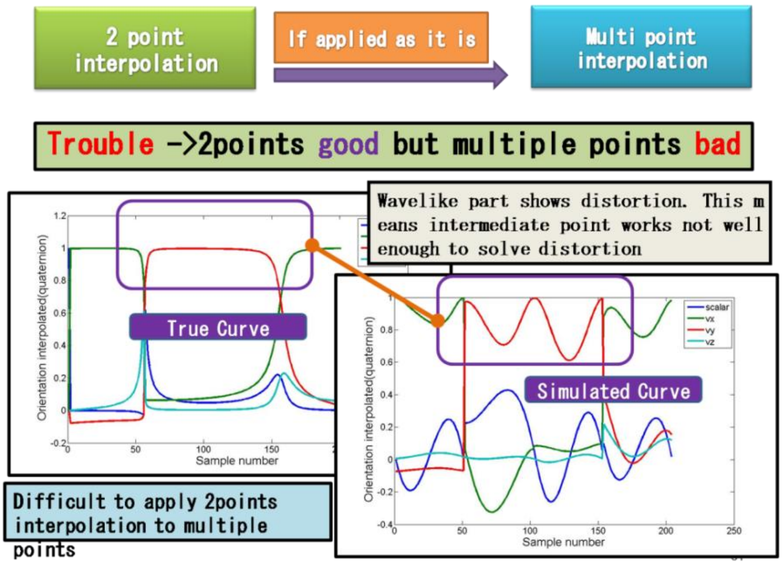

Figure 5.24 Relation between 2 point interpolation and multipoint interpolation; this comparison shows 2 point case is different to multipoint interpolation. It is because continuity condition between break points should be considered

In figure 5.25, troubled location is shown. In the figure, green curve shows the true curve which is generated by the analytical equation, blue one means curve generated by the suggested method.

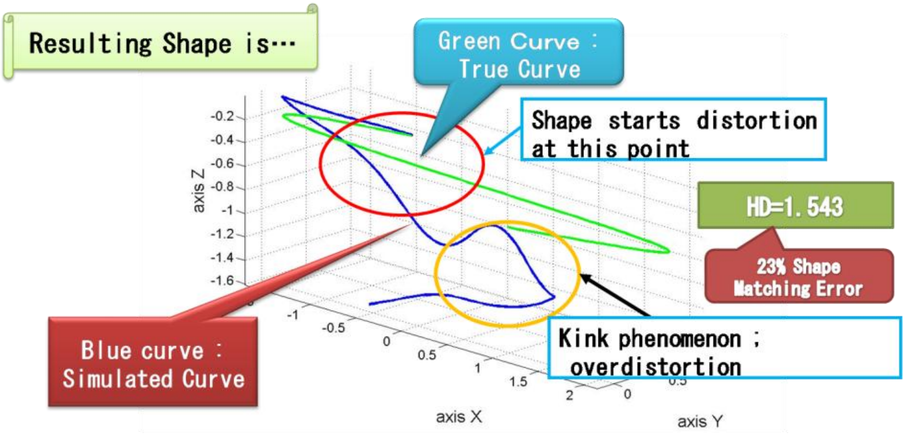

Figure 5.25 Trouble point; Shape can be distorted due to bad interpretation

SQUAD (spherical quadratic interpolation) algorithm

Squad algorithm is usually used to interpolate smoothly among multiple points smoothly. This algorithm includes the condition of C1 continuity as a condition of algorithm.

The results applying this algorithm are shown in figure 5.26. in this figure, two kinds o f continuity function was implemented and shows almost the same in the results with diff erent points near the corners.

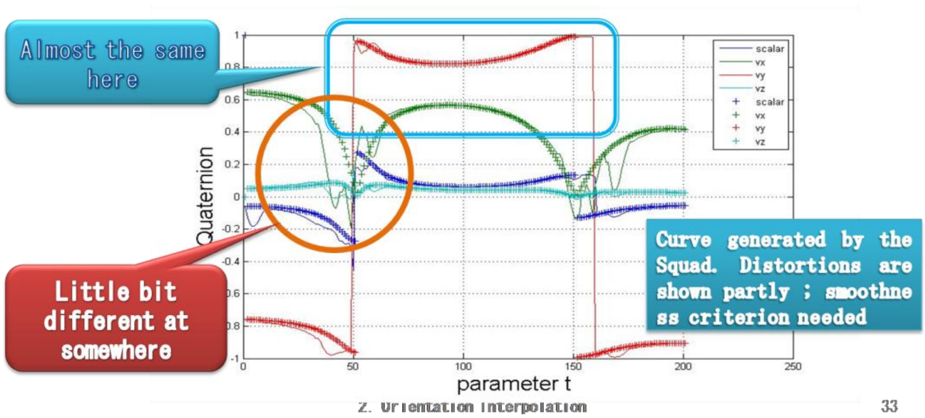

Figure 5.26 interpolation of orientation by SQUAD algorithm as a function of parameter t; unit quaternion was used as rotation. As you can see, '+'means SQUAD applied curve a nd solid line represents

In figure 5.27, the result of implementation of squad algorithm is shown.

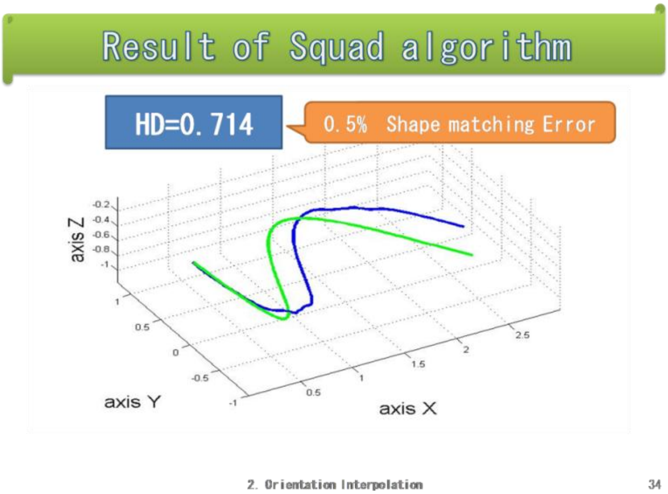

Figure 5.27 Resulting shape reconstructed using kinematic serial chain model and data gen erated by Squad algorithm

As well known in the figure, reconstructed curve resembles to the original curve. In Ha usdorf distance viewpoint, 0.7 of HD was obtained, which means reconstructed curve is al most the same to the original curve.

Representation on the 4D sphere

Rotation is expressed well by quaternion. Quaternion was used for expressing rotation i n 3D Euclidian space. But quaternion is inconvenient to understand. If we want to underst and results of quaternion operation, specially created visualization is required. Geometry is convenient to make physical amount to be visible. First of all, let us check the detail of quaternion in geometric point of view. Quaternion has 4 components: one scalar compone nt and 3 vector components. Vector represents the axis of rotation, scalar expresses magnit ude of rotation. So quaternion can be visualized if Axis-Angle representation is introduced.

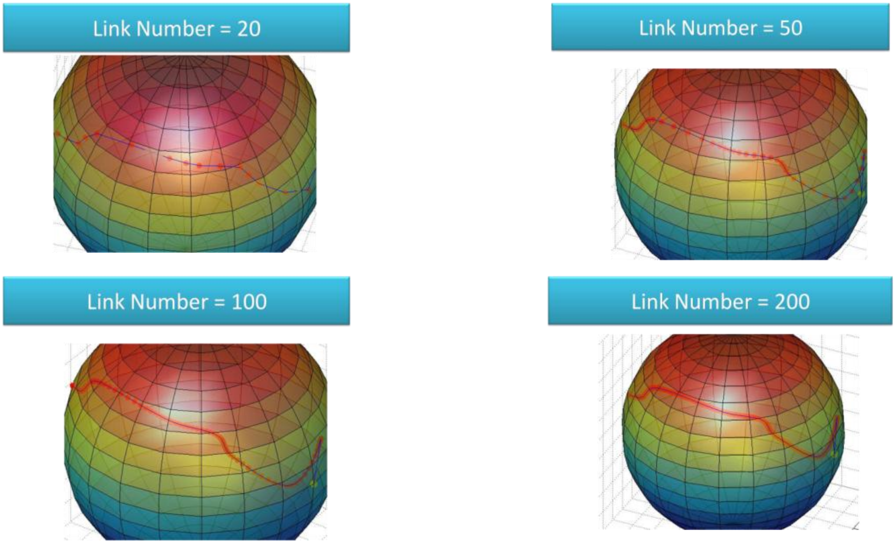

Figure 5.28 curve on the 4D sphere; this curve is not the real curve, it represents the direction of the interpolated points (points = orientation expressed by quaternion); interpolation was performed using SQUAD algorithm.

Figure 5.24 shows the progressive change of the orientation interpolation when SQUAD algorithm. SQUAD algorithm guarantees the C1 continuity of curve. In this figure, link number is changed from 20 to 200. As the number of link increases, the curve interpolated becomes smoother. Solid lines use interpolation function as ; dotted lines

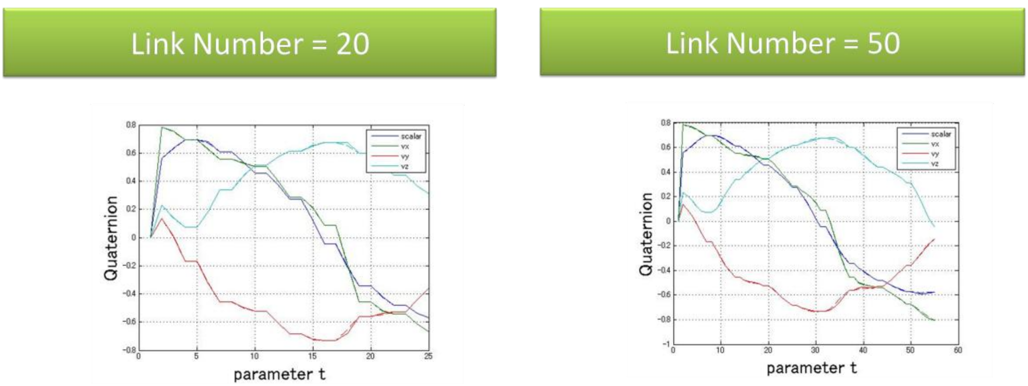

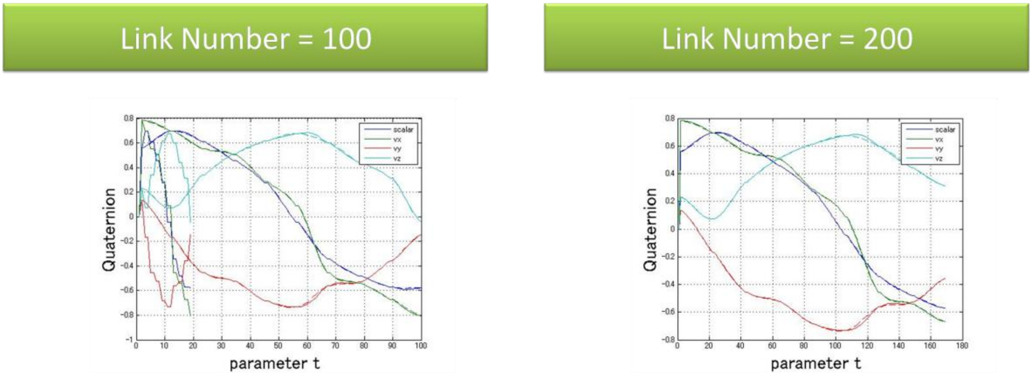

Figure 5.29 quaternion interpolations by SQUAD algorithm: as can be seen in the figure, SQUAD algorithm can remove troubles arising from the discontinuity between break points.

Figure 5.25 shows the time dependant trajectory of orientation which comes from the irregularity of cardboard. In ideal case, cardboard plane should be perpendicular to the horizontal plane. But red axis moves around during orientation change as the plane of cardboard is in reality not perpendicular to the horizontal plane.

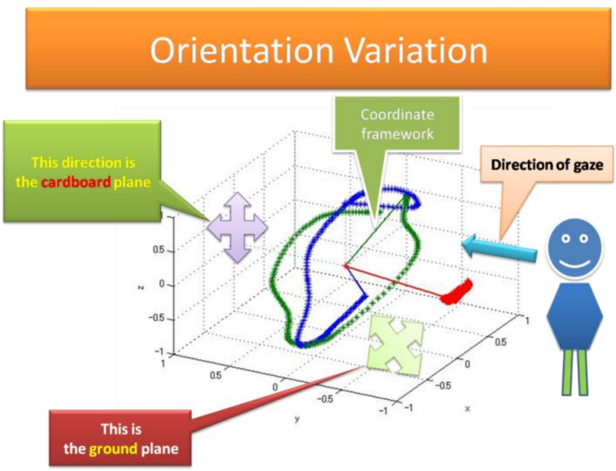

Figure 5.30 orientation variation; variation of the orientation using roll, pitch and yaw framework;

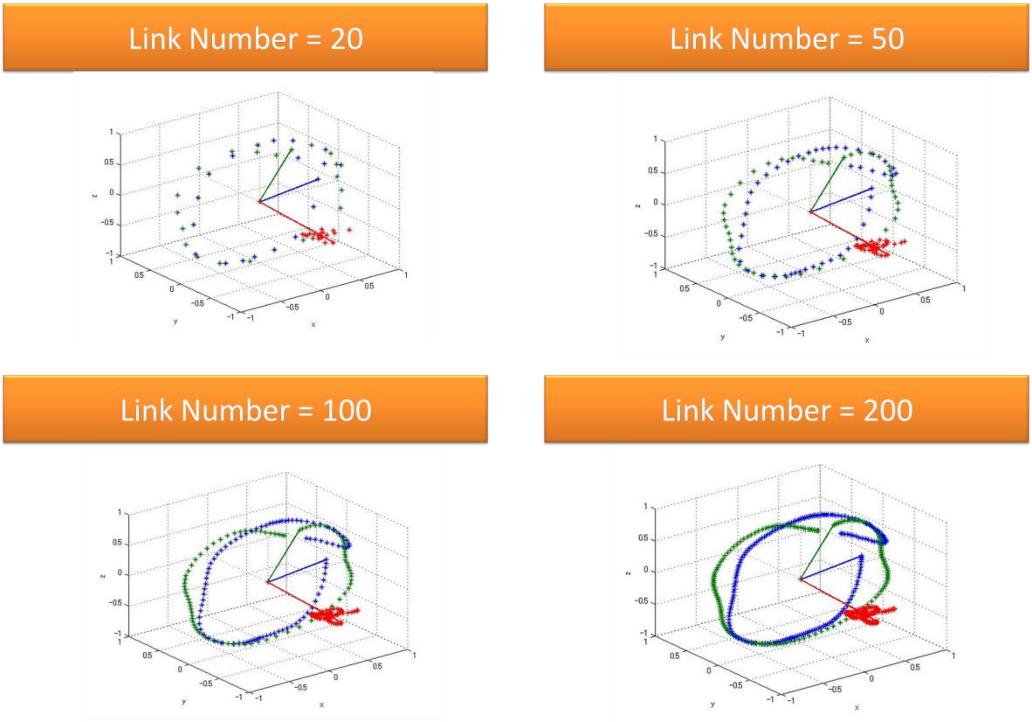

Figure 5.31 smoothness effect on the orientation variation by increase of link number:

In figure 5.26, change of smoothness of trajectory of angles due to the increase of link number is shown. In this figure also power of orientation interpolation is displayed.

Results and Discussions

In figure 5.27, the result of simulation is shown. In case that length and direction of tangent vectors on the points along the true curve are known, simulated curve imitates true one as points increase. We inspected the value of Hausdorf distance as a metric to express the degree of similarity between curves. As can be seen in the figure, the value of HD (Hausdorf Distance) goes to nearly zero. In fact, zero of HD means complete matching between two curves.

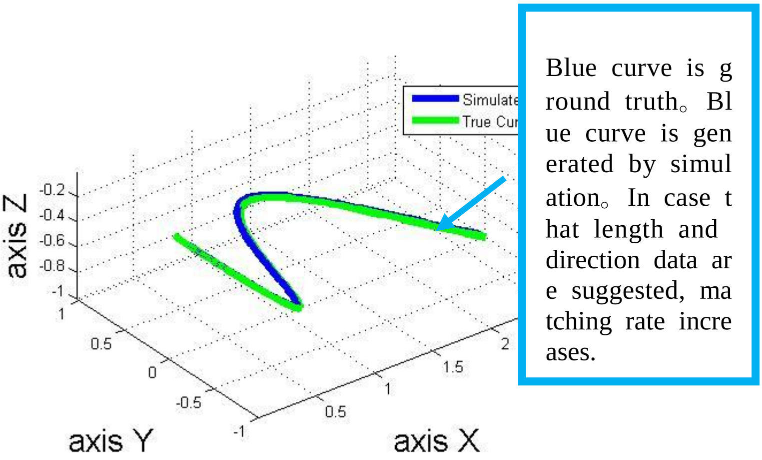

Figure 5.32 True Curve and Simulated Curve. True Curve (Green Line) is almost similar to the True Curve. **Hausdorf Distance = 0.0322**

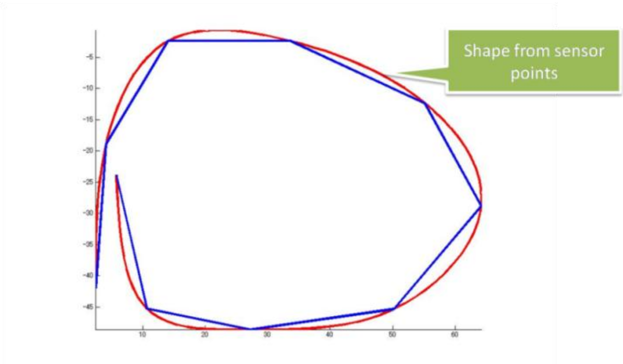

Figure 5.33 curve reconstructed from sensor data

5.13 Concluding Remarks

Until now, we have shown several evidences: experiments and related result. For successive validation as evidences, experimental procedures were explained and conditions were mentioned. Experimental procedures have their own meanings. With these procedures, we could have shown validity of preceding methodology.

Section 5.1 and 5.2 deals with hardware dependent topics. Specifically, at section 5.1, we talked how the signals are processed properly and in detail. Based on the signals, digital filtering technique was mentioned in short. Section 5.3 to 5.5 discusses each parts of methodology in detail. Generally simulation test is carried out and simple numerical calculatio ns are suggested. Section 5.3 mentions orientation interpolation with two examples.

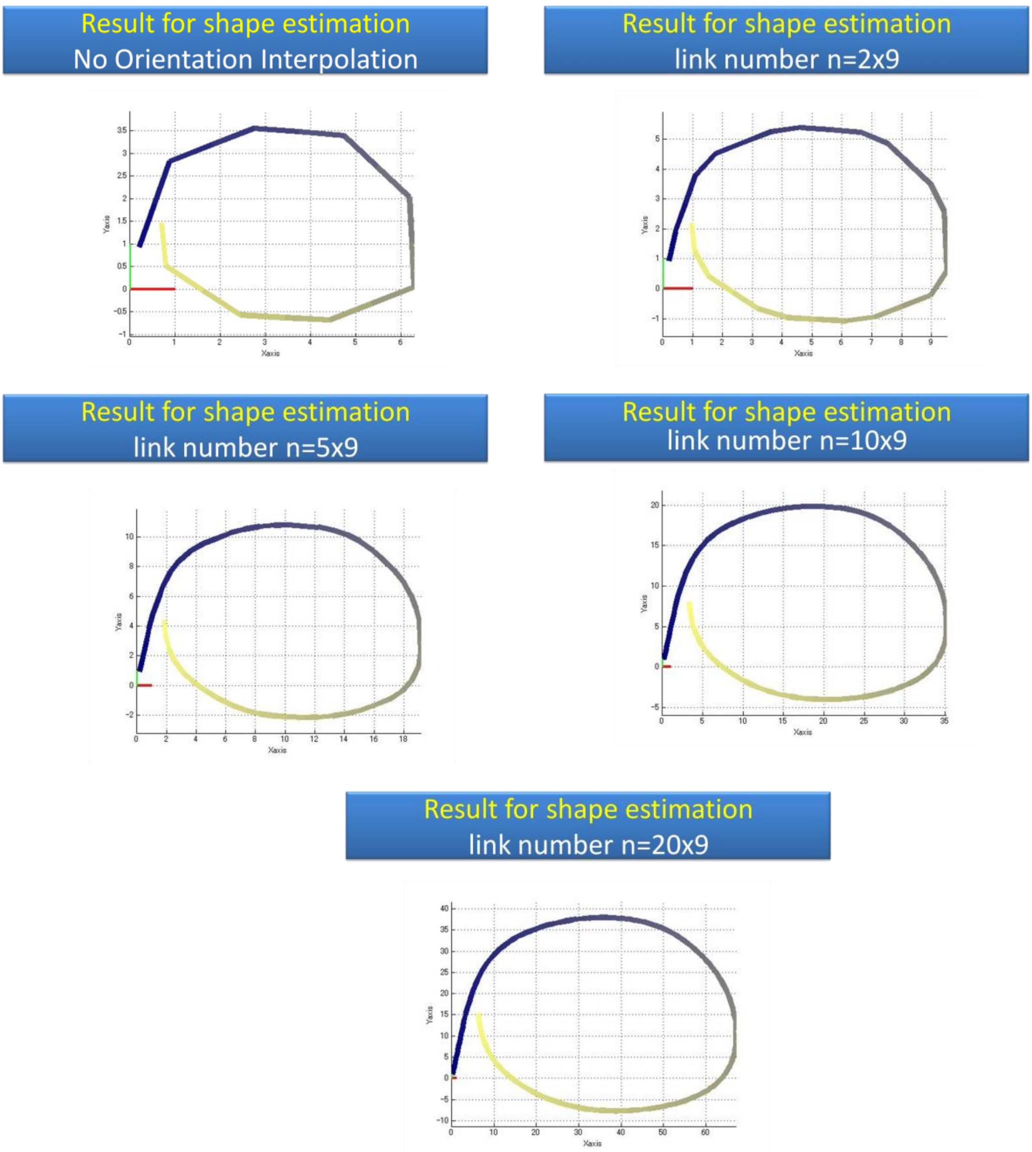

Figure 5.34 Result for shape estimation: as number of link increases, resulting shape beco mes smoother and nearer to the original shape

Linear and Bezier curve are used as interpolating one. Here also reveals difference betwee n naturalness caused by smoothness and continuity. Section 5.4 says topic of Arclength re parametrization. This is used for uniform arrangement of interpolated points. Point arrangement was distorted when orientation interpolation was implemented. In section 5.5, we showed detailed inner procedure by using simple dual quaternion calculation.

Section 5.6, 5.7 and 5.8 are concerned with accuracy and resulting visualization. Section 5.6 tells the detailed procedure for accuracy test. Two different approaches were shown. One is for comparing with ground truth curve; here sine curve. Other is accuracy evaluation through test of reducing number of sensors in the net. Section 5.7 is concerned with results and discussion of section 5.7. Finally in section 5.8, we show visualization with these methods. Final result of visualization reveals effectiveness of methodology and latent limitation on this problem solving technique.

Section 5.9 treats with accuracy verification problem using real sensor data. Suggested method was proven to work well with data coming from the sensor networks. Section 5.10 is for defining geometric metric which is used for quantifying the degree of similarity in comparing curves. Calibration target is described in detail as a preparation of experimental setup in section 5.11. In the following section 5.12, the same experiment is carried out with computer simulation.

Chapter 5 has the property of verifying methodology that was suggested in the previous chapters. Shape estimation and visualization method is fully proved to be efficient with simulation and real world data together.

Chapter 6

Conclusion & Future Works

Until now, we have investigated on how to visualize the shape of colonoscope. Motiva tion was clearly at the possibility of being helpful system as a medical device. In the mar ket, there is shape estimation system that was developed by the Olympus Co., Ltd. but thi s device was not permanently embodied in the system. In view point of medical doctor, t his could be inconvenient to manipulation. Moreover, the insertion of

6.1 Conclusion

As hardware for acquiring data, orientation sensor unit which consist of 3 axes of acce lerometer, 3 axes of gyroscope and 3 axes of magnetometer was studied and by using sen sor unit we made sensor network, which arranged a number of sensor unit along the tube in chapter 2.

In chapter 3, orientation interpolation technique was exploited based on quaternion expr ession. This was implemented on the unit quaternion sphere, which is a subspace of Speci al Orthogonal Group, SO(3) that also a subspace of Lie group.

In chapter 4, concept of Arclength Reparametrization was introduced to obtain the unif orm distance between sensors on the colonoscope. As shape is described by the Arclength parameter, Arclength representation is important. But the parameter which comes from the parametric form which was introduced for solving interpolation problem is not the same parameter of Arclength. This is why we introduce the Reparametrization by Arclength.

Kinematic chain was introduced in chapter 5. Essentially chapter 5 describes how to ca lculate the position of points which makes up of space curve. This concept was borrowed from the robotic theory. Calculating positions of points on the curve was approximated b y the serial chain model, which is usually used for the serial link robot kinematics.

6.2 Future Works

Figure 6.1 shows the concept schematic of the whole system, which we want to accomplis h as a final goal of this system. As can be seen from figure 6.1, colonoscope sensor syst em and its control system consists of future colonoscopy room. There are plausible and lat ent problem or suggestions on the future issue.

1. Research on the behavior of the physician or colonoscopist.

This research includes essentially study on the human behavior and its modeling. Sensor b ased motion analysis is one of major discipline in the human motion capture. Camera base d tracking is also an issue which receive spotlight.

2. Robot motion planning by learning

This issue can include robot motion planning by motion learning. There are researchers in Europe who are concentrating on the programming by demonstration. This group studies h ow to analyze and reconstruct the robot motion by merely watching human motion.

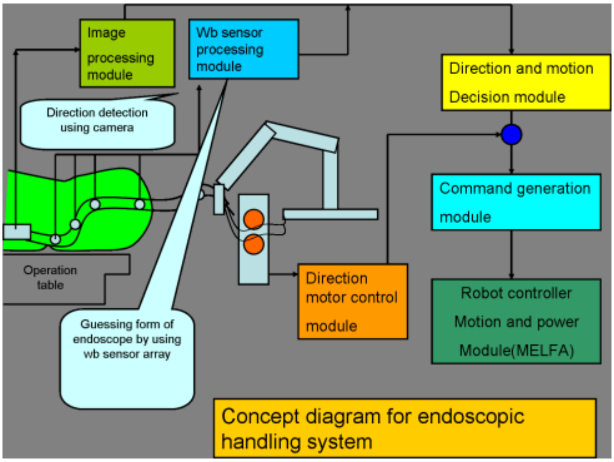

Figure 6.1 Concept diagram showing the possible layout of the endoscope handling syste m

3. Hardware structure development

This subject needs more small sized hardware which can be embodied in the commercial colonoscope system. As modern MEMS (micro electro mechanical system) Technology is evolving day by day, we can use this technology to make more compact and integrated function of system on a chip.

Small sized camera, integrated IMU sensors and its communication system should be improved in the future.

Appendix

A.1 Markov Chain Monte Carlo Method

Markov chain Monte Carlo method is widely used as alternatives to make approximation on the a posteriori probability distribution. In tracking object, traditional Kalman filtering theory had been used and it was proven to be effective in enormous area. But these methods needs exact form of distribution. In Kalman filter, the strong assumptions such as linearization and Gaussian are used, which is far away from the practical process characteristic. In order to alleviate these assumptions, Extended Kalman filter uses nonlinear function. But practically it uses derivative of the function at the point of consideration. In addition, this type of method needs concrete representation of process model.

On the contrary, the particle filtering method uses some specified number of samples to describe the process model. The theory of particle filtering brings their concepts and mathematical background from the Markov process and Monte Carlo method.

Markov process

The concept of Markovian process simplifies the relationship embedded in the complex phenomenon of real world problem. When process suffers from time passing, state which we want to see changes according to their logic. In the real world, the states of process are also closely connected to their history. If we can understand the whole relationship between all past events, then we can see the most stealthful world of the process. But it is difficult and realistically thinking, it is close to the impossibility. Here we try to relax the severe relationship of present event and the past events by introducing the simplifying concept, Markovian property.

Monte Carlo method

Monte Carlo method is usually used for approximating the integration which is shown in the process of estimation of affects of past events. This equation is called as Chapman – Kolmogolov equation. Concept underling behind the Monte Carlo method is simple. The following example will make readers get insight which can see the inner world. Let's think of calculating area of circle.

A.2 Tool as a solution of Bayesian inference [27]

Generally speaking, Bayesians tend to think uncertainty about unknown parameter val ues by probability distributions and proceed as if parameters were random quantities. For t he observed data D and unknown model parameters, we need to know the joint probabilit y distribution $P(D,\theta)$ to do inference.

$$P(D,\theta) = P(\theta)P(D|\theta) \tag{A.1}$$

, where $P(\theta)$ is called prior, and $P(D|\theta)$ is called the likelihood.
Bayes' theorem gives the posteriori distribution as

$$P(\theta|D) = \frac{P(\theta)P(D|\theta)}{\int P(\theta)P(D|\theta)} \tag{A.2}$$

In equation (A.7), the denominator is not a function of θ and is usually difficult to ev aluate. We have

$$P(\theta|D) \propto P(\theta)P(D|\theta) = P(\theta)L(\theta;D) \tag{A.3}$$

Understanding and using the posterior distribution is at the heart of Bayesian inferen ce, where one is interested in making inferences using various features of the posterior dis tribution. Since similar problems arise in frequentist applications, We change the notation t o make it more general. Let X represents a vector of d random variables, with distributio n denoted by $\pi(x)$. The goal is to obtain the expectation

$$\mathrm{E[f(X)]} = \frac{\int f(x)\pi(x)dx}{\int \pi(x)dx} \tag{A.4}$$

With MCMC methods, we only have to know the distribution of X up to the constant of normalization. Most methods in statistical inference that use simulation can be reduced to the problem of finding integrals.

Monte Carlo integration estimates the integral E[f(x)] of equation (A.9) by obtaining sampl es $X_t, t = 1, \dots, n$ from the distribution $\pi(x)$ and get

$$\mathrm{E}[f(\mathrm{X})] \approx \frac{1}{n}\sum_{\mathrm{t}=1}^{\mathrm{n}} f(\mathrm{X}_t) \tag{A.5}$$

The above approximation can be made as accurate as needed by increasing n if X_t are in dependent.

A.3 Axis angle representation

The axis angle representation of a rotation, also known as the exponential coordinate s of a rotation, parameterizes a rotation by two values: a unit vector indicating the directi on of a directed axis and an angle describing the magnitude of the rotation about the axis.

The rotation occurs in the sense prescribed by the right hand rule as depicted in Figure A.1.

This representation evolves from Euler's rotation theorem, which implies that any rotation or sequence of rotations of a rigid body in a three dimensional space is equivalent to a p ure rotation about a single fixed axis.

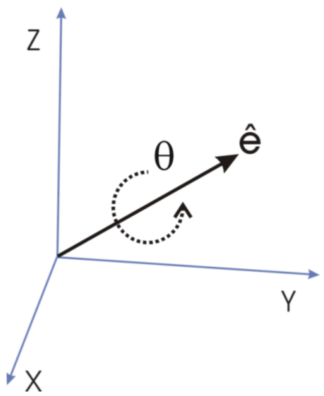

Figure A.1 Axis angle representation of rotation

The axis-angle representation is equivalent to the more concise rotation vector, or Euler ve ctor representation. In this case, both the axis and the angle are represented by a non nor malized vector co-directional with the axis whose magnitude is the rotation angle.

Rodrigues' rotation formula can be used to apply to a vector a rotation represented by an axis and an angle.

The axis angle representation is convenient when dealing with rigid body dynamics. It is useful to both characterize rotations and also for converting between different representa tions of rigid body motion, such as homogeneous transformations and twists.

Suppose you are standing on the ground and you pick the direction of gravity to be the n egative z direction. Then if you turn to your left, you will travel $\frac{\pi}{2}$ radians (or 90 degree s) about the z axis. In axis-angle representation, this would be

$$< axis, angle >= \left(\begin{bmatrix} a_x \\ a_y \\ a_z \end{bmatrix}, \theta \right) = \left(\begin{bmatrix} 0 \\ 0 \\ 1 \end{bmatrix}, \frac{\pi}{2} \right) \tag{A.6}$$

This can be represented as a rotation vector with a magnitude of $\frac{\pi}{2}$ pointing in the z direc tion.

$$\begin{bmatrix} 0 \\ 0 \\ \frac{\pi}{2} \end{bmatrix}$$

A.4 Quaternion [3]

Quaternion was developed by Sir. William Rowan Hamilton in October of 1843. The motive of developing quaternion is well described in [4].

Quaternion Algebra

The four dimensional space of Quaternions H, is spanned by real axis and 3 further ortho normal axes, spanned by the vectors, I, j, k called the principal imaginaries, which obey t he Hamilton's rules.

$$\mathbb{i}^2 = \mathbb{j}^2 = \mathbb{k}^2 = \mathbb{i}\mathbb{j}\mathbb{k} = -1 \tag{A.7}$$

These imaginaries signify three dimensional vectors.

$$\mathbb{i} = (1,0,0) \tag{A.8}$$

$$\mathbb{j} = (0,1,0) \tag{A.9}$$

$$\mathbb{k} = (0,0,1) \tag{A.10}$$

Multiplication of these imaginaries resembles a cross product

$$\begin{matrix} \mathbb{i}\mathbb{j} = \mathbb{k} & \mathbb{j}\mathbb{k} = \mathbb{i} & \mathbb{k}\mathbb{i} = \mathbb{j} \\ \mathbb{j}\mathbb{i} = -\mathbb{k} & \mathbb{k}\mathbb{j} = -\mathbb{i} & \mathbb{i}\mathbb{k} = -\mathbb{j} \end{matrix} \tag{A.11}$$

Conversion of Matrix to Quaternion

The following contents come from Appendix of Ken Shuemake [5]. He described int eresting and funny method on how to get quaternion components from rotation matrix.

$$w = \frac{1}{4}(1 + M_{11} + M_{22} + M_{33}) \tag{A.12}$$

$$w^2 > \varepsilon ?$$

TRUE FALSE

$$w = \sqrt{w^2} \qquad\qquad w = 0$$

$x = (M_{23} - M_{32})/4w$

$y = (M_{31} - M_{13})/4w$

$z = (M_{12} - M_{21})/4w$

$x^2 = -{}^1\!/_2\,(M_{22} + M_{33})$

$x^2 > \varepsilon?$

TRUE

$x = \sqrt{x^2}$

$y = {}^{M_{12}}\!/_{2x}$

$z = {}^{M_{13}}\!/_{2x}$

FALSE

$x = 0$

$y^2 = {}^1\!/_2\,(1 - M_{33})$

$y^2 > \varepsilon?$

TRUE

$y = \sqrt{y^2}$

$z = {}^{M_{23}}\!/_{2y}$

FALSE

$y = 0$

$z = 0$

Conversion of Euler angles to quaternion [5]

There are twelve possible axis conventions for Euler angles. The one used here is roll, pitch, and yaw, as used in aeronautics. A general rotation is obtained by first yawing aro und the z axis by an angle of ϕ, then pitching around the y axis by ϑ, and finally rollin g around the x axis by ψ. Using the way quaternion components describe a rotation, we f irst obtain a quaternion for each simple rotation.

$$q_{roll} = \left[cos\frac{\psi}{2}, (sin\frac{\psi}{2}, 0,0)\right] \tag{A.13}$$

$$q_{pitch} = \left[cos\frac{\vartheta}{2}, (0, sin\frac{\vartheta}{2}, 0)\right] \tag{A.14}$$

$$q_{yaw} = \left[cos\frac{\phi}{2}, (0,0, sin\frac{\phi}{2})\right] \tag{A.15}$$

Multiplying these together in the right order gives the desired quaternion q = $q_{yaw}\, q_{pitch} q_{roll}$ with components.

$$w = cos\frac{\psi}{2}cos\frac{\vartheta}{2}cos\frac{\phi}{2} + sin\frac{\psi}{2}sin\frac{\vartheta}{2}sin\frac{\phi}{2} \tag{A.16}$$

$$x = \sin\frac{\psi}{2}\cos\frac{\vartheta}{2}\cos\frac{\phi}{2} - \cos\frac{\psi}{2}\sin\frac{\vartheta}{2}\sin\frac{\phi}{2} \quad \text{(A.17)}$$

$$y = \cos\frac{\psi}{2}\sin\frac{\vartheta}{2}\cos\frac{\phi}{2} + \sin\frac{\psi}{2}\cos\frac{\vartheta}{2}\sin\frac{\phi}{2} \quad \text{(A.18)}$$

$$z = \cos\frac{\psi}{2}\cos\frac{\vartheta}{2}\sin\frac{\phi}{2} - \sin\frac{\psi}{2}\sin\frac{\vartheta}{2}\cos\frac{\phi}{2} \quad \text{(A.19)}$$

A.5 Dual Quaternion and Clifford Algebra

Dual quaternion was created by the Sir W. Clifford in 1890. The following is for th e basic algebra of dual quaternion. A dual quaternion is a vector of the form

$$\widehat{\mathbf{Q}} = \begin{pmatrix} \hat{\mathrm{d}} \\ \hat{\mathrm{a}} \\ \hat{\mathrm{b}} \\ \hat{\mathrm{c}} \end{pmatrix} \quad \text{(A.20)}$$

where the components $\hat{\mathrm{d}}, \hat{\mathrm{a}}, \hat{\mathrm{b}}$ and $\hat{\mathrm{c}}$ are dual numbers. In order to express in a compact not ation the basic algebraic operations of dual quaternions, it is convenient to split the dual q uaternion in a dual scalar part $\hat{\mathrm{d}}$ and dual vector part $\hat{\mathbf{v}} = \hat{a}\vec{\imath} + \hat{b}\vec{\jmath} + \hat{c}\vec{k}$ as follows.

$$\widehat{\mathbf{Q}} = \hat{d} + \hat{\mathbf{v}} \quad \text{(A.21)}$$

1. Sum

$$\widehat{\mathbf{Q}}_{\mathbf{1}} + \widehat{\mathbf{Q}}_{\mathbf{2}} = \hat{\mathrm{d}}_1 + \hat{\mathrm{d}}_2 + \hat{\mathbf{v}}_{\mathbf{1}} + \hat{\mathbf{v}}_{\mathbf{2}} \quad \text{(A.22)}$$

2. Product

$$\widehat{\mathbf{Q}}_{\mathbf{1}} * \widehat{\mathbf{Q}}_{\mathbf{2}} = \begin{pmatrix} \hat{\mathrm{d}}_1\hat{\mathrm{d}}_2 - < \hat{\mathbf{v}}_{\mathbf{1}}, \hat{\mathbf{v}}_{\mathbf{2}} > \\ \hat{\mathrm{d}}_1\hat{\mathbf{v}}_{\mathbf{2}} + \hat{\mathrm{d}}_2\hat{\mathbf{v}}_{\mathbf{1}} + \hat{\mathbf{v}}_{\mathbf{1}} \times \hat{\mathbf{v}}_{\mathbf{2}} \end{pmatrix} \quad \text{(A.23)}$$

Where $< \hat{\mathbf{v}}_{\mathbf{1}}, \hat{\mathbf{v}}_{\mathbf{2}} >$ and $\hat{\mathbf{v}}_{\mathbf{1}} \times \hat{\mathbf{v}}_{\mathbf{2}}$ denote the dot and vector product, respectively.

3. Conjugation

$$\widehat{\mathbf{Q}} = \hat{d} - \hat{\mathbf{v}} \quad \text{(A.24)}$$

4. Norm

$$\|\widehat{\mathbf{Q}}\| = \sqrt{\widehat{\mathbf{Q}} * \widehat{\mathbf{Q}}^*} - \hat{\mathbf{v}} \quad \text{(A.25)}$$

5. Inverse

$$\hat{\mathbf{Q}}^{-1} = \frac{\hat{\mathbf{Q}}^{*}}{\|\hat{\mathbf{Q}}\|^{2}} \tag{A.26}$$

6. Exponential

$$\exp(\hat{\boldsymbol{Q}}) = \exp(\hat{d})\begin{pmatrix} \cos(\|\hat{\mathbf{v}}\|) \\ \frac{\hat{\mathbf{v}}}{(\|\hat{\mathbf{v}}\|)}\sin(\|\hat{\mathbf{v}}\|) \end{pmatrix} \tag{A.27}$$

The extension of Euler's identity to dual quaternions is expressed by the follow ing unit dual quaternion

$$\exp\left(\hat{\mathbf{u}}\frac{\hat{\theta}}{2}\right) = \cos\frac{\hat{\theta}}{2} + \sin\frac{\hat{\theta}}{2}\hat{\mathbf{u}} \tag{A.28}$$

7. Logarithm

$$\ln(\hat{\boldsymbol{Q}}) = \begin{pmatrix} \ln(\|\hat{\mathbf{Q}}\|) \\ \frac{\hat{\mathbf{v}}}{\|\hat{\mathbf{v}}\|}\arccos\left(\frac{\hat{d}}{\|\hat{Q}\|}\right) \end{pmatrix} \tag{A.29}$$

If $\hat{Q}$ is unit dual quaternion expressed by (A.22), then

$$\ln(\hat{\boldsymbol{Q}}) = \hat{\mathbf{u}}\frac{\hat{\theta}}{2} \tag{A.30}$$

8. Power

$$\hat{\boldsymbol{Q}}^{t} = \exp(\ln(\hat{\boldsymbol{Q}})t) \tag{A.31}$$

A.6 Denavit - Hartenberg Representation [118]

Denavit-Hartenberg (abbreviated D-H, hereafter) representation of the forward kinematics is used widely in the robotics community. In the following, the convention of representatio n is exploited for reference.

Step 1: Locate and label the joint axes $z_0, \ldots, z_{n-1}$

Step 2: Establish the base frame. Set the origin anywhere on the z_0 axis. The x_0 and y_0 axes are chosen conveniently to form a right hand frame. For $i = 1, \ldots, n-1$, perform step3 to 5.

Step 3: Locate the originO_i where the common normal to z_i and z_{i-1} intersects z_i. If z_i intersects z_{i-1} locate O_i at the intersection. If z_i and $z_{i-1}$are parallel, locate O_i in any convenient position along z_i.

Step 4: Establish x_i along the common normal between $z_{i-1}$and z_i through O_i or in th e direction normal to the z_{i-1} - z_i plane if z_{i-1} and z_i intersect.

Step 5: Establish y_i to complete a right-hand frame.

Step 6: Establish the end-efffector frame $o_n x_n y_n z_n$. Assuming the *n-th* joint is revolute, set $z_n = a$ along the directionz_{n-1}. Establish the origin O_n conveniently along the z_n, pre ferably at the center of the gripper or at the tip of any tool that the manipulator may be carrying. Set $y_n = \boldsymbol{s}$ in the direction of the gripper closure and set $x_n = \boldsymbol{n}$ as $\boldsymbol{s} \times \boldsymbol{a}$**.** If th e tool is not the simple gripper set x_n and y_n conveniently to form a right hand frame.

Step 7: Create a table of link parameters $a_i, d_i, \alpha_i, \theta_i$.
a_i *= distance along* x_i *from* O_i *to the intersection of the* x_i *and* z_{i-1} *axes.*
d_i *= distance along the* z_{i-1} *from* O_{i-1} *to the intersection of the* x_i *and* z_{i-1} *axes.*
d_i *is variable if joint i is prismatic.*
α_i *= the angle between* z_{i-1} *and* z_i *measured about* x_i
θ_i *= the angle between* x_{i-1} *and* x_i *measured about* z_{i-1}. θ_i *is variable if joint i is revo lute.*

Step 8: form the homogeneous transformation matrices A_i.

Step 9: Form $T_n^0 = A_1, \ldots, A_n$. This then gives the position and orientation of the tool fra me expressed in the base coordinates.

A.7 Spherical Joint

Spherical joint is shown in figure A.2, in which the joint axes z_3, z_4, z_5 intersect at O. the Denavit-Hartenberg parameters are shown in Table A.1.

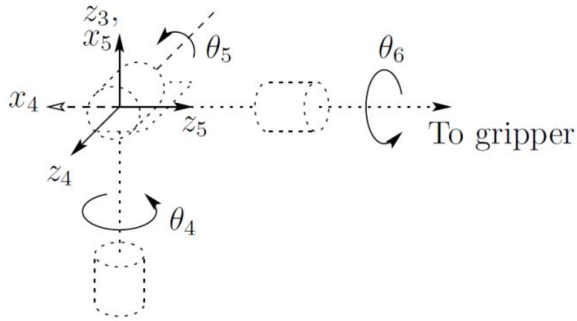

Figure A.2 Spherical Joint representation using 3 axes of revolution joints

We show now that the final three joint variables, θ_4 , θ_5, θ_6 are the Euler angles $\emptyset, \theta, \psi$ respectively, with respect to the coordinate frame $o_3x_3y_3z_3$. To see this we need o nly compute the matrices A_4, A_5 and A_6 using Table A.1

Table A.1 D-H parameters for Spherical Joint

Link	a_i	α_i	d_i	θ_i
4	0	-90	0	θ_4
5	0	+90	0	θ_5
6	0	0	d_6	θ_6

$$A_4 = \begin{bmatrix} c_4 & 0 & -s_4 & 0 \\ s_4 & 0 & c_4 & 0 \\ 0 & -1 & 0 & 0 \\ 0 & 0 & 0 & 1 \end{bmatrix} \quad (A.32)$$

$$A_5 = \begin{bmatrix} c_5 & 0 & s_5 & 0 \\ s_5 & 0 & -c_5 & 0 \\ 0 & -1 & 0 & 0 \\ 0 & 0 & 0 & 1 \end{bmatrix} \quad (A.33)$$

$$A_6 = \begin{bmatrix} c_6 & -s_6 & 0 & 0 \\ s_6 & c_6 & 0 & 0 \\ 0 & 0 & 1 & d_6 \\ 0 & 0 & 0 & 1 \end{bmatrix} \tag{A.34}$$

Multiplying these together yields

$$T_6^3 = A_4 A_5 A_6 = \begin{bmatrix} R_6^3 & O_6^3 \\ 0 & 1 \end{bmatrix}$$

$$= \begin{bmatrix} c_4c_5c_6 - s_4s_6 & c_4c_5s_6 - s_4c_6 & -c_4s_5 & c_4s_5d_6 \\ s_4c_5c_6 + c_4s_6 & s_4c_5s_6 + c_4c_6 & s_4s_4 & s_4s_5d_6 \\ -s_5c_6 & s_5s_6 & c_5 & c_5d_6 \\ 0 & 0 & 0 & 1 \end{bmatrix} \tag{A.35}$$

Comparing the rotational part R_6^3 of T_6^3 with the Euler angle transformation shows th at θ_4 , θ_5, θ_6 can indeed be identified as the Euler angles $\emptyset, \theta, \psi$ with respect to the coor dinate frame $o_3x_3y_3z_3$. T_6^3 becomes the basic homogeneous transformation matrix in our a pplication. If we rewrite this as roll, pitch and yaw angle style, then the final transformati on matrix becomes as follows.

$$T_6^3 = A_\theta A_\emptyset A_\varphi = \begin{bmatrix} R_6^3 & O_6^3 \\ 0 & 1 \end{bmatrix}$$

$$= \begin{bmatrix} c_\theta c_\emptyset c_\varphi - s_\theta s_\varphi & c_\theta c_\emptyset s_\varphi - s_\theta c_\varphi & -c_\theta s_\emptyset & c_\theta s_\emptyset d_6 \\ s_\theta c_\emptyset c_\varphi + c_\theta s_\varphi & s_\theta c_\emptyset s_\varphi + c_\theta c_\varphi & s_\theta s_\theta & s_\theta s_\emptyset d_6 \\ -s_\emptyset c_\varphi & s_\emptyset s_\varphi & c_\emptyset & c_\emptyset d_6 \\ 0 & 0 & 0 & 1 \end{bmatrix} \tag{A.36}$$

Bibliography

[1] Helmut Messman,"Atlas of colonoscopy:techniques, diagnosis, interventional procedures", 2006 Georg Verlag, Thieme, ISBN 3-13-140571-6(alk. Paper)

[2] Yoto Suzuki, Yoshikazu Mukaeda, Zhuohua Lin, Luca Bartolomeo, Kazuko Itoh, Hiroyuki Ishii, Salvatore Sessa, Massimiliano Zecca, Atsuo Takanishi, "Performance evaluation of WB-3 ultra-miniaturized Inertial measurement unit", conference of Japanese robotics society,

[3] Christopher Konvalin,"Calculating Heading, Elevation and Bank Angle",Technical Report, Doc. Number:MTD-0801,Rev.1.0, June 4, 2008, MEMSense.

[4] John C. Hart, George K. Francis, Louis H. Kaufman, "Visualizing quaternion rotation", ACM Transactions of Graphics, Vol. 13, No. 3, July 1994, Pages 256-276

[5] Ken Shuemake, "Animating Rotation with Quaternion Curves", SIGGRAPH, Vol. 19, No. 3, 1985.pp248-254.

[6] J. Deutscher, B. North, B. Bascle and A. Blake, "Tracking through singularities and discontinuities by random sampling", the 7th Proc. of IEEE conference on computer vision.Vol.2, pp1144 - 1149

[7] S.J. Phee, W. S. Ng, I.M. Chen, F. Seow-Choen, B. L. Davies, "Locomotion and Steering Aspects in Automation of colonoscopy", IEEE Engineering in Medicine and Biology Magazine, Nov/Dec 1997, p85-96

[8] Martin D. Cooney, Christian Becker-Asano, Takayuki Kanda, Aris Alissandrakis, Hiroshi Ishiguro, "Full-body Gesture Recognition Using Inertial Sensors for Playful Interaction with Small Humanoid Robot", 2010 IEEE/RSJ int. conf. on Intelligent Robots and Systems, Oct., 18-22, 2010, Taipei, Taiwan pp2276-2282

[9] Gerald Glanzer, Thomas Bernoulli, Thomas Wiebflecker and Ulrich Walder, "Semi auto nomous Indoor Positioning Using MEMS based Inertial Measurement Units and Building I nformation", proc. of 6th workshop on positioning, navigation and communication 2009, pp 135-139

[10] Zhi-Qiang, Jian-Kang Wu, "a Novel Hierarchical Information Fusion Method for Thre e Dimensional Upper Limb Motion Estimation", IEEE transactions on instrumentation and measurement, Vol. 60, No. 11, Nobember 2011

[11] Salvatore Sessa, Massimiliano Zecca, Zhuohua Lin, Tomoya Sasaki, Kazuko Itoh, Ats uo Takanishi, "Waseda Bioinstrumentation System #3 as a tool for objective rehabilitation measurement and assessment – development of the inertial measurement unit – ", 2009 IE EE 11th intl, conf. on rehabilitation robotics, Kyoto, Japan, June 23-26, 2009, pp115-120

[12] Chul W. Kang, Chan G. Park, " Attitude Estimation with Accelerometers and gyros Using Fuzzy Tuned Kalman Filter", Proc. of European Control Conf. 2009, Budapest, Hun gary, Aug. 23-26, 2009, pp3713-3718

[13] Seong-hoon P. Won, Wael W. Melek, Farid Golnaraghi," A Kalman/Particle Filter-Bas ed Position and Orientation Estimation Method Using a Position Sensor/Inertial Measureme nt Unit Hybrid System", IEEE transactions on industrial electronics. Vol. 57, No.5, May 2 010

[14]Oliver Amft, Holger Junker, Gerhard Troster, "Detection of eating and drinking arm ge stures using inertial body worn sensors", Proc. of 2005 9th IEEE Int. Symposium on Wear able Computers (ISWC'05), pp1-4

[15] Lorna Herda, Raquel Urrtasun, Pascal Fua, Andrew Hanson, "An Automatic Method f or Determining Quaternion Field Boundaries for Ball and Socket Joint Limits", Automatic face and gesture recognition, 5th IEEE int. conf. pp88-93,2002

[16] J. Zuo, G. Yan, Z. gao, "A micro creeping robot for colonoscopy based on the earth

worm", Journal of medical Engineering & Technology, Vol. 29, No.1, Jan./Feb. 2005, pp1-7

[17] Ji Hoon Kim, Hyung Gi Min, Jae Dong Cho, JaeHoon Jang, SungHa Kwon, Euntae Jeong, "Design of angular estimator of inertial sensor using the least square method", World Academy of Science, Engineering and Technology 2009.

[18] Daniel Roetenberg, Per J. Slycke and Peter H. Veltink, "Ambulatory Position and Orientation tracking Fusing Magnetic and Inertial Sensing", IEEE transactions on Biomedical Engineering, Vol.54, No.5,May 2007

[19] Gul N. Khan, Duncan F Gillies, "Extracting contours by perceptual grouping", Journal of Image and Vision Computing, Vol.10, Issue 2, March 1992, pp77-88

[20] I. M. Chen, Song H. Yeo, Yan Gao," Locomotive gait generation for inchworm like robots using finite state approach", Robotica (2001) Vol.19, pp535-542

[21] Gang Chen, Minh T. Pham, "A Semi automonous Micro-robotic System for Colonoscopy", Proc. of the 2008 IEEE Int. Conf. on Robotics and Biomimetics, Bangkok, Thailand, Feb. 21-26, 2009

[22] Seong Y. Cho, "MEMS based Pedestrian navigation System", Journal of navigation (2006), 59, pp135-153

[23] Hiromasa Yamashita, Daeyoung Kim, Nobuhiko Hata, Takeyoshi Dohi, "Multi slider linkage mechanism for endoscopic forceps manipulator", Proc. of the 2003 IEEE/RSJ, Intl. Conf. on Intelligent Robots and Systems, Vol.3, pp2577-2582, Las Vegas, Nevada October 2003.

[24] J. Szewczyk, V. de Sars, Ph. Bidaud, G Dumont, "An Active tubular polyarticulated micro-system for flexible endoscope", Proc. of ISER '00 Experimental Robotics VII, springer-Verlag London, UK, 2001.

[25] Dan Simon, “Kalman filtering”, Journal of Embedded Systems programming, June 2001, pp72-79

[26] John W. Peterson, “Arc Length Parameterization of Spline curves”, Journal of Computer Aided Design, 2006.

[27] Yundong Tu, “Markov Chain Monte Carlo: Methods and Programming in MatLab”, University of California, Refer discussion note #2009-01, October 10, 2009

[28] Christopher Bishop, “Pattern recognition and machine learning”, Springer. 2009.

[29] Sebastian O.H. Madgwick, “An efficient orientation filter for inertial and inertial/magnetic sensor arrays”,

[30] Rong Zhu, Zhaoying Zhou, “A Real-time Articulated Human Motion Tracking Using Tri-Axis Inertial/Magnetic Sensors Package”, IEEE trasactions on Neural systems and rehabilitation engineering, Vol. 12, No.2, June, 2004

[31] Choukroun, D, Bar-Itzhack, I.Y., Oshman, Y.,”Novel quaternion Kalman filter”, IEEE Transactions on Aerospace and Electronic Systems, Jan. 2006, Vol. 42, Issue 1, page 174-190, ISSN 0018-9251

[32] Qi Cheng, Bondon P, “A new unscented particle filter”, IEEE international conf. on Acoustics, Speech and Signal Processing, 2008, ICASSP, pp3417-3420, ISSN 1520-6149

[33] Sun Young Yi, Hyun Soo Woo, Woojin Ahn, Woo Seok Kim, Doo Yong Lee,”Clinical Evaluation of the KAIST-EWha Colonoscopy Simulator II”, SICE-ICASE, 2006, International Joint Conference, 18-21 Oct.,2006, pp5350-5354, E-ISBN 89-950038-5

[34] Sun Young Yi, Kum Hei Ryu, Hyun Soo Woo, Woojin Ahn, Woo Seok Kim, Doo Yong Lee, “Quantitative Analysis of Colonoscopy skills using the KAIST-Ewha Colonoscopy Simulator II”, Frontiers in the Convergence of Bioscience and Information Technologies, 2007, FBIT2007, 11-13 Oct. 2007, pp519-524, ISBN 978-0-7695-2999-8

[35] JungHwan Oh, Sae Hwang, Yu Cao, Tavanapong. W, Danyu Liu, Wong, J. degroen, P.C.,"Measuring Objective Quality of Colonoscopy", IEEE transactions on Biomedical Engi neering, Sept. 2009, Vol. 56, Issue:9, pp 2190-2196, ISSN 0018-9294

[36] Menciassi, A, Dario, P.,"Miniaturized robotic devices for endoluminal diagnosis and s urgery: A single-module diagnosis and a multiple-module approach", IEEE Intl. Conf. of E ngineering in Medicine and Biology Society, 2009. EMBC2009, pp 6842-6845, E-ISBN:97 8-1-4244-3296-7

[37] Kassim, I. , Phee, L. , Ng, W.S. , Feng Gong , Dario, P. , Mosse, C.A. ," Locomot ion techniques for robotic colonoscopy", IEEE Engineering in Medicine and Biology Maga zine, May-June 2006, Vol. 25, Issue:3, pp 49-56, ISSN:0739-5175

[38] Phee, S.J. , Ng, W.S. , Chen, I.M. , Seow-Choen, F. ; Davies, B.L. ," Locomotion a nd steering aspects in automation of colonoscopy. I. A literature review", IEEE Engineerin g in Medicine and Biology Magazine, Nov/Dec 1997, Vol. 16, Issue:6, pp85-96, ISSN:073 9-5175

[39] Phee, L. ; Accoto, D. ; Menciassi, A. ; Stefanini, C. ; Carrozza, M.C. ; Dario, P. ," Analysis and development of locomotion devices for the gastrointestinal tract", IEEE Tran sactions on Biomedical Engineering, June 2002, Vol.49, Issue:6, pp613-616, ISSN:0018-929 4.

[40] Ikuta, K.; Tsukamoto, M.; Hirose, S.," Shape memory alloy servo actuator system wit h electric resistance feedback and application for active endoscope", IEEE International Co nference on Robotics and Automation, 1988, Proceedings 1988, 24-29 Apr 1988, pp 427 - 430 vol.1, Print ISBN: 0-8186-0852-8

[41] Phee, S.J.; Ng, W.S.; Chen, I.M.; Seow-Choen, F.; Davies, B.L.;" Automation of colo noscopy. II. Visual control aspects", IEEE Engineering in Medicine and Biology Magazine, Issue, May/Jun 1998, Vol. 17, Issue:3, pp: 81 – 88, ISSN : 0739-5175

[42] Menciassi, A. ; Park, J.H. ; Lee, S. ; Gorini, S. ; Dario, P. ; Jong-Oh Park," Roboti c solutions and mechanisms for a semi-autonomous endoscope", International Conference o n Intelligent Robots and Systems, 2002. IEEE/RSJ, Vol. 2, pp: 1379 – 1384, Print ISBN: 0-7803-7398-7

[43] Khessal, N.O. ; Teng Mei Hwa ; Dina Tan ; Teng Leong Chew," The development of an automated robotic colonoscope",

[44] Dario, P.; Mosse, C.A.," Review of locomotion techniques for robotic colonoscopy", I EEE International Conference Proceedings on Robotics and Automation, 2003. pp: 1086 - 1091 vol.1, ISSN: 1050-4729

[45] Jonghoon Park," Interpolation and tracking of rigid body orientations", 2010 Internati onal Conference on Control Automation and Systems (ICCASpp: 668 – 673, E-ISBN: 978-89-93215-02-1

[46] Chessel, A.; Fablet, R.; Cao, F.; Kervrann, C.," Orientation Interpolation and Applicat ions", 2006 IEEE International Conference on Image Processing, pp: 1561 – 1564, ISSN: 1522-4880, E-ISBN: 1-4244-0481-9

[47] Nielson, G.M. ," ν-Quaternion splines for the smooth interpolation of orientations", I EEE Transactions on Visualization and Computer Graphics, Vol.: 10, Issue:2, pp: 224 – 2 29, ISSN:1077-2626

[48] Dapeng Han; Xiao Fang; Qing Wei,"Rotation interpolation based on the geometric str ucture of unit quaternions", IEEE International Conference on Industrial Technology, 2008 (ICIT 2008), 21-24 April 2008, pp: 1 – 6, E-ISBN: 978-1-4244-1706-3

[49] Jan-Phillip Tiesel," Tweaking Keyframe Animation with an Accelerometer Interface A Mobile Low-cost Motion Capture System based on Accelerometers," Bachelor Report, Ma trikel-Nr. 1674708, Universität Bremen - Fachbereich 3 Studiengang Digitale Medien Som mersemester 2006

[50] Verena Elisabeth Kremer," Quaternions and SLERP" Technical Report, University of Saarbrucken, Department for Computer Science, Seminar Character Animation, Supervisor: Michael Kipp, SS 2008

[51] Milos Zefran, Vijay Kumar, "Interpolation schemes for rigid body motions", Technical Report, California Institute of Technology, Pasadena, CA, USA

[52] Andrew Hansen, "Quaternion Frenet Frames: Making Optimal Tubes and Ribbons", C omputer Science Dept. Indiana Univ. ftp://ftp.cs.indiana.edu/pub/techreports/TR407.pdf

[53] Young Soo Suh, "Orientation Estimation Using a Quaternion-Based Indirect Kalman F ilter With Adaptive Estimation of External Acceleration", IEEE Transactions on Instrument ation and Measurement, Dec. 2010, Vol.: 59, Issue:12 pp: 3296 – 3305, ISSN: 0018-945 6

[54] F. C. PARK, BAHRAM RAVANI," Smooth Invariant Interpolation of Rotations", AC M Transactions on Graphics, Vol. 16, No. 3, July 1997, Pages 277–295.

[55] Subae Cho, "Statistical Analysis of Orientation Trajectories via Quaternions with Appl ications to Human Motion" A dissertation for Doctor of Philosophy in Statistics in The University of Michigan, 2006

[56] Berthold K. P. Horn "Closed-form solution of absolute orientation using unit Quaterni ons" Journal of the Optical Society of America A, Vol. 4page 629, April 1987

[57] Huiyu Zhou ; Huosheng Hu, "Kinematic model aided inertial motion tracking of hum an upper limb", 2005 IEEE International Conference on Information Acquisition, 27 Jun e-3 July 2005, 6 pp. Print ISBN: 0-7803-9303-1

[58] F. C. Park, Bahram Ravani, "Smooth Invariant Interpolation of Rotations", ACM Tran sactions on Graphics, Vol. 16, No. 3, July 1997, pp 277-295

[59] Huyghe, B. ; Doutreloigne, J. ; Vanfleteren, J.,"3D orientation tracking based on unsc ented Kalman filtering of accelerometer and magnetometer data", IEEE Sensors Applicati ons Symposium, 2009.(SAS 2009). 17-19 Feb. 2009, pp: 148 – 152, E-ISBN: 978-1-424

4-2787-1

[60] Yun Xiaoping ; Bachmann, E.R. ; McGhee, R.B.," A Simplified Quaternion-Based Al gorithm for Orientation Estimation From Earth Gravity and Magnetic Field Measurements ", IEEE Transactions on Instrumentation and Measurement, March 2008, Vol. 57, Issue:3 p p: 638 – 650, ISSN : 0018-9456

[61] Bachmann, E.R. ; Xiaoping Yun ; McKinney, D. ; McGhee, R.B. ; Zyda, M.J.," Des ign and implementation of MARG sensors for 3-DOF orientation measurement of rigid bo dies ", IEEE Proceedings, International Conference on Robotics and Automation, 2003(ICR A '03), pp: 1171 - 1178 vol.1,ISSN: 1050-4729

[62] Gebre-Egziabher, D.; Elkaim, G.H.; Powell, J.D.; Parkinson, B.W., " A gyro-free quat ernion-based attitude determination system suitable for implementation using low cost senso rs", IEEE Position Location and Navigation Symposium, 2000, pp: 185 – 192, Print ISBN: 0-7803-5872-4

[63] Edwan, E. ; Knedlik, S. ; Loffeld, O. ," Constrained Angular Motion Estimation in a Gyro-Free IMU" IEEE Transactions on Aerospace and Electronic Systems, Vol. : 47 , Issue:1 pp: 596 – 610, ISSN : 0018-9251

[64] Shen, Y. ; Huper, K. ; Leite, F.S.," Smooth interpolation of orientation by rolling and wr apping for robot motion planning" Proceedings 2006 IEEE International Conference on Robotics and Automation, 2006 (ICRA 2006), 15-19 May 2006, pp: 113 – 118, ISSN : 1050-4729

[65] Dapeng Han; Xiao Fang; Qing Wei, "Rotation interpolation based on the geometric st ructure of unit quaternions"IEEE International Conference on Industrial Technology, 2008 (ICIT 2008), 21-24 April 2008, pp: 1 – 6, E-ISBN: 978-1-4244-1706-3

[66] Alexander Kirillov, Jr.," Introduction to Lie Groups and Lie Algebras", Department of Mathematics, SUNY at Stony Brook, Stony Brook, NY 11794,USA,URL: ht tp://www.math.sunysb.edu/~kirillov

[67] Anish K Mampetta,"A Lie group formulation of Kinematics and Dynamics of serial Manipulators", Course Project Report, 16-741: Mechanics of Manipulation, Spring 2006, Robotics Institute, Carnegie Mellon University, Pittsburgh, PA 15213, amampett@andrew.cmu.edu

[68] J.M. Selig, "LIE GROUPS AND LIE ALGEBRAS IN ROBOTICS", South Bank University, London SE1 0AA, U.K, http://www.prometheus-us.com/asi/algebra2003/papers/selig.pdf

[69] Matt Gravelle, "Quaterions and their Applications to Rotation in 3D Space", Technical report, May 1, 2006, http://www.morris.umn.edu/academic/math/Ma4901/gravelle.pdf

[70] Rong Zhu ; Zhaoying Zhou," A real-time articulated human motion tracking using tri-axis inertial/magnetic sensors package" IEEE Transactions on Neural Systems and Rehabilitation Engineering, Volume : 12 , Issue:2, pp: 295 – 302, ISSN : 1534-4320

[71] Jung Keun Lee; Park, E.J.,"A Fast Quaternion-Based Orientation Optimizer via Virtual Rotation for Human Motion Tracking", IEEE Transactions on Biomedical Engineering, Volume: 56 , Issue: 5 , Digital Object Identifier: 10.1109/TBME.2008.2001285 ,2009 , pp: 1574 – 1582

[72] David Eberly, "Key Frame Interpolation via Splines and Quaternions", Geometric Tools, LLC, http://www.geometrictools.com/

[73] Tony Barrera, Barrera Kristiansen AB, Anders Hast,"incremental spherical lineaer interpolation", Creative Media Lab,. University of Gävle. Ewert Bengtsson, http://www.ep.liu.se/ecp/013/004/ecp01304.pdf

[74] Erik B. Dam, Martin Koch, Martin Lillholm, "Quaternions, Interpolation and Animation", Technical Report DIKU-TR-98/5, Department of Computer Science, University of Copenhagen, Universitetsparken 1, DK-2100 Kbh Denmark, July 17, 1998, http://www.itu.dk/people/erikdam/DOWNLOAD/98-5.pdf

[75] Jonghoon Park, "Interpolation and tracking of rigid body orientations", 2010 International Conference on Control Automation and Systems (ICCAS), pp: 668 – 673, ISBN: 978-89-93215-02-1

[76] Guenter, B.; Parent, R., "Computing the arc length of parametric curves", IEEE Computer Graphics and Applications, May 1990, Volume : 10 , Issue:3, pp: 72 – 78, ISSN : 0272-1716

[77] F. C. Park," Smooth invariant interpolation of rotations", ACM Transactions on Graphics (TOG),Volume 16 Issue 3, July 1997, ACM New York, NY, USA

[78] Hongling Wang, Joseph Kearney, Kendall Atkinson, "Arc-length Parameterized Spline Curves for Real Time Simulation", Dept. of Computer Science , U. of Iowa, http://www.math.uiowa.edu/ftp/atkinson/CurvesAndSurfacesArcLength.pdf

[79] Jim Armstrong, "Catmull-Rom Splines", TechNote TN-06-001, January 2006. http://www.algorithmist.net/media/catmullrom.pdf

[80] "The de Casteljau Algorithm for Evaluating Bezier Curves", From Rockwood "Interactive Curves and Surfaces", JDill deCasteljau.doc 29Oct00, http://www.genie-meca.ac-aix-marseille.fr/Productique/PDF/361_deCasteljau_john.pdf

[81] Richard J Sharpe, Richard W Thorne, "Numerical method for extracting an arc length parameterization from parametric curves", J. of Computer Aided Design, Vol. 14, No.2, March 1982

[82] University of Calgary Graphics Jungle project,"Interpolation and Motion", CPSC 587 2005.

[83] David Arnold, "Curvature in Matlab", Math 50C – Multivariable calculus, David-Anorld@Eureka.redwoods.cc.ca.us

[84] Yuanxin Wu, Xiaoping Hu, Meiping Wu and Dewen Hu," Strapdown Inertial Navigat ion using dual quaternion Algebra: Error Analysis", IEEE transactions on aerospace and el ectronic systems, Vol. 42, No.1, January 2006

[85] Bedia Akyar,"Dual Quaternions in Spatial Kinematics in an Algebraic Sense", Turk J. Math, 32(2008), pp 373 – 391

[86] Chapter 15, Clifford Algebra Synthesis of Serial Chains

[87] Chapter 3 Forward Kinematics: The Denavit - Hartenberg Convention; www.cs.duke.edu/.../chap3-forward-kinematics.pdf

[88] Ettore Pennestri, Pier Paolo Valentini, " Dual Quaternions as a Tool for rigid body motion analysis: a Tutorial with an application to biomechanics", Multibody Dynamics 2009, ECCOMAS Thematic Conference, K. Arczewski, J. Frqczek, M.Wojtyra(eds.) Warsaw, Poland, 29 June 2 – July 2009

[89] Denavit – Hartenberg Convention, PPT matrial in the internet site ; opencourses.emu.edu.tr/mod/.../view.php?...true

[90] A Perez Gracia and J M McCarthy, "Kinematic synthesis of spatial serial chains using Clifford algebra exponentials", J. Mechanical Engineering Science 2006, Proc. IMechE Vol 220 Part C, JES166, Special Issue paper 1.

[91] Jim Byrnes, "Computational Noncommutative Algebra and Applications", Nato Science Series II. Mathematics, Physics and Chemistry – Vol. 136, KLUWER Academic Publishers, eBook ISBN; 1-4020-2307-3

[92] B Mourrain, N. Stolfi ",Applications of Clifford Algebras in Robotics", Computational Kinematics, D. Reidel, Dordrecht, 1995 – Citeseer

[93] J. M. Selig, "Clifford Algebra and Robot Dynamics", Handbook of Geometric Computing, 2005, Springer

[94] Alyn Rockwood and Dietmar Hildenbrand, "Engineering Graphics in Geometric Algeb ra", Geometric Algebra Computing in Engineering and Computer Science, Springer, ISBN 978-1-84996-107-3

[95] David Hestenes, Ernest D. Fasse, "Modeling Elastically Coupled Rigid Bodies with G eometric Algebra", geocalc.clas.asu.edu/pdf.../ElasticModeling.pdf

[96] R. Wareham, J. Lasenby," Rigid-Body Pose and Position Interpolation using Geometri c Algebra", www-com-serv.eng.cam.ac.uk

[97] Alba Perez, J. M. McCarthy," Dual Quaternion Synthesis of Constrained Robotic Syst ems", Journal of Mechanical Design, May 2004, Vol. 126 pp425 – 435

[98] Hai-Jun Su," Computer aided Constrained Robot Design Using Mechanism Synthesis Theory", Dissertation Paper in Mechanical and Aerospace Engineering, University of Califo rnia Irvine

[99] Hoang-Lan Pham, Veronique Perdereau, Bruno Vilhena Adorno, Philippe Fraisse, "Pos ition and Orientation Control of Robot Manipulators Using Dual Quaternion feedback", 201 0 IEEE/RSJ International Conference on Intelligent Robots and Systems (IROS), Oct. 2010 ,pp: 658 - 663 , Taipei ISSN: 2153-0858

[100] Serdar Kucuk and Zafer Bingul,"Robot Kinematics: Forward and Inverse Kinematics", Industrial Robotics-Theory Modelling Control, ISBN 3-86611-285-8, pp 964, ARS/pIV, Ge rmany, December 2006

[101] Pasquale Gervasi," Serial Manipulator Kinematics with Dual Quaternions and Grassm annians", Thesis, Dept. of Mechanical Eng. Center for Intelligent Machines, McGill Univer sity, Montreal, Quebec, Canada, September 1999.

[102] Jingzhou Yang, Xuemei Feng, Joo H. Kim, "Review of biomechanical models for h uman shoulder complex", Int. J. Human Factors Modelling and Simulation, Vol. 1, No. 3,

2010, pp 271- 293

[103] Alba Perez Gracia, “Synthesis of Spatial RPRP closed Linkages for a Given Screw System”, D. Pisla et al. (eds.), New Trends in Mechanism Science:Analysis and Design, Mechanisms and Machine Science 5, DOI 10.1007/978-90-481-9689-0_2, 11 © Springer Sc ience+Business Media B.V. 2010
[104] C.piro and D. Accardo, “a vertical gyro model based on particle filters”, IEEEAC p aper #1529, Version 2, Updated December 5, 2006.

[105] J. Michael McCarthy, Gim Song Soh,” Geometric Design of Linkages”, Interdisciplin ary Applied Mathematics, Volume 11 2011, ISBN: 978-1-4419-7891-2 (Print) 978-1-4419-7 892-9 (Online)

早稲田大学　博士（工学）　学位申請　研究業績書

氏 名　Jaewoo Lee　(李宰雨)　　印

(2013年　2月25現在）

種 類 別	題名	発表・発行掲載誌名	発表・発行年月	連名者（申請者含む）
1. 論文	Analysis of the colon by the biodynamic model and application to the colonoscopy robot design	Proceedings of 2011 IEEE International Conference Robotics and Biomimetics (ROBIO 2011), pp. 1844-1849	2011年12月	Jaewoo Lee Genya Ukawa Shuna Doho Hiroyuki Ishii Atsuo Takanishi
	Non visual sensor based shape perception method for gait control of flexible colonoscopy robot	Proceedings of 2011 IEEE International Conference Robotics and Biomimetics (ROBIO 2011), pp. 577-582,	2011 年 12 月	Jaewoo Lee Genya Ukawa Shuna Doho Zhuohua Lin Hiroyuki Ishii Massimiliano Zecca Atsuo Takanishi
	Simulation model which can visualize the shape of the colonoscopy using orientation sensor network	Proceedings of Biomechanics 2011, Track 751-025,	2011 年 11 月	Jaewoo Lee, Genya Ukawa, Shuna Doho, Zhuohua Lin, Hiroyuki Ishii, Atsuo Takanishi
	Shape visualization method of flexible colonoscopy using non visual sensor network for monitoring of operation	Proceedings of 33rd Annual International Conference of the IEEE Engineering in Medicine and Biology Society (EMBC 2011)	2011年9月	Jaewoo Lee, Hiroyuki Ishii, Atsuo Takanishi
	Shape estimation method of flexible endoscope using sensor network in the endoscope handling Robot system.	Computer Assisted Radiology and Surgery - 25th International Congress and Exhibition(CARS 2011) Vol.6, Supplement 1, S127-128	2011年6月	Jaewoo Lee, Junichi Kinoshita, Genya Ukawa, Daisuke Kikuchi, Hiroyuki Ishii, Kazuko Itoh, Makoto Hashizume Atsuo Takanishi

				室,

種 類 別	題名	発表・発行掲載誌名	発表・発行年月	連名者（申請者含む）
	Development of a colon endoscope robot that adjusts its locomotion through the use of reinforcement learning	International Journal of Computer Aided Radiology and Surgery Vol.5, p317-325	2010年5月	Gabriele Trovato, Masaki Shikanai, Genya Ukawa, Junichi Kinoshita, Natsuki Murai, Jaewoo Lee, Hiroyuki Ishii, Atsuo Takanishi, Kazuo Tanoue, Satoshi Ieiri, Kozo Konishi, Makoto Hashizume

種 類 別	題名	発表・発行掲載誌名	発表・発行年月	連名者（申請者含む）
2. 講演	Empirical analysis of mechanical characteristics of the colon for robot design and evaluation of design parameter	Journal of Japan Society of Computer Aided Surgery : J.JSCAS 12(3), pp. 456-457	2010 年 11 月	Jaewoo Lee Junichi Kinoshita Genya Ukawa Daisuke Kikuchi Hiroyuki Ishii Kazuko Itoh Makoto Hashizume Atsuo Takanishi
	Development of automatic visual inspection system for irregular formed materials with ill reflectivity in mixed production line	第 27 回日本ロボット学会学術講演会予稿集, 2R1-03	2009年9月	Jaewoo Lee